PHYSICAL REVIEW LETTERS

VOLUME 7 NUMBER 12

DECEMBER 15, 1961

Published by the

AMERICAN PHYSICAL SOCIETY

Published in Two Sections

Section 1

PHYSICAL REVIEW LETTERS

Containing short communications dealing with important new discoveries or topics of high current interest in rapidly changing fields of research, and abstracts of Articles to be published in future issues of THE PHYSICAL REVIEW.

Published by the

AMERICAN PHYSICAL SOCIETY

Officers

President

F. SEITZ
University of Illinois
Urbana, Illinois

Vice-President

W. V. HOUSTON
Rice University
Houston, Texas

Secretary

K. K. DARROW
Bell Telephone Laboratories
(retired)
Office:
Columbia University
New York 27, New York

Deputy Secretary

W. W. HAVENS, JR.
Columbia University
New York 27, New York

Treasurer

S. L. QUIMBY
Columbia University
New York 27, New York

Deputy Secretary for the Pacific Coast

HOWARD SHUGART
University of California
Berkeley, California

Managing Editor

S. A. GOUDSMIT
Brookhaven National Laboratory
Upton, Long Island, New York

Editors

S. A. GOUDSMIT and S. PASTERNACK

Assistant Editor

A. HERSCHMAN

Publication Manager

M. J. FLEMING

Communications intended for this Journal should be short (about 800 words) and self-contained; they should not contain more than two figures. The results of an extended research program should not be presented as a series of Letters in place of a comprehensive Article.

Manuscripts, which must be in duplicate, should be submitted to S. A. Goudsmit, Editor, The Physical Review, Brookhaven National Laboratory, Upton, New York. The authors' institutions are requested to pay a publication charge of $35 per page which, if honored, entitles them to 100 free reprints. For abstracts, a publication charge of $8 will be requested.

Subscription Price

	U. S. and Canada	Elsewhere
Physical Review Letters		
Members of the American Physical Society	$ 5.00	$ 6.00
Nonmembers	10.00	11.00

Back Numbers

Single Copies	1.50
Complete Volumes	
I (July 1 - December 15, 1958)	15.00
II (January 1 - June 15, 1959)	15.00
III (July 1 - December 15, 1959)	15.00
IV (January 1 - June 15, 1960)	15.00
V (July 1 - December 15, 1960)	15.00
VI (January 1 - June 15, 1961)	15.00

Subscriptions, renewals, orders for back numbers, and changes of address should be sent to the American Institute of Physics, 335 East 45th Street, New York 17, New York.

Physical Review Letters is published semi-monthly by the American Physical Society at Columbia University, New York, N. Y.

Second-class postage paid at New York, N. Y.

VOLUME 7, NUMBER 12 DECEMBER 15, 1961

PHYSICAL REVIEW LETTERS

SECTION 2

ABSTRACTS OF ARTICLES TO BE PUBLISHED IN THE PHYSICAL REVIEW

In this section are printed the abstracts of Articles that have been forwarded to The American Institute of Physics for publication in The Physical Review. In quoting information obtained from this section before the appearance of the corresponding Article, reference should be made to "Physical Review (to be published)" rather than to this Journal.

THERMODYNAMIC BEHAVIOR OF LIQUID HELIUM-THREE IN ITS POSSIBLE SUPERFLUID PHASE. I. Toshio Soda, Department of Physics, University of California, Berkeley, California, and Ramabadhra Vasudevan,* Department of Physics, University of California, La Jolla, California (Received March 17, 1961; revised manuscript received October 23, 1961).

The thermodynamic behavior of liquid He^3 in its possible superfluid phase is investigated by extending the methods of Brueckner et al. They suggest that such a correlated phase can exist at very low temperatures due to the fact that there exist attractive D-state interactions near the Fermi surface. The free energy and the energy gap of the system for D-state interactions corresponding to different pure azimuthal modes are calculated at different temperatures. It is found that $l=2$, $m=2$ and $l=2$, $m=1$ modes correspond to the lowest free energy of the system near the critical temperature. In the intermediate range of temperatures the free-energy curves for the two modes, when the computations are made numerically, come out to be very nearly the same. But actually it can be shown by an analytical method that they are identical. The $l=2$, $m=0$ mode yields a higher free energy for all temperatures less than the critical temperature. The mixing of modes is investigated near the critical temperature. Any linear combination of all the modes $l=2$, $m=0$, 1, -1, 2, and -2 does not seem to lead to a lower free energy than that of the $l=2$, $m=\pm 2$ and $m=\pm 1$ modes. The correlation lengths at different temperatures are also analyzed. The specific heat and entropy curves for the $l=2$, $m=2$ mode are given.

*Now at the Physics Department, University of California, Berkeley, California.

EXACT EVOLUTION OF REDUCED DISTRIBUTION FUNCTIONS IN A HOMOGENEOUS DENSE CLASSICAL FLUID. Frank C. Andrews,* Department of Chemistry, University of California, Berkeley, California (Received October 4, 1961).

The exact evolution of reduced distribution functions is studied for a homogeneous dense classical fluid by methods which are equivalent to the diagram technique of Prigogine and coworkers. No diagrams or Fourier expansion are used in this work, however. So long as only short-range order is present in the fluid, exact equations for the evolution of the momentum distribution function and for reduced s-particle distribution functions are obtained. They are seen to be non-Markovian in a sense explicitly related to the finite duration of a collision. Simple Markovian equations—a generalized master equation for momenta and a functional equation for correlations—result only when the momentum distribution changes negligibly in times of the order of the duration of a collision.

*Present address: Chemistry Department, University of Wisconsin, Madison, Wisconsin.

APPROACH TO EQUILIBRIUM IN A DENSE CLASSICAL FLUID. Frank C. Andrews,* Department of Chemistry, University of California, Berkeley, California (Received October 4, 1961).

The equation derived in a previous paper for the exact evolution of the momentum distribution function of a homogeneous dense classical fluid is studied. The Markovian form of this equation is found to drive the momentum distribution monotonically to an arbitrary function of the kinetic energy of the system. This function must be canonical if it factorizes in momentum space.

Incorporation of the non-Markovian effects in the evolution equation through a simple approximation does not destroy the approach to equilibrium. Since reduced s-particle distribution functions previously were shown to be functionals of the momentum distribution, they also monotonically approach equilibrium.

*Present address: Chemistry Department, University of Wisconsin, Madison, Wisconsin.

EVOLUTION OF REDUCED DISTRIBUTION FUNCTIONS FOR INHOMOGENEOUS DENSE CLASSICAL FLUIDS. Frank C. Andrews,* Department of Chemistry, University of California, Berkeley, California (Received October 4, 1961).

The evolution of reduced distribution functions is studied for an inhomogeneous dense classical fluid by methods previously used to study homogeneous fluids. So long as only short-range order is present in the fluid and the variation in properties caused by the inhomogeneity is negligible over distances of the order of the region of a collision, then the evolution equations for the one-particle and s-particle distribution functions are obtained. They take a simple Markovian form if the one-particle distribution changes negligibly in times of the order of the duration of a collision. The operators involved in the evolution equations are studied. Their physical meaning and relationship to the classical Boltzmann equation are considered.

*Present address: Chemistry Department, University of Wisconsin, Madison, Wisconsin.

CALCULATION OF THE SUPERCONDUCTING STATE PARAMETERS WITH RETARDED ELECTRON-PHONON INTERACTION. P. Morel, French Embassy, New York, New York, and P. W. Anderson, Bell Telephone Laboratories, Murray Hill, New Jersey (Received October 10, 1961).

The energy gap and other parameters of the superconducting state are calculated from the Bardeen-Cooper-Schrieffer theory in Gor'kov-Eliashberg form, using a realistic retarded electron-electron interaction via phonons and including the Coulomb repulsion. The solution is facilitated by observing that only the local phonon interaction, mediated entirely by short-wavelength phonons, is important, and that a good approximation for the phonon spectrum is therefore an Einstein model rather than a Debye model. The resulting equation is solved by an approximate iteration procedure. The results are similar to earlier gap equations but the derivation gives a precise meaning to the interaction and cutoff parameters of earlier theories. The numerical results are in good order-of-magnitude agreement with the observed transition temperatures but lead to an isotope effect at least 15% less than the accepted $-\frac{1}{2}$ exponent (T_c proportional to $M^{-1/2}$). Also, the present theory predicts that all metals should be superconductors, although those not observed to do so would have remarkably low transition temperatures.

INTERBAND TRANSITIONS IN SUPERCONDUCTORS. G. Dresselhaus and M. S. Dresselhaus, Lincoln Laboratory, Massachusetts Institute of Technology, Lexington, Massachusetts (Received October 9, 1961).

When the photon energy is such that an interband transition occurs between the valence and conduction bands in the normal state, small differences in the optical properties of the normal and superconducting metals can arise. Using a simple energy-gap model for the superconductor, the change in the reflectivity and transmission is calculated and is shown to be measurable over a narrow frequency range, assuming realistic values for the pertinent parameters. This type of experiment may be useful for studies of both interband transitions in normal metals and anisotropy of the energy gap in superconductors.

SUPERPOSITION OF PERIODIC POTENTIALS AND HOMOGENEOUS FIELDS. G. H. Wannier, University of Oregon, Eugene, Oregon, and D. R. Fredkin,* Bell Telephone Laboratories, Murray Hill, New Jersey (Received September 5, 1961).

Following up an earlier communication, wave functions are constructed for a superposition of a periodic electric potential and a uniform magnetic field. The wave functions are not themselves solutions of the Schrödinger equation, but yield the traditional effective Hamiltonian for this problem. Contrary to the electric field case the manifold of states linked by the "band index" does not form a Bloch band; the reason is that the cellular transforms of the Bloch-like functions are modi-

fied by the Peierls phase. At present, the derivation of these results is in closed form, but justifiable only "to all powers of the magnetic field." This was also the case for the previous electric derivation. The limitation may not be genuine. The second half of the paper does in fact prove directly the existence of closed Bloch bands in the presence of a homogeneous electric field; the case of free electrons is given as an example. One expects from this that the new results for the magnetic field are, at least in part, also independent of the power series method used for their justification.

*Permanent address: University of California, La Jolla, California.

ANTIFERROMAGNETIC STRUCTURE OF $CrVO_4$ AND THE ANHYDROUS SULFATES OF DIVALENT Fe, Ni, and Co. B. C. Frazer and P. J. Brown, Brookhaven National Laboratory, Upton, New York (Received September 22, 1961).

The antiferromagnetic structures of $CrVO_4$, $FeSO_4$, $NiSO_4$, and $CoSO_4$ have been determined from neutron diffraction data collected from polycrystalline samples. All of these compounds have the same orthorhombic crystal structure. In this structure the magnetic ions form face-centered sheets which stack at d_{002} intervals in the $\vec{c}$ direction. The magnetic structure found for $CrVO_4$ consists of ferromagnetically ordered sheets which stack antiferromagnetically. The single spin direction is found to be inclined at angles $\Phi_a = 27 \pm 15°$, $\Phi_b = 64 \pm 10°$, and $\Phi_c = 81 \pm 15°$ with the crystallographic axes. A somewhat more logical spin orientation, which is close to being within experimental error, would be parallel to the $\vec{a}$ axis. The Cr^{+++} moment at 4.2°K is $(2.1 \pm 0.2)\mu_B$. The magnetic structures of $FeSO_4$ and $NiSO_4$ both have antiferromagnetic sheets with ferromagnetic coupling between the sheets. In both cases the spin direction is parallel to the $\vec{b}$ axis. The moments at 4.2°K are $(4.1 \pm 0.4)\mu_B$ for Fe^{++}, and $(2.1 \pm 0.1)\mu_B$ for Ni^{++}. In $CoSO_4$ there is also antiferromagnetic ordering within each sheet, but the coupling between sheets does not lead to a collinear spin structure. Instead there are two spin directions that alternate in successive sheets. The spin vectors are found to lie in the YZ plane at alternately clockwise and counterclockwise angles of $25 \pm 2°$ from the b axis as translations are made along the $\vec{c}$ axis. The Co^{++} moment at 4.2°K is $(3.3 \pm 0.2)\mu_B$. This magnetic structure found for $CoSO_4$ is very similar to a structure predicted recently for $CuCl_2 \cdot 2H_2O$ by Moriya on the basis of anisotropic superexchange calculations.

MAGNETOACOUSTIC EFFECTS IN NONDEGENERATE SEMICONDUCTORS. Harold N. Spector,* Institute for the Study of Metals, University of Chicago, Chicago, Illinois (Received October 11, 1961).

A self-consistent, semiclassical treatment is given for the attenuation of a sound wave in a nondegenerate impurity semiconductor with spherical energy bands, using the formalism developed by Cohen, Harrison, and Harrison. A treatment is given for propagation both parallel and perpendicular to the magnetic field and the behavior of the attenuation is examined for a wide range of frequencies, magnetic fields, and mean free paths. The phenomena studied include saturation with frequency in longitudinal magnetic fields, and cyclotron resonance and magnetoplasma effects in transverse magnetic fields. A magnetoplasma resonance for the transverse polarized waves in a longitudinal magnetic field has been discovered and has been identified with a resonance calculated by Cohen, Harrison, and Harrison. A qualitative physical interpretation of the various effects found in the detailed calculations is also presented.

*Presently National Science Foundation Postdoctoral Fellow at the Hebrew University, Jerusalem, Israel.

EFFECT OF ORDER ON THE HALL CONSTANTS OF Ni_3Mn. James A. Dreesen, Carnegie Institute of Technology, Pittsburgh, Pennsylvania (Received July 24, 1961).

Hall effect measurements as a function of temperature are reported for ordered and disordered Ni_3Mn. At low temperatures the ordinary Hall coefficient is found to be negative for both the ordered and disordered alloy. It is shown that the apparent positive value of the ordinary Hall coefficient in the disordered alloy at room temperature is due to the near coincidence of the Curie temperature of this alloy with room temperature. This results in a positive contribution to the measured value of the ordinary Hall coefficient from the extraordinary effect, a smaller contribution being present at low temperatures. An

approximate correction is made for this contribution, with the result that the true ordinary coefficient in disordered Ni_3Mn is found to be nearly equal to that in the ordered alloy. Furthermore, its absolute magnitude and temperature dependence are much like that of Cu-Ni and pseudonickel alloys. On this basis it is concluded that ordering has much less effect on the band structure of this alloy than was previously assumed.

EFFECT OF AN IMPURITY LAYER ON SURFACE WAVES. Harvey Kaplan, Syracuse University, Syracuse, New York (Received October 9, 1961).

We study here the effects of a homogeneous impurity mass layer on the surface waves of a semi-infinite monatomic square lattice with nearest and next nearest neighbor central springs. In the long-wavelength limit the impurity layer does not alter the surface waves from those of a pure semi-infinite lattice. However, depending upon the ratio of the impurity mass to the host mass, and for wavelengths shorter than a critical wavelength, the long-wavelength surface wave may disappear and new surface waves with frequencies either higher or lower than the spectrum of the pure infinite lattice may appear. The relationship of this model to the analogous one- and three-dimensional problems is discussed.

We expect this theory to be applicable to problems such as the effect of an oxide layer on the surface vibrations of a crystal.

SPECIFIC HEAT OF Cr-Fe ALLOYS FROM -140 TO 350°C. Klaus Schröder, University of Illinois, Urbana, Illinois (Received August 14, 1961).

The specific heat of bcc iron-chromium alloys has been measured in an adiabatic calorimeter in the temperature range from -140 to 350°C. Isothermal plots of c_p versus composition revealed two maxima at higher temperatures. One occurred independently of temperature at 19 at.% Fe and was associated with the peak in the density-of-states curve; the other was temperature dependent and was associated with the transition from ferromagnetism to paramagnetism. Lattice and electronic contributions could be separated from each other for alloys with high chromium concentration. The Debye θ did not vary noticeably with composition, but the electronic specific heat showed a maximum.

LOW-TEMPERATURE HEAT CAPACITY OF A SUPERCONDUCTING ALLOY OF ALUMINUM. F. A. Otter* and D. E. Mapother, University of Illinois, Urbana, Illinois (Received October 9, 1961).

The specific heat of a precipitation-hardening alloy of aluminum (Alcoa 6063) has been measured down to 1.8°K in both the annealed and hardened conditions. From 1.8 to 4.2°K, the data for both conditions are well represented by $C=\gamma T+1.944\times10^{6}(T/\theta_D)^3$ mjoule/mole-deg with $\gamma=1.33\pm0.02$ mjoule/mole-deg^2 and $\theta_D=430\pm4$°K for the annealed condition. In this temperature range, both γ and θ_D increase for the alloy in the hardened condition. The changes are $d\gamma/\gamma=(1.1\pm0.5)\%$ and $d\theta_D/\theta_D=(1.3\pm0.6)\%$. No change in θ_D was observed from 10 to 20°K. The change in θ_D is quantitatively consistent with previous work on the shift of the superconducting critical field curve of this alloy with hardening. Both the present change in θ_D and the previously reported shift in H_c indicate an internal compressive stress in the fully hardened alloy which is believed to arise from coherency stress in the early stages of precipitation. The observed change in γ seems inconclusive with respect to the coherency stress hypothesis for reasons which are discussed.

*Present address: Ohio University, Athens, Ohio.

COLOR CENTERS IN CsCl-TYPE ALKALI HALIDES. Herbert Rabin and James H. Schulman,* U. S. Naval Research Laboratory, Washington, D. C. (Received October 11, 1961).

A study of x-ray induced color centers in the CsCl-type alkali halides has been made at room, liquid nitrogen, and liquid helium temperatures. The gross features of this coloration are similar to those observed in NaCl-type alkali halides, namely a principal absorption band in the visible portion of the spectrum with other absorptions at both longer and shorter wavelengths. The absorption spectra observed vary with the temperature of irradiation; the bands show characteristic thermal shifting and broadening, bleach under both thermal and optical excitation, and demonstrate much of the usual color-center behavior. At the same time some characteristics of the

cesium halides appear to be unique, in particular the multiplicity in structure which makes its appearance in the principal absorption bands of CsCl and CsBr at liquid helium temperature. Since the principal absorption gives every evidence of being associated with the F center, one possible explanation of the component structure is that it arises from higher excited states of the F center.

*Presently on leave at the U. S. Office of Naval Research, London, England.

PARAMAGNETIC RESONANCE OF THE COBALT ION IN RUTILE SINGLE CRYSTAL. E. Yamaka* and R. G. Barnes, Institute for Atomic Research and Department of Physics, Iowa State University, Ames, Iowa (Received September 11, 1961).

The electron paramagnetic resonance of Co^{2+} in single-crystal rutile (TiO_2) has been investigated at 3-cm wavelength and 4.2°K. The angular dependence of the resonance pattern indicates that the Co^{2+} ion enters substitutionally for the Ti^{4+} ion in the lattice. Strongly anisotropic values of the splitting factor g and hfs constant A are obtained, which may be understood in terms of a fairly large charge transfer to the surrounding ions.

*On leave from the Electrical Communication Laboratory, Tokyo, Japan.

DRIFT MOBILITIES OF ELECTRONS AND HOLES AND SPACE-CHARGE-LIMITED CURRENTS IN AMORPHOUS SELENIUM FILMS. J. L. Hartke,* University of Illinois, Urbana, Illinois (Received October 11, 1961).

The band model has been applied to semiconducting amorphous selenium. Drift mobilities in pure films agreed well with previous results of Spear, and some evidence was obtained that the shallow electron and hole traps were caused by imperfections, further considerations suggesting that the traps were distributed continuously in energy. Electron drift mobilities were reduced when arsenic was added to the films but their temperature dependence was unchanged, suggesting that arsenic increased the concentrations of imperfections which produce shallow electron traps. Hole ranges were $(2\text{-}4)\times10^{-6}$ cm^2/volt and exhibited no observable temperature dependence, while electron ranges were $(1\text{-}2)\times10^{-7}$ cm^2/volt at 300°K and decreased with decreasing temperature.

Gold and tellurium electrodes were used to inject holes into amorphous selenium, producing space-charge-limited currents at high fields. The observed currents indicated hole capture centers distributed uniformly in energy in a region extending downwards from 1 ev above the valence band edge. The densities of these levels were 10^{15} cm^{-3} ev^{-1}. Electrical conductivities of 10^{-14} to 10^{-16} ohm^{-1} cm^{-1} were obtained at low fields. The lowest value of conductivity agreed well with values extrapolated from liquid selenium. The drift of photoinjected electrons in the presence of space-charge-limited currents was used to probe the electric field. The general spatial dependence was that expected of space-charge-limiting by holes, but could not be explained quantitatively.

*Present address: Zerox Corporation, Rochester, New York.

PHOTOEMISSION AND BAND STRUCTURE OF THE SEMICONDUCTING COMPOUND CsAu. W. E. Spicer, RCA Laboratories, Princeton, New Jersey (Received October 5, 1961).

The energy distribution of the photoelectrons and the quantum efficiency of the photoemission from CsAu were measured in the spectral range from 1.6 to 6.2 ev. From the measurements the following conclusions were drawn: For $h\nu > 4.0$ ev, photoelectrons are excited principally from the valence band; for $h\nu < 4.0$ ev, photoelectrons are excited from states near the bottom of the conduction band. A bandgap of $2.6(\pm 0.2)$ ev and an electron affinity of $1.5(\pm 0.2)$ ev are deduced.

KNIGHT SHIFT AND QUADRUPOLE INTERACTION IN Tc METAL. William H. Jones, Jr., and Frederick J. Milford, Battelle Memorial Institute, Columbus, Ohio (Received October 4, 1961).

The nuclear magnetic resonance of the Tc^{99} nucleus in technetium metal has been observed. The shape and position of the resonance are due to combinations of isotropic and anisotropic Knight shifts; first and second order quadrupole interactions; and dipolar broadening. The various contributions have been separated by studying the characteristics of the resonance as a function of frequency.

ULTRAVIOLET ABSORPTION OF KI DILUTED IN KCl CRYSTALS. Herbert Mahr, Laboratory of Atomic and Solid-State Physics, Cornell University, Ithaca, New York (Received October 2, 1961).

The absorption of KI diluted in KCl single crystals was studied for concentrations of 10^{-3} to 10^{-5} mole fraction KI in the temperature range from 80°K to 700°K. The exact shape of the long-wavelength absorption peak, which is Gaussian around the maximum and exponential at the edge, was measured quantitatively over four orders of magnitude. The total integrated absorption is proportional to the iodide concentration which was determined chemically. In the limit of high temperatures the half-width of the band is proportional to the square root of the temperature and the edge follows Urbachs law. Deviations at low temperatures were shown to arise from zero-point oscillations. The results were compared with models for localized excitons.

REFLECTIVITY OF GRAY TIN SINGLE CRYSTALS IN THE FUNDAMENTAL ABSORPTION REGION. Manuel Cardona and D. L. Greenaway, Laboratories RCA Ltd., Zurich, Switzerland (Received October 2, 1961).

Single crystals of gray tin have been grown by the method of Ewald from a mercury solution. The reflection coefficient of a surface of growth has been measured in the fundamental absorption region. The reflectivity shows two maxima as in other semiconductors with diamond and zinc blende structure. The lower energy maximum exhibits a doublet structure. The energy at which this maximum occurs is interpreted as the energy gap at the L point of the Brillouin zone. The energy separation of the doublet components gives the spin-orbit splitting of the valence band at the L point. From the measured value of the L gap the transverse effective mass at the bottom of the conduction band is estimated to be $0.06m$. Several general conclusions about the systematics of the band structure in all semiconductors with diamond and zinc blende structure are presented.

EFFECT OF QUARTIC ANHARMONICITY ON THE INFRARED ABSORPTION OF ALKALI HALIDE CRYSTALS. D. W. Jepsen, Thomas J. Watson Research Center, International Business Machines Corporation, Yorktown Heights, New York, and R. F. Wallis, U. S. Naval Research Laboratory, Washington, D. C. (Received September 11, 1961).

A classical theory is given for the influence of quartic anharmonicity terms on the infrared lattice vibration spectra of ionic crystals. It is found that quartic anharmonicity introduces terms in the damping constant which are proportional to the square of the absolute temperature. A frequency renormalization is found to be necessary in order to make the simple classical theory go through for quartic terms.

EXTREME ULTRAVIOLET ABSORPTION BY LITHIUM FLUORIDE. A. Milgram* and M. Parker Givens, University of Rochester, Rochester, New York (Received August 30, 1961).

A study was made to determine the absolute value of the absorption coefficient for lithium fluoride between 10 and 110 ev. The first exciton level in the fundamental absorption was found to be at 12.9 ev. Absorption structure attributed to the fluorine 2s electrons and lithium 1s electrons was observed. The energy band gap was estimated to be less than 14 ev. The absorption structure associated with the Li K electrons was found at energies corresponding to transitions by the 2s electrons of the free Li^+ ion. A duplication of this structure at a higher energy suggested the possibility that a multiple process was involved in the photon absorption.

*Present address: Research Department, Carrier Research and Development Company, Syracuse, New York.

MAGNETISM OF KCl. E. Sonder, Solid State Division, Oak Ridge National Laboratory, Oak Ridge, Tennessee (Received October 2, 1961).

At room temperature KCl has a diamagnetic susceptibility of 1.04×10^{-6} cgs units per cm^3. The value at liquid nitrogen temperatures is $\frac{1}{2}\%$ smaller. As the temperature is lowered further, a paramagnetic contribution inversely proportional to the temperature becomes apparent in additively or gamma-ray colored material. The magnitude of this paramagnetic contribution, which is proportional to the number of one-electron imper-

fection centers, is compared to the optical absorption of electron excess centers, to yield a value of 0.6 for the oscillator strength of the F band, and strong evidence that the M center is not paramagnetic. The results also indicate that the M center absorbs under the F band as well as in the M band.

TRANSITIONS TO METALLIC STATES IN IONIC CRYSTALS, WITH PARTICULAR REFERENCE TO CESIUM IODIDE. M. Flower and N. H. March, Department of Physics, The University, Sheffield, England (Received May 31, 1961; revised manuscript received November 6, 1961).

Shock-wave experiments by Alder and Christian have indicated that metallic transitions might occur in certain ionic crystals. Therefore, one heavy ionic crystal, CsI, has been studied by the cellular method of band theory, both for the normal lattice parameter and for a reduced spacing corresponding to an estimated pressure of ~250 000 atmospheres. Our principal conclusion is that the energy gap between valence and conduction bands varies little with pressure in the range we consider. A gap of 6 or 7 ev is obtained with our relatively crude potential. The width of the valence band is estimated at 3-4 ev and with our potential, and neglect of spin-orbit effects, a state at the zone edge along [100] appears to be the highest in this band, while the conduction band minimum is at $\vec{k}=0$. The results under normal conditions are in good agreement with the photoemission experiments of Philipp, Taft, and Apker, both for the gap and the valence bandwidth, but the shock-wave experiments of Alder and Christian cannot be understood along the present lines. Later static pressure experiments by Griggs et al. are not, however, in conflict with our findings.

NUCLEAR SPIN ABSORPTION SPECTRA IN SOLIDS. A. G. Anderson, International Business Machines Research Laboratory, San Jose, California (Received October 5, 1961).

Nuclear magnetic spin absorption spectra in both parallel and perpendicular ac and dc magnetic fields are reported for lithium nuclei in lithium metal. This is a case where the predominant interactions are the Zeeman interaction of the nuclear magnetic moment with the dc field and the magnetic dipole-dipole interaction between nuclei in fixed lattice positions. For an applied dc field, H_0, the spectrum consists of absorption around zero frequency, around $\omega=\gamma H_0$, and around $\omega=2\gamma H_0$. Linewidths and relative amplitudes observed experimentally are in good agreement with the theory, which predicts linewidths of approximately the same magnitude for all lines and line amplitudes which vary as H_0^{-4}, H_0^{0}, or H_0^{-2}. At applied dc fields, which are large compared with the internal magnetic dipole-dipole fields, an additional absorption is observed for the parallel-field case at very low frequencies; this is attributed to the relatively long time required for establishment of internal equilibrium at these fields.

Absorption spectra are reported for lithium-magnesium alloys. In these alloys addition of magnesium produces electric quadrupole broadening of the lithium absorption spectra. The zero-field absorption spectrum of copper is also reported.

LOW-ENERGY SCATTERING OF A CHARGED PARTICLE BY A POLARIZABLE SYSTEM. Thomas F. O'Malley, Leonard Rosenberg,* and Larry Spruch, Physics Department, Washington Square College and Institute of Mathematical Sciences, New York University, New York, New York (Received October 12, 1961).

In the scattering of a particle (or system) of charge Ze by a neutral system with an electrical polarizability α, an electric dipole moment is induced which generates an effective potential that behaves asymptotically as $-\frac{1}{2}Z^2e^2\alpha/r^4$. Due to this effective long-range interaction, effective-range theory in its normal form is not applicable. Thus, for the scattering of a particle with an incident orbital angular momentum of zero, for example, the expansion of $k\cot\eta(0)$ includes terms in k and in $k^2\ln k$, in addition to the usual constant and k^2 terms. The effective range, r_0, as normally defined is infinite but one can define a quantity r_{p0} which explicitly takes into account the long-range character of the effective potential. For $L>0$ it is $k^2\cot\eta(L)$ which approaches a constant as k approaches zero rather than $k^{2L+1}\cot\eta(L)$ as for a short-range potential. The above results can have serious consequences in the scattering of electrons and of positrons by neutral spherically symmetric atoms. Some detailed consideration is given to the scattering by hydrogen atoms.

The formulation of effective-range theory which is given is valid when Pauli exchange between the two colliding systems is possible. The method used for taking into account the effect of the Pauli principle (this method would be the same for long-range and short-range forces) is rather more convenient than in the usual presentation.

*Present address: Physics Department, University of Pennsylvania, Philadelphia, Pennsylvania.

ELECTRON TRIPLET PRODUCTION BY HIGH-ENERGY PHOTONS IN HYDROGEN. Duane C. Gates, Robert W. Kenney, and William P. Swanson, Lawrence Radiation Laboratory, University of California, Berkeley, California (Received June 13, 1961).

The 323-Mev hardened bremsstrahlung beam from the Berkeley synchrotoron was used to produce electron-positron pairs and triplets in a 4-in.-diam liquid hydrogen bubble chamber. It was found that the experimental triplet cross sections for detectable recoils (momentum greater than 0.27 Mev/c) and for recoils with momentum greater than mc rise logarithmically with photon energy to 100 Mev, then level off at approximately 2.8 mb and 1.5 mb, respectively. The total triplet cross section agrees with that of Borsellino above 20-Mev photon energy. No contribution due to exchange terms was found. The positron energy distribution agrees with that of Wheeler and Lamb. The recoil momentum distribution agrees substantially with that of Suh and Bethe. Approximately one event due to multiple pair production was expected. None was found.

LEVEL STRUCTURE OF Cr^{52}. R. R. Wilson, A. A. Bartlett, J. J. Kraushaar, J. D. McCullen,* and R. A. Ristinen, Department of Physics, University of Colorado, Boulder, Colorado (Received July 31, 1961; revised manuscript received November 22, 1961).

The low excited states of Cr^{52} have been investigated by studying the decay of Mn^{52} using scintillation spectrometers and a double-focusing beta-ray spectrometer. In addition to the three strong lines at 0.74, 0.94, and 1.43 Mev, a number of weak transitions have been observed that require the addition of at least one new level at 3.614 Mev and which yield information on the spins and parities of the various levels. The following gamma rays have been observed: 1.434 Mev (100%), 1.332 Mev (5.7%), 1.246 Mev (5.8%), 1.214 Mev (2.9%), 0.935 Mev (83.9%), 0.847 Mev (2.6%), 0.744 Mev (81.9%), and 0.346 Mev (0.9%), in addition to several weaker and more uncertain lines. A decay scheme has been constructed which consists of levels at 1.434 Mev (2+), 2.369 Mev (4+), 2.648 Mev, 2.766 Mev (4+), 3.112 Mev (6+), 3.161 Mev (1, 2, 3), 3.614 Mev (5+, 6+), and 3.832 Mev (5+, 6+). A comparison has been made between the experimentally determined level structure and several theoretical calculations.

Mn^{54} (290 day) was present in the Mn^{52}. The energy of the Mn^{54} gamma-ray transition was determined to be 834.9 ± 1.1 kev.

*Now at Princeton University, Princeton, New Jersey.

MOMENTUM DISTRIBUTIONS FOR PROTONS IN Li^6 IN THE CLUSTER MODEL. J. Strnad, Physical Institute of University and J. Stefan Institute, Ljubljana, Yugoslavia (Received October 16, 1961).

The momentum distributions for protons with two different binding energies as measured in quasi-elastic scattering on Li^6 are calculated in a simplified cluster model. It is assumed that clusters in nuclei are well separated and cluster-model wave functions which are not antisymmetrized are used. The simplification seems to be justifiable in this case. With the cluster-model wave functions of Pearlstein, Wildermuth, and Tang, experimental data from quasi-elastic scattering of protons on Li^6 can be reproduced, whereas this could not be achieved with the simple shell model.

LOW-ENERGY PROTON PRODUCTION BY 160-Mev PROTONS. Raymond Fox* and Norman F. Ramsey, Cyclotron Laboratory, Harvard University, Cambridge, Massachusetts (Received October 11, 1961).

Energy and angular distributions of emitted protons in the energy range 5 to 23 Mev from lead, tantalum, tin, and zinc when bombarded by 160-Mev protons were obtained. A peak was obtained in each of the energy distributions slightly below the Coulomb barrier of each element. The magnitude of the peaks increased with a decrease in the Coulomb barrier of the element. The angular dependence of the heights

of the peaks for all of the elements was approximately isotropic. The angular distributions of the emitted protons with energies above the Coulomb barrier increased in the forward direction. The results are compared with previous related experiments and possible sources of disagreement are discussed.

*Now at the Lawrence Radiation Laboratory, University of California, Livermore, California.

NEUTRON INDUCED FISSION OF Pu^{241}. H. L. Smith, R. K. Smith, and R. L. Henkel, Los Alamos Scientific Laboratory, University of California, Los Alamos, New Mexico (Received October 9, 1961).

The neutron-induced fission cross section for Pu^{241} was measured at neutron energies between 0.25 and 21 Mev. The fission excitation function is similar to other even-odd fissionable nuclei and shows a cross section of 1.68 ± 0.08 barns at 3 Mev. A rough correlation is developed from fission systematics which allows predictions of 3-Mev cross sections. U^{235} fission cross section values between 10 and 21 Mev (previously unpublished) are also tabulated.

INTERNAL BREMSSTRAHLUNG SPECTRUM ACCOMPANYING 1S ELECTRON CAPTURE IN DECAY OF Fe^{55}, Cs^{131}, and Ti^{204}. M. H. Biavati, S. J. Nassiff,* and C. S. Wu, Columbia University, New York, New York (Received October 2, 1961).

The internal bremsstrahlung spectra in coincidence with the K x rays resulting from 1S electron capture in Fe^{55} and Cs^{131} have been measured. The results are in good agreement with Martin and Glauber's revised calculations including relativistic and screening effects. The shape of the coincidence spectra exhibits a maximum at the predicted energy and then drops off in intensity toward the low-energy region. This is markedly different from that of the total bremsstrahlung spectrum which rises continuously toward the low-energy region. In the case of Cs^{131}, the shape of the bremsstrahlung spectrum pertaining to the radiative capture of P electrons as obtained by subtracting from the total spectrum the spectrum due to S-electron capture is also in good accord with that predicted. An estimate of the total probability for bremsstrahlung production during 1S electron capture as obtained by comparing the corresponding bremsstrahlung spectrum with the x-ray intensity gives for Fe^{55} $(1.5 \pm 0.8) \times 10^{-5}$ and for Cs^{131} $(1.4 \pm 1) \times 10^{-5}$, which is in fair agreement with the theoretical prediction including relativistic corrections. The end point of the 1S electron capture bremsstrahlung spectrum of Tl^{204} was also measured and found to be 310 ± 10 kev.

*Now at Comision Nacional de Energia Atomica, Buenos Aires, Argentina.

CONVERSION-ELECTRON ANGULAR CORRELATIONS FOR STRIPPING REACTIONS. Eugene V. Ivash, Department of Physics, University of Texas, Austin, Texas (Received October 2, 1961).

The $(d, p; e)$ and $(d, n; e)$ angular correlation between the outgoing proton or neutron of a stripping reaction and a possible internal conversion electron, is theoretically investigated. Expressions for the correlation function similar to those for $(d, p; \gamma)$ and $(d, n; \gamma)$ angular correlations are obtained, differing only in the presence of the particle parameters $b_\nu(LL'; e)$. It is suggested that conversion-electron correlations for stripping reactions may prove useful as a nuclear spectroscopic tool for the heavier nuclei.

COULOMB EXCITATION OF LEVELS IN Se^{77}. R. L. Robinson, F. K. McGowan, and P. H. Stelson, Oak Ridge National Laboratory, Oak Ridge, Tennessee (Received October 13, 1961).

An investigation has been made of the gamma rays which de-excite levels of Se^{77} that have been Coulomb excited by means of variable-energy alpha particles (2.1 to 8.0 Mev). The energies (in kev), spins and parities, and $B(E2)_{ex}$'s (in units of $e^2\ cm^4 \times 10^{-50}$) found for the levels are: 242 ± 2, 3/2-, and 18.2 ± 1.6; 248 ± 5, 5/2-, and 0.37 ± 0.09; 440 ± 4, 5/2-, and 25.9 ± 1.7; and 515 ± 8, 3/2-, and 1.0 ± 0.2. New evidence for the two close-lying levels at 242 and 248 kev has been provided by coincidence studies. A comparison of the $B(E2)_{ex}$'s to the $B(E2)_{sp}$ suggests that the 242- and 440-kev levels result from collective excitations of the ground-state configuration, and that the 248- and 515-kev levels result from changes in the ground-state configuration. Be-

sides the ground-state transitions from these Coulomb-excited levels, gamma rays with energies of 87, 161, 203, and 283 kev were observed. Excitation curves of the 87- and 161-kev transitions indicate that they cascade from the 248-kev level. From the measurements of the gamma-ray angular distributions, values for $(E2/M1)^{1/2}$ of 0.18 ± 0.03 and 0.05 ± 0.03 were obtained, respectively, for the 242-kev gamma ray and for the 203-kev gamma ray, which originates at the 440-kev level.

ALPHA PARTICLES FROM Be^9 AND C^{12} BY 25-Mev ALPHA-PARTICLE BOMBARDMENT. Lynn B. Brown and H. B. Knowles, Lawrence Radiation Laboratory, University of California, Livermore, California (Received October 12, 1961).

Alpha-particle spectra from thin beryllium and carbon targets have been taken at 47.5° laboratory angle, and an alpha energy of 25.41 Mev. The center-of-mass spectra of both nuclei indicate that the four-body reactions $Be^9(\alpha; 3\alpha, n)$ and $C^{12}(\alpha; 4\alpha)$ are greatly preferred over the three-body reactions $Be^9(\alpha; \alpha, n)Be^8$ and $C^{12}(\alpha; 2\alpha)Be^8$. Several inelastic levels of both nuclei appear, and the recoil-decay alpha particles from the 9.61-Mev level of C^{12*} are seen. The Fermi statistical model is invoked in an attempt to establish that the multibody reactions are reasonably representative of the proportions of the two- and three-cluster configurations in the ground states of the two nuclei, and that the three-cluster configurations are preferred.

CROSS SECTIONS FOR THE $B^{11}(n,\gamma)B^{12}$ REACTION. W. L. Imhof, R. G. Johnson, F. J. Vaughn, and M. Walt, Lockheed Missiles and Space Company, Research Laboratories, Palo Alto, California (Received October 2, 1961).

Cross sections for the reaction $B^{11}(n,\gamma)B^{12}$ were measured by an activation technique for neutron energies from 139 kev to 2325 kev and at thermal energy. Resonances in the reaction were observed at neutron energies of 430 kev, 1030 kev, 1280 kev, and 1780 kev. Since the resonance at 1030 kev did not correspond to a known level in B^{12}, the total neutron cross section for boron was measured with 4-kev resolution in the neutron energy region between 950 kev and 1350 kev. An S-wave resonance was observed in the total cross section at 1027 ± 10 kev. This resonance corresponds to a level in B^{12} at an excitation energy of 4.31 Mev; it most probably has spin and parity of 1^-, and a width of 10 ± 4 kev. From an analysis of the capture cross-section resonances, the radiation widths of the levels were found to be 0.3 ev at 430 kev, 0.3 ev at 1027 kev, 0.2 ev at 1280 kev, and 0.9 ev at 1780 kev, with estimated uncertainties of 50%. The measured value of the $B^{11}(n,\gamma)B^{12}$ cross section for thermal neutrons was 5 ± 3 mb.

SIMPLE NUCLEAR REACTIONS OF Ga^{69} AND Ga^{71} WITH HIGH-ENERGY PROTONS. Norbert T. Porile, Chemistry Department, Brookhaven National Laboratory, Upton, New York (Received October 9, 1961).

Excitation functions in the energy range of 0.5-2.9 Bev have been measured for several (p,xn), (p,pxn), and $(p,3pxn)$ reactions of Ga^{69} and Ga^{71}. The cross section for the (p,pn) reactions are about 57 mb at 2.9 Bev and 69 mb at 0.5 Bev. The cross sections for the (p,pxn) reactions decrease monotonically as x increases and are some 30-250 times larger than the isobaric (p,xn) reaction cross sections. The results are compared with Monte Carlo cascade and evaporation calculations. Good agreement is obtained at 0.5 Bev except in the case of the (p,pn) reaction. In the Bev region the agreement is less widespread. The (p,pn) cross sections are compared with a calculation that takes the effects of shell structure and a diffuse nuclear surface into account. Some preliminary conclusions about the availability of the $1f_{7/2}$ shell for (p,pn) reactions in this mass region are drawn on the basis of this comparison.

HIGH-ENERGY INTERFERENCE EFFECT OF BREMSSTRAHLUNG PRODUCTION IN A SINGLE CRYSTAL OF SILICON. A. N. Saxena,* High-Energy Physics Laboratory, Stanford University, Stanford, California (Received September 18, 1961; revised manuscript received November 10, 1961).

In an experiment performed at Stanford to look for the interference effect of the bremsstrahlung production by 575-Mev electrons in a single crystal of silicon, the ratio of the charges collected in the two halves of a double ion chamber were

used to detect the enhancement of the soft component of the bremsstrahlung. The data, presented in the form of a three-dimensional plot of the ratio vs the angles of rotation between the lattice normal and the electron beam about the horizontal and the verticle axes, clearly showed the enhancement. Comparison of the experimental result and the theory showed good agreement. The resolution of this experiment was poor; hence the central minimum predicted by the theory could not be observed. This minimum, however, has been observed by Bologna et al. at Frascati.

*Now at the Research and Development Department, Fairchild Semiconductor Corporation, Palo Alto, California.

PRECISION MEASUREMENT OF THE μ^+ LIFETIME. Richard A. Lundy, Enrico Fermi Institute for Nuclear Studies, The University of Chicago, Chicago, Illinois (Received September 28, 1961).

A new precision measurement of the lifetime of the positive muon, $\tau(\mu^+)$, is described. On the basis of 12 internally consistent, independent determinations performed under a variety of experimental conditions we obtain $\tau(\mu^+) = (2.203 \pm 0.004)$ μsec. These determinations were performed by means of an improved version of Swanson's "digitron"—a digital electronic time interval measuring device—embodying a CW oscillator and several protective features. The available experimental conditions, in particular concerning the percentage of background events, were greatly superior to those available in earlier experiments here and elsewhere. Particular attention was paid to sources of systematic error, such as time dependence of background events and rate dependence of the over-all measuring process. All sources of background have been localized, their effects quantitatively exhibited and, in general, suppressed electronically during actual lifetime determinations.

The prediction of the conserved vector-current theory, using $ft(0^{14}) = (3069 \pm 13)$ sec and $m_\mu = 206.76\, m_e$, is (including radiative corrections) $\tau(\mu^+) = 2.298 \pm 0.05$ μsec, and thus in disagreement with the experimental value reported here. This discrepancy is even greater than with the somewhat higher values obtained for $\tau(\mu^+)$ by other workers; these values are briefly reviewed.

A full discussion of the logical operation of the digitron, and of time-interval measuring devices in general, is presented. In Appendix I a general formalism is given which establishes the connection between arbitrary interval distributions presented at the input of such devices and their corresponding output interval distributions.

PROPERTIES OF Σ DECAYS AND THE Σ^0 LIFETIME. J. Dreitlein* and H. Primakoff, Department of Physics, University of Pennsylvania, Philadelphia, Pennsylvania (Received July 18, 1961).

The consequences of a possible nonconservation of parity in the electromagnetic decay, $\Sigma^0 \to \Lambda^0 + \gamma$, are deduced and an experimental test of parity conservation is proposed. In order to devise a method to determine the Σ^0 lifetime, $\tau(\Sigma^0)$, a study is made of $\Lambda^0 \to \Sigma^0$ conversion in Λ^0-nucleus collisions and it is found that the $\Lambda^0 \to \Sigma^0$ conversion induced by the nuclear Coulomb field, with cross section proportional to $Z^2/\tau(\Sigma^0)$, is the dominant process at large Z for Σ^0 generation in approximately forward directions. In addition, the implications of a principle of "minimal weak coupling" (involving a conserved baryon-meson polar-vector current) are exhibited for $\Sigma^\pm \to \Lambda^0$ strangeness-conserving leptonic decays and are used to propose a further conceivable method to determine the Σ^0 lifetime. Throughout the discussion, the various cross sections and decay rates are given for the two possible relative intrinsic parities of the Λ^0 and Σ^0.

*Present address: Stanford University, Stanford, California.

SINGLE VIRTUAL PARTICLE EXCHANGE MODEL OF HIGH-ENERGY INELASTIC GLANCING COLLISIONS. Freda Salzman* and George Salzman,† Department of Physics, University of Colorado, Boulder, Colorado (Received August 15, 1961).

A general formulation, based upon the ideas of field theory, is given for the single virtual particle exchange model of high-energy inelastic glancing or "peripheral" collisions. The main assumption of the model is that there is a region of the final-state phase space in which the cross section is dominated by single virtual particle exchange graphs of a particular kind. A general discussion is given of the kinematics and of the region of applicability of the model. It is shown that, unlike the situation in elastic scattering, inelastic

processes can occur with timelike momentum transfer, and an example in which this happens is discussed. The region in which it appears most reasonable to use the model is that characterized by final states which consist of two well-defined groups of particles. An argument based on unitarity is given which strongly suggests that the energy dependence of this part of the peripheral nucleon-nucleon cross section is less than logarithmic at very high energies.

*On leave of absence during the 1961-62 academic year at the University of Rome, Rome, Italy.

†On leave of absence during the 1961-62 academic year at the Italian National Laboratory, Frascati, Italy.

DETERMINATION OF THE COUPLING STRENGTH OF ρ MESONS AND NUCLEONS. P. Burt and W. K. R. Watson,* Jet Propulsion Laboratory, California Institute of Technology, Pasadena, California (Received October 6, 1961).

Consideration of pion-nucleon elastic scattering in the forward direction at high energies indicates a possible method of determining the coupling strength of the ($I=1$, $J=1$) two-pion resonance (ρ meson) with nucleons for zero momentum transfer. As a specific example, we consider the case of π^-, p elastic scattering and show that $g^2\rho_{NN}/4\pi\hbar c \simeq 0.2$.

*Present address: University of California, Riverside, California.

SPIN SUSCEPTIBILITY OF NORMAL FERMION SYSTEMS. Ronald M. Rockmore, Department of Physics, Brandeis University, Waltham, Massachusetts and The RAND Corporation, Santa Monica, California (Received September 20, 1961).

The calculation of the induced spin density of a normal fermion system, such as the electron gas in the limit of small wave numbers, is carried beyond the random phase approximation (R.P.A.) by the method of canonical transformation so as to include the first non-R.P.A. corrections. An expression for the induced spin density in the same limit exact to all orders of particle-particle coupling is then derived by more general methods of many-body perturbation theory. It depends only on the knowledge, to all orders of interparticle coupling, of the effective mass and the forward scattering of quasi-particles at the Fermi surface, and also yields the results of the extended R.P.A. on appropriate expansion. In the limit of zero wave number, the resulting expression for the magnetic susceptibility is found identical with that deduced by Landau from a phenomenological basis and may be regarded as an additional confirmation of the microscopic validity of the theory of the Fermi liquid.

ISOBAR MECHANISM FOR PION-BARYON HIGHER RESONANCES. San Fu Tuan, Department of Physics, Brown University, Providence, Rhode Island (Received October 9, 1961).

Peierls' isobar mechanism is extended to pion-hyperon interactions on the assumption that Y_1^* is the $\pi\Lambda$ isobar whose mass lies below the $\bar{K}N$ threshold and of spin parity $P_{3/2}$. It is shown that this mechanism, when combined with experimental data currently available, does suggest that a pion-hyperon resonance in the $I=1$ channel at c.m. energy 1645 Mev with spin-parity assignment $D_{3/2}$ is possible. This resonance state is expected to reflect in the total K^--p and K^--n (pure $I=1$) cross sections as resonance peaks centered at around 685-Mev/c K-meson lab momentum. Experimental implications of this isobar model for pion-baryon interactions as well as certain mathematical difficulties associated with the over-all validity of such a mechanism are also discussed.

RENORMALIZATION OF QUANTUM ELECTRODYNAMICS IN A CLASSICAL GRAVITATIONAL FIELD. Ryoyu Utiyama,* Institute of Field Physics, University of North Carolina, Chapel Hill, North Carolina (Received August 10, 1961).

The divergences of the Green's functions of electrons and photons in a classical gravitational field are investigated and are found to be removable by the introduction of suitable counter terms into the Lagrangian. These counter terms are obtained by rewriting the conventional renormalization technique in a generally covariant way. It is shown that infinite renormalization constants identical to those appearing in conventional quantum electrodynamics are sufficient for the removal of all divergences also when a gravitational field is present. No other renormalization is necessary. The segregation of the divergences is accomplished by making use of the transformation properties of the Green's functions under (i) general coordinate transforma-

tions, (ii) Vierbein rotations, and (iii) gauge transformations.

*On leave of absence from Osaka University, Osaka, Japan.

GROUND-STATE ENERGY OF THE NUCLEON. Richard J. Drachman, Brandeis University, Waltham, Massachusetts (Received June 23, 1961).

Halpern's method of moments has been applied to the intermediate-coupling reduced Hamiltonian, whose lowest eigenvalue is a variational upper bound to the ground-state energy of the nucleon in the fixed-source model of meson theory. The results compare favorably with an earlier intermediate-coupling calculation of Friedman, Lee, and Christian, and agree with direct moment-method results. A discussion of the relationship between the present work and a Tamm-Dancoff approximation for the reduced Hamiltonian is included.

MINIMUM PRINCIPLE FOR MULTICHANNEL SCATTERING. Leonard Rosenberg* and Larry Spruch, Physics Department, Washington Square College and Institute of Mathematical Sciences, New York University, New York, New York (Received October 4, 1961).

The usual variational principles of scattering theory are simply stationary principles. In a recent series of papers, all restricted to single-channel scattering, conditions were established under which variational principles can be found which are much more powerful in that the functional that represents the variational estimate is not simply stationary in the neighborhood of the exact scattering solution but is rather an extremum. A lower bound was obtained on the single real parameter, $\tan\eta_c$, which characterizes the scattering in the (uncoupled) channel c. The conditions previously established allowed for composite bound states, for the Pauli principle, for arbitrary angular momenta, and for long-range and in particular Coulomb potentials; at nonzero energies, the various potentials had to be truncated. The present paper deals with the extension to multichannel scattering in which each of the open channels contains only two systems. The bounds are now on linear combinations of the elements of the reactance matrix or of the derivative matrix. The potentials must be truncated in a fashion very similar to that used in Wigner-Eisenbud theory.

*Present address: Physics Department, University of Pennsylvania, Philadelphia, Pennsylvania.

EXTRAPOLATION TO CUTS AND THE SCATTERING OF ELECTRONS AND POSITRONS. S. D. Drell and R. H. Pratt, Institute of Theoretical Physics, Department of Physics, Stanford University, Stanford, California (Received August 28, 1961).

The low-momentum-transfer region of strong-interaction processes may be discussed in terms of one-pion-exchange graphs. This success of "extrapolation to poles" suggests, as an extension, "extrapolation to cuts" corresponding to low-mass intermediate states containing two or more particles. We find that this extrapolation may be performed in the case of electromagnetic interactions, owing to the vanishing photon mass. For small-angle scattering of relativistic electrons in a pure Coulomb field, $\sin^4(\theta/2)(d\sigma/d\Omega) = a_0 + a_1 \sin(\theta/2) + \cdots$, where a_0 is given precisely by the one-photon pole and a_1 (obtained exactly to all orders in $Z\alpha$) comes from the many-photon terms. For scattering by finite nuclei we further find that, for fixed momentum transfer, the ratio of second to first Born approximation decreases as $(\text{energy})^{-1}$ at high energies. This leads to a simple approximate formula for the ratio $R \equiv (\sigma_- - \sigma_+)/(\sigma_- + \sigma_+)$ of electron and positron scattering, and to a simple method of determining the charge form factors of intermediate-Z nuclei.

VECTOR MESONS AND NUCLEON-NUCLEON POTENTIALS. R. S. McKean, Jr., University of Washington, Seattle, Washington (Received September 18, 1961).

The role of the π-π resonances in the nucleon-nucleon force is considered on a model which treats these resonances as particle exchanges. The nucleon form factors are used to obtain the resonance parameters; thus the coupling constant of the "particles" to the nucleon are the only free parameters. It is found that the qualitative features of the central, spin-orbit, and tensor potentials in all states can be reproduced, except that the central repulsive core has too long a range. These results suggest that π-π effects

dominate rather than supplement the usual uncorrelated 2π, 3π contribution to the nucleon-nucleon force.

PERTURBATION THEORY OF PION-PION INTERACTION. I. RENORMALIZATION. Tai Tsun Wu, Gordon McKay Laboratory, Harvard University, Cambridge, Massachusetts and the Institute for Advanced Study, Princeton, New Jersey (Received October 9, 1961).

The problem of pion-pion scattering is studied on the basis of the model of a four-particle direct interaction without derivative coupling. Renormalization is carried out for this model with a detailed analysis of overlap insertions. To every finite order in the renormalized coupling constant, it is shown that the unitarity relation holds and that the Feynman integral representation is still valid, and hence renormalization has no effect on analytic properties.

ACNODES FOR PION-NUCLEON SCATTERING. Francis R. Halpern, University of California, San Diego, La Jolla, California (Received October 2, 1961).

An implicit expression is found for the occurrence of acnodes on the Landau curves of a certain fifth order Feynman diagram. These acnodes are investigated in cases in which the lines of the graph are either pions or nucleons and in these cases are shown to give no singularities on the physical sheet. To find the Landau curves, the internal momentum vectors of the diagram have been parameterized.

PHYSICAL REVIEW
LETTERS

VOLUME 7 DECEMBER 15, 1961 NUMBER 12

BETA-GAMMA PHASE TRANSFORMATION IN SOLID He^3

J. P. Franck*
Division of Pure Physics, National Research Council, Ottawa, Canada
(Received November 14, 1961)

It was reported recently by Schuch and Mills[1] that solid He^3 at a temperature of about 18.75°K and close to the melting line has a face-centered cubic structure. This new phase has been designated the γ phase. It was obvious from this result that solid He^3, like solid He^4,[2,3] must exhibit a phase transformation from the hexagonal close-packed β phase to face-centered cubic structure. In this laboratory we are currently carrying out measurements of the specific heat of He^3 and He^4 at high densities in the temperature range 3 to 30°K. As part of this program a calorimetric investigation of the β-γ phase transformation in solid He^3 was made. From this the β-γ phase boundary close to its intersection with the melting line was established. In addition the latent heat of transformation was obtained. Both results were used in order to calculate the change in entropy and molar volume upon transformation.

The apparatus used is an adiabatic calorimeter suitable for operation in the temperature range 3 to 30°K. The helium sample is contained in a steel cell of 1.48-cm^3 volume. The cell is connected through a steel capillary of 0.1-mm bore to a high-pressure Toepler pump. A second capillary of the same bore leads to a small coil which is used as a rough pressure indicator. The helium is usually compressed into the cell near 20°K to the required density. The calorimeter is then rapidly cooled below the freezing temperature. While taking measurements both capillaries are thermally anchored to a liquid helium bath. In this way the capillaries are blocked by a plug of solid helium. The measurements are therefore made at virtually constant volume.

Temperatures are measured with an Allen-Bradley carbon resistor which is calibrated against the vapor pressures of hydrogen and helium near their normal boiling points. Clement's two-constant interpolation formula[4] is used. It is known[5] that this formula leads to deviations from true temperature of the order of 0.01°K near 18°K.

The transformation was investigated in two helium samples of different molar volume. As the samples were held at constant volume melting took place over a finite temperature interval. The temperatures at the onset of melting, T_m, could be obtained from heating curves and were used for characterizing the samples. From this temperature the pressure P_m at the onset of melting and the molar volume V could be calculated by using the data of Grilly and Mills[6,7] (see Table I). The amount of helium in the cell was calculated from V and the calibrated cell volume. The temperatures of the phase transition was obtained by taking heating curves at constant energy input. A typical example is shown in Fig. 1. The transition temperature was taken at the point where the heating curve first deviates from a straight line. Thermal as well as instrumental relaxation probably obscured the natural width of the transition. Several determinations were made for each sample; the results are listed separately in Table I.

The specific heat of both samples was determined in the vicinity of the transition temperature. It was found that the specific heat below and above the transition forms a continuous curve within the experimental error of about 1%. The Debye temperatures θ_D at the transition are 105.7°K for sample 1 and 109.2°K for sample 2.

Table I. Transition temperature T_{tr}, latent heat L, and transition pressure P_{tr} for βHe^3 - γHe^3.

Sample	T_{tr}, °K	L, cal/mole	P_{tr}, atm
No. 1	17.803	0.068	
T_m = 17.95°K	17.803	0.071	
P_m = 1629.1 atm	17.778	0.061	
V = 11.70 cm³/mole	17.815		
Average:	17.800 ±0.015	0.067 ±7%	1626.8
No. 2			
T_m = 18.67°K	17.879	0.065	
P_m = 1728.5 atm	17.877	0.068	
V = 11.56 cm³/mole		0.067	
Average:	17.878 ±0.015	0.067 ±2%	1715.7

In addition to this, the average specific heat was measured for temperature intervals that included the complete phase transition. The heating intervals were varied between 0.15 and 0.27°K. An additional heat capacity, when compared with the interpolated specific heat from outside the transition, was observed in these intervals and attributed to the latent heat of transition. The results of all determinations are listed separately in Table I. As the latent heat L is determined as a difference of two big quantities, the scatter in L is rather large.

The pressure P_{tr} at the transition temperature T_{tr} can be obtained from the pressure at the onset of melting by the relation:

$$P_{tr} - P_m = \int_{T_m}^{T_{tr}} (\partial P/\partial T)_V dT = \int_{T_m}^{T_{tr}} (\partial S/\partial V)_T dT.$$

This makes use of a Maxwell thermodynamic relation and the quantity $(\partial S/\partial V)_T$ is known experimentally. The difference $P_{tr} - P_m$ is -2.3 atm for sample 1 and -12.8 atm for sample 2.

The phase diagram in the pressure-temperature plane is given in Fig. 2. Here the melting line is taken from the data of Grilly and Mills.[7] The intersection of the β-γ phase boundary with the melting line is found at $T = 17.780 \pm 0.015$°K and $P = 1608 \pm 2$ atm. The slope of the phase boundary

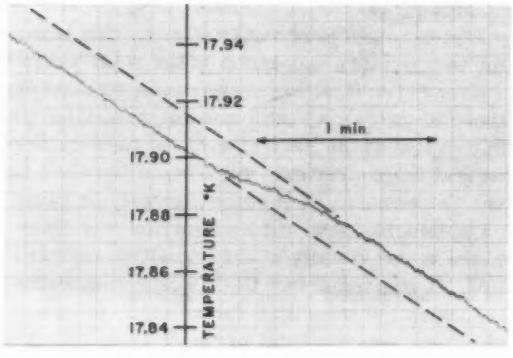

FIG. 1. A heating curve showing the β-γ transition in solid He^3 at a molar volume of 11.56 cm³/mole.

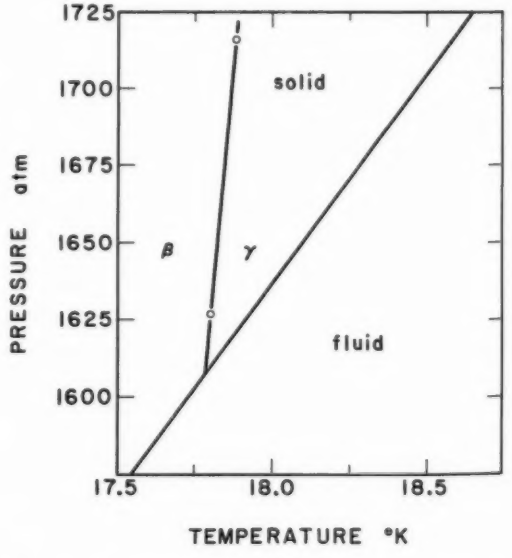

FIG. 2. The phase diagram of He^3 in the vicinity of the β-γ transition.

is $dP/dT = 1140$ atm/deg.

The change of entropy ΔS and of molar volume ΔV upon transformation can be derived from the Clausius-Clapeyron equation using the experimentally determined values of dP/dT, L, and T_{tr}. This gives $\Delta S = 0.0041$ cal/mole deg, and $\Delta V = 1.4_8 \times 10^{-4}$ cm^3/mole. ΔV constitutes $1.2_7 \times 10^{-3}$% of the molar volume.

It may be added that the corresponding transition in solid He^4 (αHe^4 - βHe^4) has also been observed in a previous experiment with this apparatus. The transition occurred at 14.99°K for a sample of molar volume 11.77 cm^3/mole. The latent heat of transition was 0.060 cal/mole.

The author wishes to acknowledge the constant help and encouragement received from Dr. J. S. Dugdale.

---

*National Research Council Postdoctorate Fellow.

[1]A. F. Schuch and R. L. Mills, Phys. Rev. Letters 6, 596 (1961).

[2]J. S. Dugdale and F. E. Simon, Proc. Roy. Soc. (London) A218, 291 (1953).

[3]R. L. Mills and A. F. Schuch, Phys. Rev. Letters 6, 263 (1961).

[4]J. R. Clement, in Temperature, Its Measurement and Control in Science and Industry (Reinhold Publishing Corporation, New York, 1955), Vol. 2, p. 380.

[5]J. P. Franck and D. L. Martin, Can. J. Phys. 39, 1320 (1961).

[6]R. L. Mills and E. R. Grilly, Phys. Rev. 99, 480 (1955).

[7]E. R. Grilly and R. L. Mills, Ann. Phys. 8, 1 (1959).

PRECISE OBSERVATION OF THE PROFILE OF THE FRAUNHOFER STRONTIUM RESONANCE LINE. EVIDENCE FOR THE GRAVITATIONAL RED SHIFT ON THE SUN

J. E. Blamont and F. Roddier

Service d'Aéronomie, Observatoire de Meudon, Seine et Oise, France

(Received November 15, 1961)

We wish to report a measurement of the profile of the solar strontium resonance line $^1P_1 - {}^1S_0$, 4607.3 A, by a method permitting high resolution. Observation of this profile on the limb of the Sun as well as the center of the disk permits an unambiguous separation of wavelength shifts caused by mass motion on the Sun and the gravitational red shift. The shift attributable to the relativistic effect is found to be very close to the theoretical value. The success of this observation of the red shift is due to the fact that in this experiment atoms are used as a clock both on the Sun and the Earth. This removes errors made in wavelength calibration.

In our method of spectroscopic analysis the light to be analyzed excites the optical resonance of the vapor of a metal. The intensity of the light reemitted by the vapor, proportional to the incident intensity, is measured at right angles to the exciting beam by a photomultiplier. The scattering frequency is shifted by applying a magnetic field to the vapor. The variation in intensity of the reemitted light as a function of the field gives the profile of the exciting light. We have used this method on the D lines of sodium of the twilight glow,[1] the study of sources in the laboratory,[2] the fluorescence of the Moon and Venus,[3] and the detection of the dayglow.[4]

In order to study the profile, it is necessary to use only one component (through a circular analyzer) of a resonance line with normal Zeeman effect and without hyperfine structure. We have operated on an atomic beam of strontium in order to minimize the width of the absorption line. This beam and the discussion of its use on solar light have been discussed earlier.[5]

The strontium (Fig. 1) is placed in a steel vessel heated to 600°C in a silica tube, water-cooled at the end. Two diaphragms delimit the beam whose half-aperture ratio is $\frac{1}{20}$. The metal beam passes through an observation chamber where it is excited by a light beam of half-aperture-angle $\frac{1}{20}$. The excitation can be caused by a white light source or by the light coming from an image of the Sun, of diameter 11 cm, formed by an objective of 30-cm diameter. The angle used on the Sun varies from 30″ to 1′. A mirror is used to observe the light emitted parallel to the magnetic axis; the half-angle of observation is $\frac{1}{10}$ in order to remove mixing with π components. Stray light is measured with the metal beam turned off. The ratio of intensity of stray light to resonance light is 1 to 3; of resonance light to noise, 20 to 1.

The beam geometry is such that the Doppler

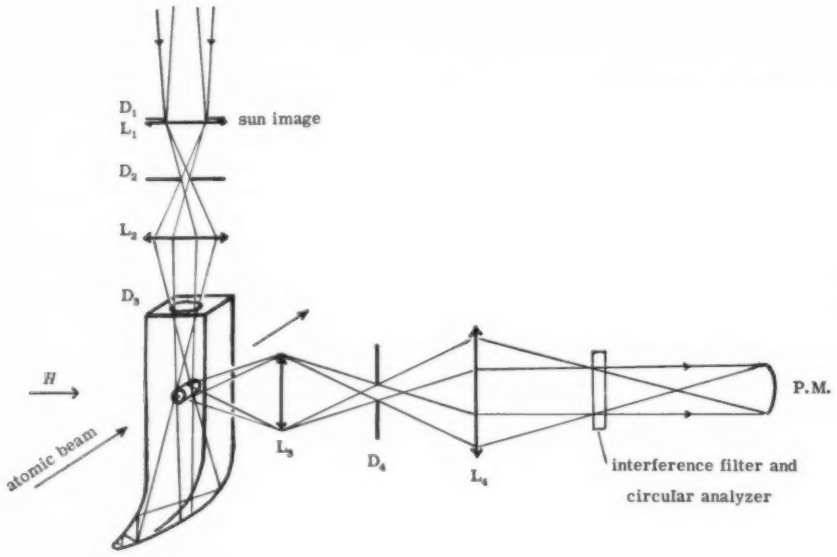

FIG. 1. Schematic diagram of the experiment. D_1: diaphragm defining a part of the solar image; D_2, D_3, D_4: diaphragms removing the stray light; L_1, L_2, L_3, L_4: converging lenses.

shape of the absorption line has a theoretical width of 8×10^{-4} A. But at an oven temperature of 550°C and above, the width of the profile is increased to 10^{-3} A at 550°C and 2×10^{-3} A at 640°C by self-absorption of the light in the dense beam. We have traced a curve of growth (re-emitted energy as a function of the beam density for white light excitation) and conclude that at our temperature we explore the solar spectrum with a saturated profile of (1 to 2)$\times10^{-3}$ A half-width.

When the beam is excited by a white source, the intensity re-emitted would be invariant with the field if the beam were optically thin. This is not the case and because of multiple scattering effects which we have discussed elsewhere,[4] the intensity varies with the field. The response of the beam has to be calibrated with a white light source before any spectrum is taken. Solar observations have been corrected for this white light effect, measured in every experiment since it depends on the beam density. The order of magnitude of the effect is 5 to 10% for 10^4 gauss.

At the center of the solar disk, the intensity at the line bottom is 40% of the continuum intensity, just reached at 10^4 gauss, much less than the 60% indicated by the Utrecht Atlas. The line is strongly asymmetrical; the line shape varies from day to day due to observation of different solar regions, but the axis of the line (middle of horizontal chords) is extremely regular [Fig. 2(a)]. The indicated shifts towards the red are corrected for relative motions of the earth. Observed fluctuations around the given values can amount to 10^{-3} A. The theoretical value of the gravitational red shift is 9.76×10^{-3} A. The observed shift at the bottom is very near the relativistic value.

At the limb of the solar disk (1′ of arc from the edge) the intensity at the bottom is 55% of the continuum intensity. The line axis has a completely different shape than at the center [Fig. 2(b)]. At the line bottom the axis stays vertical at a constant value shifted towards the red by 12×10^{-3} A. This value finds a complete interpretation if we add to the mentioned relativistic shift the pressure red shift of the Lindholm effect. Lindholm's theory,[6] good enough for a resonance line, predicts a shift of 2.4×10^{-3} A for the considered line with $T = 5700$°K and 10^{17} hydrogen atoms/cm^3. The theoretical red shift is thus 12.16×10^{-3} A which is exactly the experimental value.

This means that at the center of the disk the measurements are affected by a third effect, a violet shift, which may be due to convective motions. This effect taking place at a certain depth is naturally displaced towards the continuum for the limb observations. If we superpose center and limb profiles, keeping the ratio of intensities constant, the two axes coincide on some interval. This asymmetry has been predicted by Schröter[7] in a model which reduces the photosphere to a mixture of hot ascending and cool descending currents whose speeds vary with altitude. The line

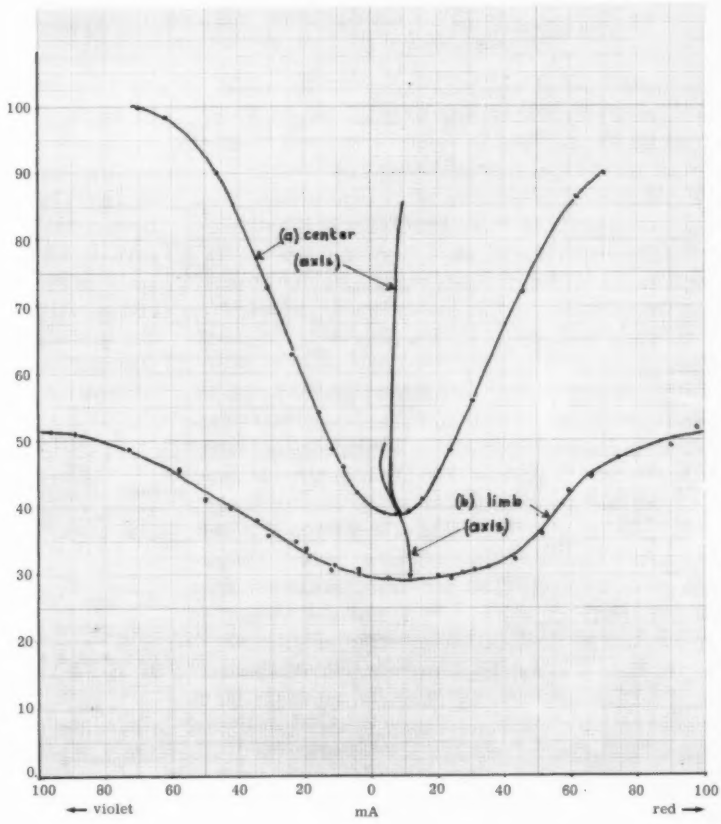

FIG. 2. Two profiles obtained August 5, 1961, between 16.00 and 17.00 U.T. (a) Center of the disk; (b) at 1′ from the limb.

shape of a group of spots has been obtained and exhibits elaborate structure due to Zeeman effect.

[1]J. E. Blamont, Compt. rend. 237, 1320 (1953).
[2]M. Babillot, Diplôme d'Etudes Supérieures, University of Paris, 1961 (unpublished).
[3]J. E. Blamont, Ann. Astrophys. (to be published).
[4]J. E. Blamont and T. M. Donahue, Compt. rend. 251, 2750 (1960); J. Geophys. Research 66, 3099 (1961).
[5]F. Roddier, Diplôme d'Etudes Supérieures, University of Paris, 1960 (unpublished).
[6]E. Lindholm, Arkiv Mat. Astron. Fysik 28B, No. 3 (1942).
[7]E. Schröter, Z. Astrophys. 41, 141 (1956).

GRAVITATIONAL INSTABILITY OF A MAGNETIZED PLASMA

B. Lehnert
Royal Institute of Technology, Stockholm, Sweden
(Received October 26, 1961; revised manuscript received November 30, 1961)

The instability of a plasma which is supported under gravity by a magnetic field has earlier been studied by Kruskal and Schwarzschild[1] and by Rosenbluth and Longmire[2] who found that density perturbations were growing at an exponential rate. Later investigations[3,4] indicated that the instability could be suppressed, or at least reduced in its growth rate, for sufficiently small density gradients. A different mechanism for its suppression has recently been based on the effects of the finite Larmor radius.[5]

In the present report the problem will be reconsidered in terms of the fluid equations. We assume a two-dimensional case with a homogeneous, magnetostatic field $\vec{B}$ in the z direction of a rectangular coordinate system, a homogeneous gravitational field $\vec{g}$ in the y direction, and a plasma with the unperturbed density distributions of ions and electrons given by $N(y)$. The perturbed densities of ions and electrons are $n_i = N + \tilde{n}_i$ and $n_e = N + \tilde{n}_e$, where $\tilde{n}_i$ and $\tilde{n}_e$ are small compared to N. The electric field $\vec{E}$ consists of the unperturbed part $\vec{E}_0$ and the perturbation $\tilde{E}$. Ions and electrons are assumed to have mass velocities $\vec{v}_i$ and $\vec{v}_e$ situated in the xy plane.

Among the approximations to be made the inertia of electrons will be neglected since the electron mass m_e is much smaller than the ion mass m_i. The center of mass of the plasma is assumed to be at rest in the unperturbed state and only small mass velocities of the ions are considered where $(\vec{v}_i \cdot \vec{\nabla})\vec{v}_i$ is unimportant. Further, we assume small ratios between particle pressure and "magnetic pressure" and small characteristic velocities compared to the speed of light c in such a way that W_i and $W_e \ll V_A \ll c$, where W_i and W_e are the thermal velocities of ions and electrons and V_A is the Alfvén velocity. Then, the influence of the induced magnetic field on the drifts of the density distributions is negligible and the electric field can be expressed by $\vec{E} = -\vec{\nabla}\phi$. We also assume the characteristic length $|N/N'|$ (with $N' \equiv dN/dy$) of the unperturbed density to be much larger than the characteristic lengths $L_x = 2\pi/k_x$ and $L_y = 2\pi/k_y$ of the density perturbation, which in their turn should be much larger than the ion and electron Larmor radii ρ_i and ρ_e. Finally, the unperturbed thermal velocity spectra of ions and electrons are supposed to be peaked around the constant values W_{i0} and W_{e0} and to give rise to scalar pressures $\frac{1}{2} m_i W_{i0}^2 N$ and $\frac{1}{2} m_e W_{e0}^2 N$ which are isotropic in the xy plane. Collisions are neglected. The equivalent magnetic moment of a gyrating particle is then constant at least in first order[6] in the ratios $\rho_i(1/L_x + 1/L_y)$ and $\rho_e(1/L_x + 1/L_y)$. Since B is constant, the "thermal" energies $\frac{1}{2} m_i W_i^2$ and $\frac{1}{2} m_e W_e^2$ as well as ρ_i and ρ_e will then also be constant in the same order in the perturbed state.

With these starting points, conservation of matter and momentum is expressed by

$$\partial n_i/\partial t + \operatorname{div}(n_i \vec{v}_i) = 0; \quad \partial n_e/\partial t + \operatorname{div}(n_e \vec{v}_e) = 0, \tag{1}$$

and

$$n_i \vec{v}_i = n_i \vec{E} \times \vec{B}/B^2 + m_i n_i \vec{g} \times \vec{B}/eB^2 - \vec{\nabla} p_i \times \vec{B}/eB^2 - m_i n_i (\partial \vec{v}_i/\partial t) \times \vec{B}/eB^2; \tag{2}$$

$$n_e \vec{v}_e = n_e \vec{E} \times \vec{B}/B^2 - m_e n_e \vec{g} \times \vec{B}/eB^2 + \vec{\nabla} p_e \times \vec{B}/eB^2, \tag{3}$$

where the scalar pressures are $p_i = \frac{1}{2} m_i W_i^2 n_i$ and $p_e = \frac{1}{2} m_e W_e^2 n_e$. Off-diagonal elements of the pressure tensor which arise from the perturbation have been neglected in Eqs. (2) and (3).

From Maxwell's equations we obtain

$$\operatorname{curl} \vec{B}/\mu_0 = e(n_i \vec{v}_i - n_e \vec{v}_e) + \epsilon_0 (\partial \vec{E}/\partial t), \tag{4}$$

where μ_0 is the magnetic permeability and ϵ_0 the dielectric constant in vacuo. A divergence operation on Eq. (4) yields in combination with Eq. (1)

$$\tilde{n}_i - \tilde{n}_e = -(\epsilon_0/e)\vec{\nabla}^2 \phi, \tag{5}$$

when $\tilde{n}_i - \tilde{n}_e$ and $\vec{\nabla}^2\phi$ are supposed to vanish in the initial state.

The unperturbed electric field is determined from Eqs. (2) and (3) and the condition that the center of mass should be at rest:

$$\vec{E}_0 = (m_i W_{i0}^2/2eN)\vec{\nabla}N - m_i \vec{g}/e, \tag{6}$$

when the thermal energy of electrons does not exceed that of ions very much. An electromagnetic force $eN(\vec{v}_{i0} - \vec{v}_{e0}) \times \vec{B}$ balances the gravitation and pressure forces in the unperturbed state,

where $\vec{v}_{i0}$ and $\vec{v}_{e0}$ are corresponding mass velocities.

The drift motion and compression of the density distributions can now be determined[4] from a divergence operation on Eqs. (2) and (3) in combination with Eqs. (1) and (6). If terms up to second order are retained,

$$-\frac{\partial \tilde{n}_i}{\partial t}=\frac{N'}{B}\frac{\partial \phi}{\partial x}+u_f\frac{\partial \tilde{n}_i}{\partial x}-\frac{\epsilon_i}{e}\vec{\nabla}^2\frac{\partial \phi}{\partial t}-\tfrac{1}{2}\rho_{i0}{}^2\vec{\nabla}^2\frac{\partial \tilde{n}_i}{\partial t}, \quad (7)$$

$$-\frac{\partial \tilde{n}_e}{\partial t}=\frac{N'}{B}\frac{\partial \phi}{\partial x}+(u_f-u_{ie})\frac{\partial \tilde{n}_e}{\partial x}, \quad (8)$$

with $u_f=\frac{1}{2}\rho_{i0}{}^2\omega_i N'/N$, $\omega_i=eB/m_i$, $\epsilon_i=Nm_i/B^2$, $u_{ie}=g/\omega_i$, and ρ_{i0} is the unperturbed ion Larmor radius. We observe that $\epsilon_0/\epsilon_i=V_A{}^2/c^2\ll 1$ and combination of Eqs. (5), (7), and (8) yields

$$\left[\vec{\nabla}^2\frac{\partial^2}{\partial t^2}-(u_{ie}-u_f+u_\lambda)\vec{\nabla}^2\frac{\partial^2}{\partial x\,\partial t}+G\frac{\partial^2}{\partial x^2}\right]\phi=0, \quad (9)$$

where $u_\lambda=\frac{1}{2}\rho_{i0}{}^2eN'/\epsilon_i B$, $G=u_{ie}\omega_i N'/N$, and use has been made of the fact that $|N/N'|$ is much larger than the characteristic lengths L_x and L_y.

For perturbations of the form $\exp[i(k_x x+k_y y+\omega t)]$, Eq. (9) gives

$$\omega=\tfrac{1}{2}(\alpha-f+\lambda)\pm\tfrac{1}{2}[(\alpha-f+\lambda)^2-4\alpha^2\gamma]^{1/2}, \quad (10)$$

in which $\alpha=k_x u_{ie}$, $f=k_x u_f$, $\lambda=k_x u_\lambda$, and $\gamma=-G/(k_x{}^2+k_y{}^2)u_{ie}{}^2$.

If α and λ within the parentheses could be dropped, Eq. (10) becomes identical with the result deduced by Rosenbluth et al.[5] for $k_y=0$. The corresponding stability condition would then become[5]

$$(k_x\rho_i)(\rho_i N'/N)>4\omega_H/\omega_i, \quad (11)$$

where the growth rate $\omega_H=(\alpha^2\gamma)^{1/2}$ represents that given by the earlier theory.[2] In addition, in the limit of very flat density distributions, i.e., when N' is very small, the frequency would become $\omega\approx-\frac{1}{2}f\pm i\omega_H$.

However, the terms α and λ are of the same order as f and cannot be dropped. From the present definitions $\lambda=f$ and there is an exact cancellation of the term leading to the condition (11). Thus, at least in the present approach, the stability criterion is not given by condition (11) but becomes instead $\gamma<\frac{1}{4}$ as deduced earlier.[3,4] The cancellation is due to the last term in Eq. (7) which represents the inertia of the electric currents produced by the perturbed density gradients. In the limit of small N' the nontrivial solution of the frequency now reduces to $\omega\approx\alpha$.

It remains to investigate whether a treatment of gravitational instability by direct application of the Boltzmann equation, as has been done by Rosenbluth et al.,[5] gives additional information beyond that obtained from the present approach. In particular, Rosenbluth[7] has pointed out that the off-diagonal elements of the pressure tensor give contributions which do not vanish when the relations corresponding to Eqs. (2) and (3) are subject to a divergence operation. This may change the results obtained here.

At the present stage it should only be pointed out that the asymptotic frequency $\omega\approx\alpha=2\pi u_{ie}/L_x$ for small gradients N' and small driving forces is physically plausible because the density clouds would then have time to move through each other and produce pulsations of the frequency α without changing noticeably during a period L_x/u_{ie}. On the other hand, the earlier solution[5] which leads to the asymptotic frequency $\omega\approx-\frac{1}{2}f\pm i\omega_H$ depends upon N' and cannot be understood in the same way from physical arguments.

---

[1]M. D. Kruskal and M. Schwarzschild, Proc. Roy. Soc. (London) A223, 348 (1954).

[2]M. N. Rosenbluth and C. L. Longmire, Ann. Phys. 1, 120 (1957).

[3]B. Lehnert, Phys. Fluids 4, 525 (1961); 4, 847 (1961).

[4]B. Lehnert, Conference on Plasma Physics and Controlled Nuclear Fusion Research, Salzburg, September, 1961 (unpublished), Paper CN-10/3.

[5]M. N. Rosenbluth, N. A. Krall, and N. Rostoker, Conference on Plasma Physics and Controlled Nuclear Fusion Research, Salzburg, September, 1961 (unpublished), Paper CN-10/170.

[6]M. D. Kruskal, Project Matterhorn Report PM-S-33, NYO-7903, 1958 (unpublished).

[7]M. N. Rosenbluth (unpublished); a private communication on this question is gratefully acknowledged by the author.

ION-PAIR RESONANCE MECHANISM OF ENERGY TRANSFER IN RARE EARTH CRYSTAL FLUORESCENCE

F. Varsanyi and G. H. Dieke
Physics Department, The Johns Hopkins University, Baltimore, Maryland
(Received November 22, 1961)

Considerable detail about the interactions in a solid can be obtained if this solid has an absorption or fluorescence spectrum with sharp lines. As crystals with complicated structure present too many possibilities, we have endeavored to study the situation in relatively simple lattices and have found hexagonal $LaCl_3$ particularly useful, where the La^{3+} ions are partly or entirely replaced by a different rare earth ion.

These crystals show bright fluorescence from relatively stable levels of the ion. The behavior of the fluorescence spectrum when the crystal is illuminated by monochromatic radiation of changing frequency[1] presents a possibility of elucidating the fundamental processes which govern the transfer of energy within the crystal and the interaction between photons and crystal energy levels.

It appears that for the interpretation of some of the observed phenomena a cooperation of pairs of ions is necessary. The following experiment shows that one photon can excite two ions simultaneously.

When pure $PrCl_3$ is illuminated with light of frequency 20475 cm^{-1}, the $^3P_0$ state is excited and fluorescence from this level is observed. The same fluorescence spectrum is observed when the frequency of excitation is changed so that higher electronic levels $^3P_1$, $^1I_6$, and $^3P_2$ are excited. The energy difference between these levels and $^3P_0$ is transferred to the lattice with a very short relaxation time. The full energy level diagram of $Pr^{3+}(4f^2)$ is shown on Fig. 1.

The striking thing is that the same fluorescence spectrum is observed at definite excitation frequencies larger than that necessary to excite the $^3P_2$ state, in a region where it is definitely known that there cannot be any absorption lines of a single Pr^{3+} ion. A representative portion of the excitation survey plate is reproduced on Fig. 2. The frequencies where fluorescence is excited agree closely with frequencies necessary to excite simultaneously one Pr^{3+} ion to the $^3P_0$ state and a second ion to one of the lower excited states. This is shown by the following relations, where the number between parentheses shows the observed excitation frequency. All observed frequencies in this spectral region are included in the table and the agreement,

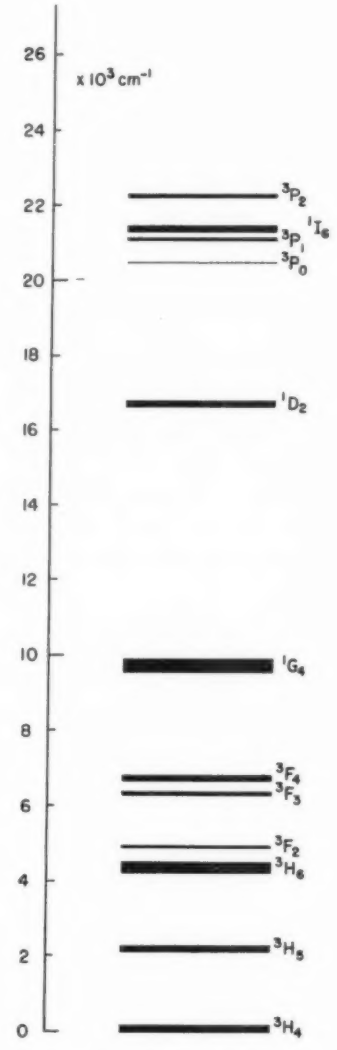

FIG. 1. Energy levels of $Pr^{3+}(4f^2)$. The width of the lines indicates the Stark splitting in a $LaCl_3$ crystal. The diagram is complete with the exception of one $^1S_0$ level which is predicted above 50000 cm^{-1} by calculations.

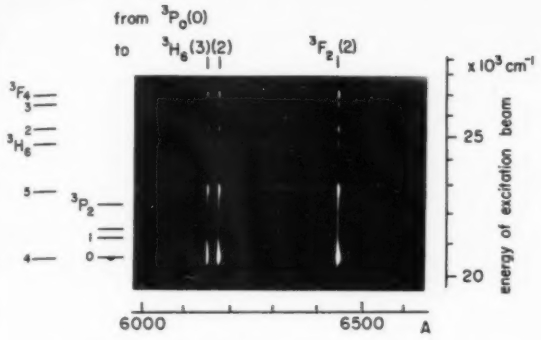

FIG. 2. Portion of the excitation survey plate taken at 4.2°K with a 100% $PrCl_3$ crystal. Any horizontal strip displays a fluorescence spectrum excited by the energy as marked on the right. Numbers in parentheses are the crystal quantum numbers of the respective Stark levels. Parts of two single-ion energy level diagrams are shown on the left to indicate the mechanism of excitation in a region with no single-ion levels.

$$^3P_0 + {}^3H_4 = 20\,475 + \quad 0 = 20\,475 \text{ cm}^{-1}, \quad (20\,500)$$
$$^3P_0 + {}^3H_5 = 20\,475 + 2115 = 22\,590 \text{ cm}^{-1}, \quad (22\,700)$$
$$^3P_0 + {}^3H_6 = 20\,475 + 4230 = 24\,705 \text{ cm}^{-1}, \quad (24\,700)$$
$$^3P_0 + {}^3F_2 = 20\,475 + 4922 = 25\,397 \text{ cm}^{-1}, \quad (25\,400)$$
$$^3P_0 + {}^3F_3 = 20\,475 + 6303 = 26\,778 \text{ cm}^{-1}, \quad (26\,800)$$
$$^3P_0 + {}^3F_4 = 20\,475 + 6700 = 27\,175 \text{ cm}^{-1}, \quad (27\,200)$$

is perfect within the limits of measurement.

The simultaneous excitation of two ions corresponds classically to the appearance of combination frequencies when two oscillators of different frequencies are linked by nonlinear forces sufficiently weak not to affect the frequencies seriously.

Optical phenomena which involve two or more crystal ions have been studied before. Schawlow, Wood, and Clogston[2] have explained the appearance of satellite lines in ruby as due to the resonance interaction of neighboring identical Cr^{3+} ions. Related are also the phenomena investigated in the field of sensitized luminescence[3] of phosphors.

The interaction of ion pairs also plays an important role in the dissipation of energy within the crystal. If a level X above a stable fluorescent level F is excited, fluorescence from F is observed and the difference $X-F$ is used for multiple phonon excitation. If $X-F$ becomes too large, the energy is not transferred directly from X to F and X becomes a stable fluorescent level. Our recent experiments have shown that if $X-F$ approaches the excitation energy of a low level of another ion, the transfer again takes place, that is to say fluorescence from F is again observed. The difference $X-F$ is then used to excite the second ion. In Er^{3+} this is found when X is approximately 6700 cm^{-1} above F. The energy of the first excited state is $Y = 6690$ cm^{-1}.

In the classical picture this process corresponds to the emission of radiation of the difference frequency of two coupled oscillators with frequencies X and Y.

This type of ion-pair interaction in fluorescence has been observed throughout the whole rare earth series and explains some peculiarities of the observed fluorescence. For the lighter rare earths the lower states are relatively close together so that the regions of phonon and ion-pair interaction overlap. This means that generally there is cascading from the higher excited states to the lower ones and only relatively few fluorescent levels exist. For the heavier ions the lowest excited state is generally several thousand cm^{-1} above the ground state, which inhibits cascading in many cases. The experimental details will be given later.

The ion-pair resonance mechanism may play an important part in the optical pumping for maser materials. It has given rise to a number of questions which are now being studied experimentally. Effective optical pumping into infrared levels with ultraviolet light and without necessarily heating the lattice is accomplished in the Pr^{3+} case described above. The surplus energy is emitted in the visible. Similar processes involving dissimilar ion pairs are also possible.

---

[1]F. Varsanyi and G. H. Dieke, J. Chem. Phys. 31, 1066 (1959).

[2]A. L. Schawlow, D. L. Wood, and A. M. Clogston, Phys. Rev. Letters 3, 271 (1959).

[3]D. L. Dexter, J. Chem. Phys. 21, 836 (1953); Phys. Rev. 108, 630 (1957); the first of these also contains many references.

OPTICAL MASER ACTION OF Nd^{+3} IN A BARIUM CROWN GLASS

E. Snitzer
American Optical Company, Southbridge, Massachusetts
(Received November 6, 1961)

Since the original suggestion for an optical maser,[1] maser oscillations have been reported in a number of crystals[2-6] and in the gas mixture of He-Ne.[7] This Letter describes a glass optical maser which operates at room temperature and contains trivalent neodymium as the active ion. The output consists of a number of sharp lines in a wavelength interval of about 30 angstroms centered at approximately 1.06 microns.

Concentrations of Nd_2O_3 varying from 0.13 to 2.0 weight percent were added to a barium crown glass whose composition is 59 wt.% SiO_2, 25% BaO, 15% K_2O, and 1% Sb_2O_3. The glass has a density of approximately 3 and a nominal index of refraction of 1.54. Because of the $4f^3$ electron configuration is well shielded in Nd^{+3}, the term values are virtually the same as one would find in a crystal or the free ion. The energy level diagram is easily identified by reference to the spectrum of $NdCl_3$.[8] There is an absorption at 880 mμ which is due to the transition from the $^4I_{9/2}$ ground state to the $^4F_{3/2}$ level, which is the level from which the fluorescence originates. There are other absorption lines in the visible and near infrared; the strongest one is at 580 mμ. The $^4I_{9/2,11/2,13/2}$ levels are the terminal states for spontaneous emission which give broad lines (several hundred angstroms wide) at 0.88 μ, 1.06 μ, and 1.3 μ. From the absorption and fluorescent spectra the lifetime for radiative decay from the $^4F_{3/2}$ state was calculated to be about 0.6 msec. The measured lifetime is 0.56 msec, which indicates a high quantum efficiency for fluorescence from the $^4F_{3/2}$ state.

The quantum efficiency, as determined by the lifetime, was checked in eight different glass bases and for a number of concentrations of Nd. The barium crown was selected because it gave the longest lifetime for fluorescent decay. There was only a barely perceptible concentration quenching for 2 wt.% Nd_2O_3. The quantum efficiency rapidly decreased for higher concentrations; for 10 wt.% Nd_2O_3 in barium crown the lifetime is less than 0.15 msec.

The glass samples were in the form of clad rods. Two cross sections were investigated, 0.012 in. and 32 microns in diameter. The cladding was an ordinary soda-lime-silicate with an index of refraction of 1.52. The samples were 3 in. long and the polished ends partially silvered for 2% transmission.

There were several reasons for using clad rods. While glass can be made with excellent optical quality, this requires large melts. In the experimental program of glass investigation that was carried out, the usual melt size was one pound. It is difficult to get such small glass melts free from stria and other imperfections. Even though the core glass was of poor optical quality, a cladding of lower refractive index can improve the mode properties.

First, some mode selection is provided by the small numerical aperture of the fiber if the indices of core and cladding are close to one another. Second, the good optical interface between the core and the cladding for a drawn glass fiber can provide high-Q surface wave modes. There is evidence for both types of modes being excited in maser oscillations in the clad Nd glass rods.

Because of the relatively strong and narrow absorption lines in Nd^{+3}, the pumping light does not penetrate very far into the sample. This suggests a small cross section for optimum pumping. A thick cladding makes it easier to handle small diameter samples. Also, the cladding glass acts as an immersion medium which increases the pumping flux density by about 50%.

Figure 1(a) shows the output as a function of time near threshold for the 0.012-in. diameter rod of 2 weight% Nd_2O_3 in the barium crown. The sample was illuminated by a G.E. FT524 flashtube with 75 microfarads charged to 2.0, 2.2, 2.4, and 2.6 kv, respectively, for the four curves shown. The time scale is 10^{-4} sec/division. Just above threshold there is a slow buildup of light, giving the hump shown at about 200 microseconds after the initiation of the flashtube light. At about 50% above threshold, "ringing" is observed in the output. Figure 1(b) shows this when pumping the same rod with an E.G. and G. FX-33 flashtube through which 50 watt-seconds was discharged. The 32-micron diameter fibers show substantially the same threshold as the 0.012-in. rod.

The 0.13 wt.% Nd_2O_3 in barium crown samples do not show ringing when illuminated with the maximum light available from the FT524. However, maser action is suggested by the appearance of a hump in the light output versus time curve for

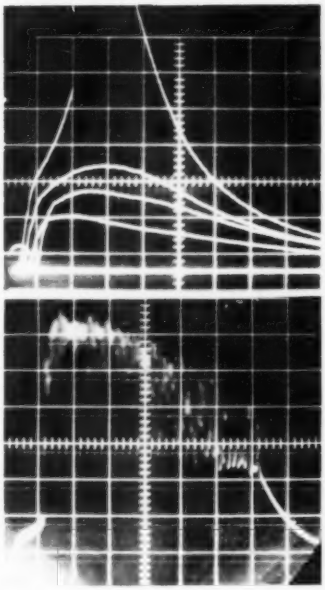

FIG. 1. Light output as a function of time from a clad 0.012-in. diameter rod of 2 wt. % Nd_2O_3 in the barium crown glass. (a) The time trace when pumped by a G. E. FT524 with 75 microfarads charged, respectively, to 2.0, 2.2, 2.4, and 2.6 kv. (b) The ringing produced by pumping with 50 watt-sec from an E. G. and G. FX-33.

discharges of the FT524 in excess of about 3000 watt-seconds.

In Fig. 2 is shown the end of the 0.012-in. rod for a single flash with the FX-33 light level at 10% above that required for ringing. The pictures were taken by use of an infrared image converter with an S-1 surface. The circular ring is at the interface between the core and cladding.

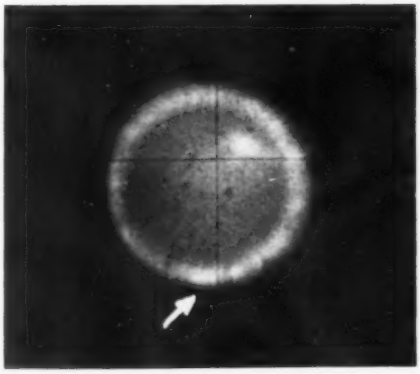

FIG. 2. The image of the end of a clad 0.012-in. diameter rod when pumped with 35 watt-sec from an E.G.G. FX-33 flashtube.

Just at threshold for ringing, only the spot shown by the arrow appeared. As the pump power was increased, the spot extended to the ring. Still further increase of pump light gave the interior filament. Finally, well above threshold the whole fiber was illuminated, but still with the surface wave modes appearing to be more strongly excited. For the 32-micron diameter fiber, threshold maser oscillations gave a uniform ring at the surface; and well above threshold the center of the fiber was filled in with light. Not all of the rods examined showed the surface waves at threshold.

The parallelism of the ends was not found to be critical. For the 3-in. long rods of 0.012-in. diameter with parallelism to 20 seconds or parallelism to only 6 minutes of arc gave the same threshold value. Various length samples were examined. There was no change in threshold power for lengths down to 2 cm. At 1 cm the threshold power doubled. Assuming a 5% absorption for the silver films on the ends with 2% transmission, this would indicate a Q of 10^6 due to scattering along the length of the rod. This corresponds to a 50% attenuation in the rod in about 8 inches. With better optical quality glass this should be improved. Measurements made on good fibers used in fiber optic devices have a 50% loss in about seven feet.

Figure 3 shows the spectrum of the maser output of one of the 0.012-in. rods taken on Kodak type 1-Z plates with a 3.4-meter focal length, plane grating spectrometer with a dispersion of 4.8 A/mm. Twenty 100-watt-sec flashes of the FX-33 flashtube were required. Except for small details the spectrum was reproducible in a given sample. From sample to sample the most intense lines occurred in about the same place, but the number of lines and the wavelength interval over which they occurred varied by a factor of two. The normal fluorescent line is about 200 A wide with no indication of lines within this interval.

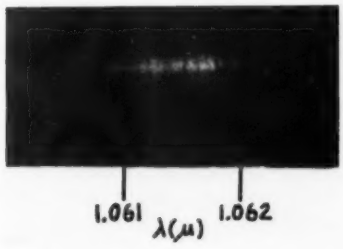

FIG. 3. The maser spectrum of 2 wt. % Nd_2O_3 in a barium crown glass.

The lines in the maser spectrum could be due either to the properties of the glass or to the effect of maser action in a resonant cavity. If the Nd^{+3} ions are in a limited number of well-defined atomic sites in the glass many lines could result,[9] similar to the satellite lines found in red ruby.[6] Alternatively, the lines could be due to the effect of the resonant cavity which gives standing waves only at discrete wavelengths.

The writer gratefully acknowledges the help given by R. Young for making the glass samples, Dr. H. Jupnik for the evaporations, E. Dixon for the studies on various length samples, and F. Hoffman for competent technical assistance during the measurements phase of this work.

[1]A. L. Schawlow and C. H. Townes, Phys. Rev. 112, 1940 (1958).

[2]T. H. Maiman, Nature 187, 493 (1960).

[3]P. P. Sorokin and M. J. Stevenson, Phys. Rev. Letters 5, 557 (1960); IBM J. Research 5, 56 (1961).

[4]W. Kaiser, C. G. Barrett, and D. L. Wood, Phys. Rev. 123, 766 (1961).

[5]I. Wieder and L. R. Sarles, Phys. Rev. Letters 6, 95 (1961).

[6]A. L. Schawlow and G. E. Devlin, Phys. Rev. Letters 6, 96 (1961).

[7]A. Javan, W. R. Bennett, and D. R. Herriott, Phys. Rev. Letters 6, 106 (1961).

[8]E. H. Carlson and G. H. Dieke, J. Chem. Phys. 34, 1602 (1961).

[9]R. C. Vickery and R. Sedlacek, Nature 181, 39 (1958).

EXPERIMENTAL OBSERVATION OF A NEW REGION OF NUCLEAR DEFORMATION*

Raymond K. Sheline,† Torbjørn Sikkeland, and Richard N. Chanda

Lawrence Radiation Laboratory, University of California, Berkeley, California

(Received November 20, 1961)

The nuclear periodic table has three or possibly four regions where nuclei have been experimentally shown to be deformed, namely $A \cong 19$ to 28 and 150 to 190, $A \geq 222$, and possibly $A \sim 8$. The work presented in this Letter gives experimental evidence for an additional region of deformation.

Figure 1 is a schematic representation of the nuclear periodic table in which previously observed regions of nuclear deformation are labeled 2, 4, 5, and 6. Up to $A \cong 40$, the line of beta stability of the nuclear periodic table involves nuclei whose neutron and proton numbers are about the same. Therefore, the first limited regions of deformation, labeled 5 and 6 in Fig. 1, have $N \cong Z$. Above $A \cong 40$, however, the line of beta stability shifts toward a higher neutron ratio. Consequently the neutron and proton shells are somewhat out of phase until one reaches the rare earths and actinides, where extended regions of deformation are observed because the 50- to 82-proton region is approximately in phase with the 82- to 126-neutron region and the 82- to 126-proton region with the 126- to 184-neutron region. On the other hand, though highly neutron-deficient and correspondingly unstable, the regions labeled 1 and 3 in Fig. 1, where $N \cong Z$, should contain deformed nuclei. We have concentrated our effort in region 1.

In order to study the energy levels of nuclei in region 1, it was necessary to discover a number of new La and Pr nuclides. We will report here only on those new nuclides whose mass number, half-life, and first excited state are relatively certain.

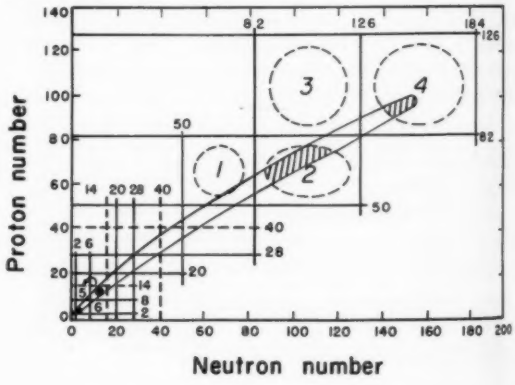

FIG. 1. Schematic representation of the nuclear periodic table showing the neutron (vertical solid lines) and proton (horizontal solid lines) closed shells. The dashed vertical and horizontal lines represent semiclosed shells, which have an effect on regions of deformation. The thin banana-shaped curve approximately encloses nuclei that have been experimentally studied. Regions where nuclei have been experimentally observed to be deformed are indicated with cross hatching. Additional regions where it is reasonable to expect to find deformed nuclei are labeled 1 and 3. This research is concerned with region 1. This figure is patterned after one suggested by E. K. Hyde.

Table I. Nuclear reactions showing cross bombardments used to produce the nuclides, La^{126}, La^{128}, and La^{130}.

New nuclide	Nuclear reactions	Heavy-ion bombarding energy (Mev)
La^{126}	$In^{115}(O^{16},5n)La^{126}$	94
	$Sb^{121}(C^{12},7n)La^{126}$	117
La^{128}	$In^{115}(O^{16},3n)La^{128}$	65
	$Sb^{121}(C^{12},5n)La^{128}$	84
	$Sb^{123}(C^{12},7n)La^{128}$	117
La^{130}	$Sb^{121}(C^{12},3n)La^{130}$	53
	$Sb^{123}(C^{12},5n)La^{130}$	84

The simplest available method of proving that nuclei are deformed involves the production of odd-odd nuclei whose decay into daughter even-even nuclei gives a characteristic low energy for the first excited state and, if possible, a rotational band built on the ground state with spins 0+, 2+, 4+, ··· and ratios of energies to the first excited state 1.0:3.33:7.00···. Accordingly, we have produced the nuclei La^{126}, La^{128}, and La^{130} with half-lives of 1.0 ± 0.3, 6.5 ± 1.0, and 9.0 ± 1.0 min, respectively.

These La nuclei have been made in a variety of ways (see Table I), using the heavy-ion current of the Berkeley Hilac. A heavy-ion bombarding energy was chosen which would give maximum yield of a desired isotope. This energy (see Table I) was estimated by using Cameron's mass table[1] and by assuming the average kinetic energy of each emitted neutron to be 4 to 5 Mev.

The reaction products recoiling out of ~1-mg/cm^2 self-supporting targets of In and Sb were caught in a 1.8-mg/cm^2 Pd foil which was then dissolved in hot aqua regia. With Ba as holdback carrier the La activities were precipitated in LaF_3 and the precipitate washed once with dilute HF. The procedure took about 1.7 min from the end of bombardment to the start of counting.

When the same targets were bombarded by ions that produce elements below La in atomic number, the chemical procedure separated only a small fraction of the activity. This suggests that the radiochemical purity of the sample was satisfactory. The purity was also checked by separating some of the La activities carrier-free by elution with ammonium α-hydroxy isobutyrate from a column of Dowex-50 cation-exchange resin.

The mass assignments are also quite definite. In the first place, there is the evidence on the mass numbers from the cross bombardments shown in Table I. In the second place the La^{126} is shown to decay into a species that has a spectrum identical[2] with that of Ba^{126}. Finally, the La^{130} emits a very strong 356 ± 4 kev gamma ray. A 359-kev gamma ray is observed[3] in the Coulomb excitation of Ba^{130}. To verify the above mass assignments, we are now determining the excitation functions.

The energy levels in the daughter nuclei Ba^{126}, Ba^{128}, and Ba^{130} are used to determine whether or not these nuclei are deformed. The first excited state of the even-even Ba nuclides including Ba^{126}, Ba^{128}, and Ba^{130} are plotted in Fig. 2. The lowering of the first-excited-state energy with mass number is similar to that observed in the normal rare earths. A more detailed analysis of these energies is therefore necessary. There are at least three ways to use the first-excited-state energy as a criterion for deformation. These are (a) a direct comparison between the energy of

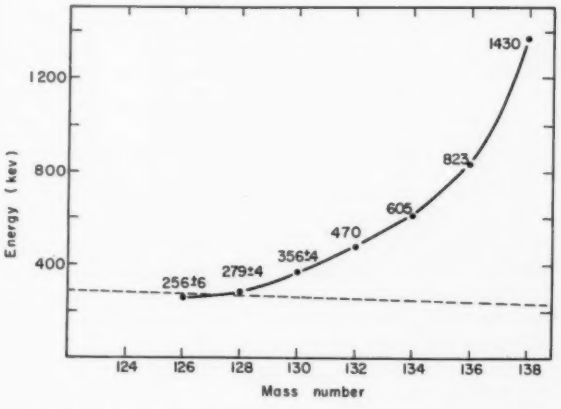

FIG. 2. First excited states of even-even Ba nuclides. The levels in Ba^{126}, Ba^{128}, and Ba^{130} are the results of this research. The dashed line shows $(E_{2+})_{crit}$, the dividing point between spherical and deformed nuclei.

the first excited state and an $(E_{2+})_{crit}$ suggested by Alder et al.,[4] (b) a determination of an empirical deformation, β_{emp}, from a relationship between $\mathcal{I}/\mathcal{I}_{rig}$ and β,[5] and (c) a comparison of β_{Mig} from the relationship of Migdahl.[6] These three methods are utilized in Table II, where comparisons are made with other nuclei with similar deformations but from other regions of deformation. A comparison of Ba^{126}, Ba^{128}, and Ba^{130} with other deformed nuclei indicates that Ba^{126} is like W^{186}, Os^{186}, and Ra^{224}. Thus all of these nuclei have a first-excited-state energy less than $(E_{2+})_{crit}$ and have very similar β_{emp} (0.19 to 0.21) and β_{Mig} (0.15 to 0.18).

Similar statements apply to a comparison of Ba^{128} to Os^{188} and Ra^{222}. On the other hand, both Ba^{130} and Os^{190} seem to be in a transition region. Their first-excited-state energies are each higher than the $(E_{2+})_{crit}$, and each has $\beta_{emp}=0.16$ and $\beta_{Mig}=0.12$. Osmium-190 has a rotational band which cannot be fitted well with the simple $I(I+1)$ relationship but is fitted by the nonaxially symmetric rotator model of Davydov and Fillipov.[7] It seems very probable that Ba^{130} would be very similar in this regard.

In addition to gamma-ray singles spectra, gamma-gamma coincidences were also taken using standard fast-slow circuitry and, in some cases, a two-dimensional coincidence analyzer. Coincidences were found in the decay of each of the La nuclides. However, the presence of the 511-kev annihilation radiation tended to obscure coincidence relationships, and it was not possible to fix unambiguously the energy of second and/or third excited states in the Ba isotopes. However, if one makes the simplest assumptions with the coincidence data, the results strongly favor a rotational band interpretation, and are inconsistent with a vibrational interpretation. Ratios of the supposed second excited states are similar to those in Column VIII of Table II. Nonetheless, none of the spins of the supposed second excited states has been measured. Consequently, a satisfactory proof of the existence of rotational states must await complete coincidence analysis.

A trend similar to Fig. 2 for the first excited states of even-even Ce nuclei has also been observed. However, in this case mass assignments and half-lives of the Pr nuclides are not nearly as certain. This evidence does tend to confirm the

Table II. Comparisons between the nuclei Ba^{126}, Ba^{128}, and Ba^{130} and nuclei from other regions of deformation.

Nucleus	E_{2+}[a] (kev)	$(E_{2+})_{crit}$[b] (kev)	$\mathcal{I}/\mathcal{I}_{rig}$[c]	β_{emp}[d]	β_{Mig}[e]	β_{exp}[f]	Ratios of energies in the rotational band
Ba^{126}	256	279	0.251	0.20	0.16		
Ba^{128}	279	272	0.225	0.18	0.15		
Ba^{130}	356	265	0.172	0.16	0.12		
Gd^{154}	123	200	0.462	0.29	0.25	0.30	1.0:3.02:5.84
Dy^{156}	138	196	0.333	0.23	0.19		1.0:2.93:5.59
W^{186}	124	147	0.273	0.20	0.17	0.24	1.0:3.28
Os^{186}	137	147	0.247	0.19	0.15	0.20	1.0:3.19:6.33
Os^{188}	155	144	0.215	0.18	0.14	0.18	1.0:3.09
Os^{190}	188	142	0.174	0.16	0.12		1.0:2.93:5.60:8.89
Ra^{222}	111	110	0.228	0.19	0.15		1.0:2.79:5.78
Ra^{224}	84.5	108	0.295	0.21	0.18		1.0:2.98
Th^{228}	72.1	106	0.341	0.23	0.20		1.0:3.14:6.33

[a] Throughout the table, energy values are taken from R. K. Sheline, Revs. Modern Phys. 32, 1 (1960) except the values for Ba^{126}, Ba^{128}, and Ba^{130} (reported herein) and Dy^{156} [see E. P. Grigor'ev and B. S. Dzhelepov, Doklady Akad. Nauk S.S.S.R. 135, 564 (1960); translation: Soviet Phys. —Doklady 3, 1243 (1961)].

[b] Values of $(E_{2+})_{crit}=13\hbar^2/\mathcal{I}_{rig}$ are given (see reference 3). This $(E_{2+})_{crit}$ is the criterion by which nuclei may be assumed to be spherical [for $E_{2+}>(E_{2+})_{crit}$] or deformed [for $E_{2+}<(E_{2+})_{crit}$]. Often the transition is not as abrupt as indicated by the single value.

[c] Ratio of $\mathcal{I}=3\hbar^2/E_{2+}$ to $\mathcal{I}_{rig}=(2MAR_0^2/5)(1+0.31\beta+\cdots)$, where $R_0=1.2A^{1/3}\times10^{-13}$ cm, $\beta=1.08/A^{1/3}$, and MA is the nuclear mass.

[d] See reference 5.

[e] Values of β_{Mig} are determined from $\mathcal{I}=(2MAR_0^2/5)(2.33\beta_{Mig}-0.1)$ (see reference 6).

[f] Experimental deformations calculated from the available values of the transition probabilities for Coulomb excitation.

existence of an extended region of deformation, however. The existence of the region of deformation labeled 1 in Fig. 1 suggests that (a) it should be possible to observe deformed even-even Nd nuclei and possibly also Sm nuclei with presently available heavy-ion beams, and (b) it is certainly feasible to observe a large number of deformed odd-A Ba, La, Ce, Pr, Nd, and Pm nuclides. The observation of odd-A nuclei in this region would be particularly interesting because it would allow assignments of Nilsson orbits in this new region of deformation.

Recent calculations on the equilibrium deformations for nuclei in regions 1 and 3 on Fig. 1 indicate a considerable deformation in each region.[8] These calculations and this experiment should provide impetus to the observation of deformations in the neutron-deficient actinides, region 3 in Fig. 1. Such experiments might be undertaken by the observation of the α fine structure resulting from the decay of even-even nuclei produced from the following types of nuclear reactions: $Pb^{204}(O^{16}, 8n)Th^{212}$ and $Hg^{196}(Ne^{20}, 8n)Th^{208}$.

We are grateful particularly to Albert Ghiorso for his encouragement and help in all phases of this research, to Daniel O'Connell for the targets, to Roberta Garrett, Suzanne Hargis, and Beverly Isaacs for help with the chemistry and plotting, to the Hilac crew for their help during bombardments, to Charles A. Corum for the design of the target assembly, and to Almon E. Larsh, Alfred Wydler, and William Goldsworthy for help with the electronics.

---

*Work supported by the U. S. Atomic Energy Commission.

†Summer visitor, on leave from Florida State University, Tallahassee, Florida.

[1]A. G. W. Cameron, Atomic Energy of Canada Limited Report AECL-433, 1957 (Chalk River Report CRP-690) (unpublished).

[2]M. I. Kalkstein and J. M. Hollander, Phys. Rev. 96, 730 (1954).

[3]L. W. Fagg, Phys Rev. 109, 100 (1958).

[4]K. Alder, A. Bohr, T. Huus, B. Mottelson, and A. Winther, Revs. Modern Phys. 28, 432 (1956).

[5]B. Elbek, in Proceedings of the International Conference on Nuclear Structure, Kingston, Canada, 1960, edited by D. A. Bromley and E. W. Vogt (University of Toronto Press, Toronto, 1960), p. 601; N. K. Glendenning and J. Sawicki, Lawrence Radiation Laboratory Report UCRL-9178, 1960 (unpublished). The parameter β_{emp} is an empirical relationship between $\vartheta/\vartheta_{rig}$ and β.

[6]A. B. Migdahl, Nuclear Phys. 13, 655 (1959).

[7]A. S. Davydov and G. F. Fillipov, Nuclear Phys. 8, 237 (1959).

[8]E. Marshalek, L. Person, and R. K. Sheline, Lawrence Radiation Laboratory (unpublished work).

ELASTIC AND INELASTIC SCATTERING OF HIGH-ENERGY PROTONS FROM HYDROGEN

G. Cocconi,* A. N. Diddens, E. Lillethun, G. Manning,†
A. E. Taylor,† T. G. Walker,‡ and A. M. Wetherell
CERN, Geneva, Switzerland
(Received November 20, 1961)

Previous measurements[1] of the momentum spectra of high-energy protons scattered from Be targets have shown the existence of an elastic peak[2] and of an inelastic bump[3] about 1 Gev/c below the elastic peak. This Letter describes measurements of p-p elastic and inelastic cross sections using a CH_2-C difference method, again with targets in the internal beam of the CERN proton synchrotron. These measurements were made at laboratory scattering angles close to 60 mrad with incident proton momenta between 12 and 27 Gev/c.

The experimental arrangement was similar to that described in reference 1, but the geometrical resolution was improved from 1% to 0.6%, and the final energy of the circulating beam in the synchrotron was stabilized to better than 0.5%. The over-all number of recorded events in this experiment was increased by using simultaneously five similar independent counter telescopes.

The CH_2 and C targets had the same surface density, about 1 g cm^{-2}, and were flipped alternately into successive beam pulses. Counts accumulated for each target were stored in separate sets of scalers. The integrated number of protons that interacted in each target was determined at the end of each run by measuring the Be^7 activity (half-life 53 days, 0.48-Mev γ ray) produced in each target. The cross section for the production of Be^7 from C is constant at[4] 11 mb from 0.2 to 5.7 Gev and is assumed here to have the same value in the region from 12 to 27 Gev.

The laboratory differential cross section for a p-p collision can be written as

$$\frac{d^2\sigma}{d\Omega dP}=\tfrac{1}{2}\sigma_{Be^7}\left(\frac{\Sigma M}{\Sigma A}\right)_{CH_2}\left[\left(\frac{N}{M}\right)_{CH_2}-R\left(\frac{N}{M}\right)_{C}\right]\frac{1}{\Delta P\Delta\Omega},$$

$$R=\left(\frac{\Sigma M}{\Sigma A}\right)_{C}\Big/\left(\frac{\Sigma M}{\Sigma A}\right)_{CH_2}, \qquad (1)$$

where σ_{Be^7} is the cross section for producing Be^7 from C, and ΣA is the integrated number of Be^7 nuclei produced during the bombardment. N is the number of protons counted in a solid angle $\Delta\Omega$ and a momentum interval ΔP for M counts in an intermediary monitor. ΣM is the integrated monitor count corresponding to ΣA.

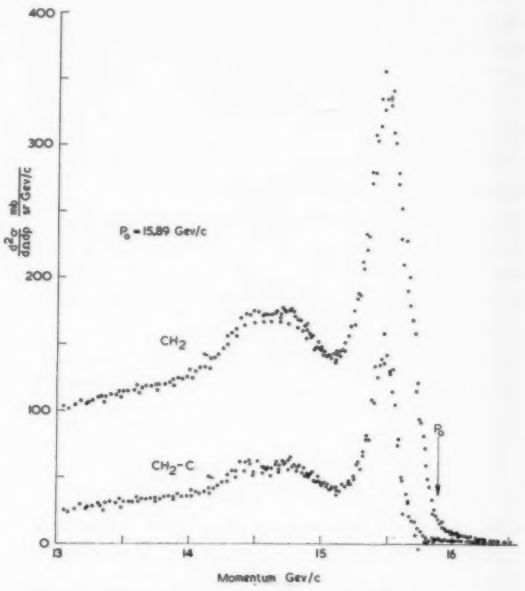

FIG. 1. Momentum spectrum of the protons from a CH_2 target and the CH_2-C difference. All experimental points from the five telescopes are shown.

Figure 1 shows a typical momentum spectrum obtained with a CH_2 target and the CH_2-C difference spectrum evaluated using Eq. (1). The experimental points recorded in all five channels are included. Figure 2 shows the p-p spectra obtained after grouping the points in small momentum intervals. All the curves of Fig. 2 show a pronounced peak at the highest momenta, followed in general by two smaller peaks at lower momenta. The first peak is identified with p-p elastic scattering, as the energy lost by the scattered proton is in agreement, within an experimental accuracy of about 100 Mev, with that calculated. The irregularities on the high-momentum side of some of the p-p elastic peaks are caused by incorrect subtraction. These occur when several measurements at different bombarding energies were made with one pair of targets and consequently an average value of R was used for all energies. A compari-

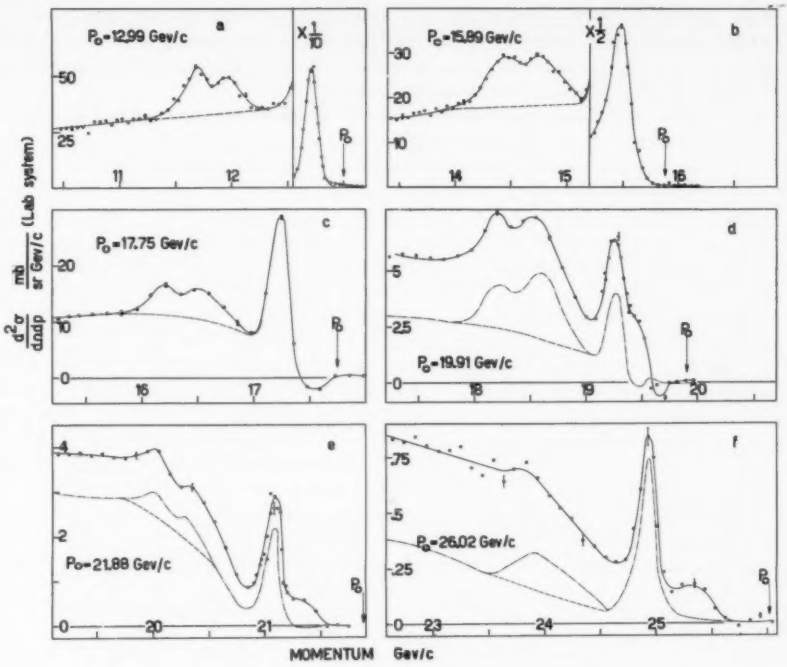

FIG. 2. Momentum spectra of protons from p-p collisions. The points shown were obtained by averaging the experimental data in small momentum intervals of about 30 Mev/c. (d), (e), and (f) show (as a broken line) the spectrum obtained by changing R [Eq. (1)] by 13%, 8%, and 14%, respectively. The broken line under the two inelastic peaks indicates the area to evaluate the cross section for the inelastic bump. These values are shown in column 10 of Table I. P_0 is the incoming proton laboratory momentum.

son of the CH_2 and C spectra indicates that the normalization constant R used in these circumstances may be in error by about 10%. The value of R has been changed empirically to make the p-p cross section above the elastic peak zero, and the resulting spectra are shown as dot-dash lines in Fig. 2. This changes the elastic cross section by $\lesssim 50\%$ and is an indication of the magnitude of one source of systematic error.

The elastic cross sections given in Table I were obtained from the area under the curves, renormalized where necessary. The statistical errors are small but the large systematic errors quoted arise from uncertainties in the values of R and σ_{Be^7}, in the computation of the focusing effects of the fringing field of the proton synchrotron, and in the amount of hydrogen lost from the CH_2 during bombardment. The hydrogen loss was measured by gravimetric analysis of the bombarded CH_2 and was found to be $\lesssim 10\%$. Figure 3 shows values of $(4\pi/\sigma_{tot})^2(1^2/k^2)(d\sigma/d\Omega)$, evaluated in the center-of-mass system [this is equal to $(d\sigma/dt)/(d\sigma/dt)_{t=0}$ if one uses the optical-theorem limit for the forward scattering amplitude], plotted against the square of the invariant four-momentum transfer, t. σ_{tot} is the total p-p cross section for the bombarding proton of wave number k in the center-of-mass system. The p-p cross sections for $t \gtrsim 0.2$ (Gev/c)^2 published by other authors[5-7] are included in Fig. 3. It can be seen that for values of $t \leq 0.5$ (Gev/c)^2, data from all energies fall approximately on a single curve,

$$\left(\frac{4\pi}{\sigma_{tot}}\right)^2 \frac{1}{k^2}\frac{d\sigma}{d\Omega} = F(t) = e^{-7.5t}.$$

This can be compared with the Gaussian approximation to the black-disk optical-model prediction and gives a value for the radius of ~1 fermi. For $t \geq 0.5$ (Gev/c)^2, $F(t)$ appears to be no longer a function of t alone but also of k for a given t. The data indicate interest in extending these measurements to different angles and energies and in particular to higher momentum transfers.

Another feature of the p-p momentum spectra is the inelastic bump and its fine structure. Figure 2 shows that at most energies two inelastic peaks are resolved. The momentum separations ΔP_1 and ΔP_2 of those from the elastic peak are given in Table I. The rest energy W^* of the recoiling system corresponding to a peak is given by

$$W^{*2} = M^2 + 2M\Delta E - t \sim M^2 + 2M\Delta P, \quad (2)$$

Table I. p-p elastic and inelastic cross sections. Θ, P_0, and t are the scattering angle, the incoming momentum, and the (4-momentum transfer)^2, respectively. ΔP_1 and ΔP_2 are the momentum separations of the inelastic peaks from the elastic peak; W_1^* and W_2^* are the corresponding rest energies of the recoiling system. $d\sigma/d\Omega$ in column 10 is the differential cross section of the inelastic bump evaluated by integrating the areas shown in Fig. 2. x means renormalized as described in text.

	Experimental conditions			Elastic peak			Inelastic peaks		
	Θ (lab) (mrad)	P_0 (lab) (Gev/c)	t (Gev/c)^2	$d\sigma/d\Omega$ (lab) (mb/sr)	Θ (c.m.) (degree)	$d\sigma/d\Omega$ (c.m.) (mb/sr)	ΔP_1 ΔP_2 (lab) (Gev/c)	W_1^* W_2^* (Gev)	$d\sigma/d\Omega$ (lab) (mb/sr)
	56.5	12.99	0.524	82	17.5	2.9	0.74 1.03	1.514 1.685	10
	56.5	15.89	0.783	20	19.2	0.59	0.72 1.01	1.504 1.678	8.4
x	56.5	17.30	0.925	6.5	20.0	0.18			
	56.5	17.75	0.978	7.6	20.2	0.21	0.71 1.01	1.499 1.680	3.5
x	56.5	18.69	1.084	2.2	20.7	0.056	0.74 1.00	1.520 1.675	2.2
x	56.5	19.56	1.184	0.76	21.2	0.018			
x	56.5	19.75	1.206	1.28	21.3	0.031	0.73 1.05	1.513 1.706	0.83
x	56.5	19.91	1.221	0.77	21.4	0.018	0.73 1.04	1.513 1.700	1.7
x	56.5	21.88	1.474	0.40	22.3	0.0088	0.71 1.07	1.50 1.72	0.25
x	56.5	22.74	1.590	0.34	22.6	0.0072			0.34
x	56.5	26.02	2.071	0.14	24.2	0.0027			0.10
	60.5	18.29	1.184	0.80	21.9	0.021	0.72 1.03	1.507 1.694	1.2
	60.5	27.83	2.372	0.055	26.6	0.0010			
Errors (all ±)									
Random				≤ 5%		≤ 5%	0.04	0.02	≤ 5%
Systematic abs.	0.5	0.3 %		50%	0.2	50%			50%
Systematic rel.		0.03%		40%		40%			40%

and is tabulated. M is the proton mass and ΔE is the laboratory energy difference of the incoming and outgoing protons. The values found for W^* are consistent with the assumption of definite rest energies for the recoil systems and the average values are 1.51 ± 0.01 Gev and 1.69 ± 0.01 Gev. As the energies of the second and third "resonances" ($T = \frac{1}{2}$) found in the π-p scattering are 1.51 and 1.69 Gev, respectively, there appears to be a connection between the inelastic bumps and these resonances. The tabulated estimates of the cross section $d\sigma/d\Omega$ for the inelastic bump were obtained by integrating the area under the bump as indicated in Fig. 2.

Several explanations have been offered for the origin of the inelastic bump,[1,8-12] but none of them explains all the features of the experimental data.

An explanation in terms of a one-meson exchange diagram in which the target proton and the pion are left in an isobaric state has been considered.[1,8] Two main objections can be raised, however. First, as the momentum transfer in the experiments was ~1 Gev/c this one-meson exchange is not expected to be the dominant process. Secondly, the model predicts a peak corresponding to the ($\frac{3}{2}$, $\frac{3}{2}$) π-p resonance in addition to the observed fine structure which arises from the $T = \frac{1}{2}$ resonances. The present results show no evidence for such a peak.[13]

Recently, it has been pointed out[11,12] that these difficulties may be overcome by considering another one-meson exchange process in which the

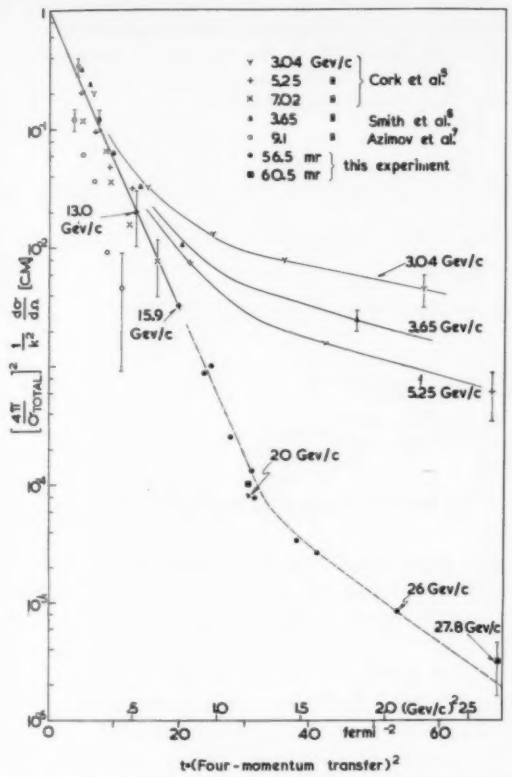

FIG. 3. The differential cross section for elastic p-p scattering, normalized to the optical-theorem value, against the square of the four-momentum transfer.

incoming proton undergoes diffraction scattering on a virtual pion of the target proton. Calculations by Drell and Hiida[12] have succeeded in predicting an inelastic bump, although its position relative to the elastic peak is less constant with energy than found in this experiment. A final-state interaction between the target proton and the pion may then qualitatively explain the double peak in the inelastic bump (the two $T=\frac{1}{2}$ resonances). The absence of the $(\frac{3}{2},\frac{3}{2})$ peak is expected since the pion and recoil nucleon are in a $T=\frac{1}{2}$ state, being formed from the target proton, and in the diffraction scattering the isotopic spin quantum number is expected to be conserved.

These experiments would not have been possible without the whole-hearted co-operation of the proton synchrotron machine group who operated the accelerator under the stringent conditions demanded by this experiment, developed new target techniques, and improved the energy stability of the machine. We should also like to thank L. Bird, R. Donnet, and C. A. Ståhlbrandt for their continuous assistance.

*Present address: Cornell University, Ithaca, New York.

†On leave of absence from the Atomic Energy Research Establishment, Harwell, England.

‡On leave of absence from Nuclear Institute for Research in Nuclear Science, Harwell, England.

[1]A. M. Wetherell, Proceedings of the Conference on Strong Interactions, Berkeley, December, 1960 [Revs. Modern Phys. 33, 382 (1961)]; G. Cocconi, A. N. Diddens, E. Lillethun, and A. M. Wetherell, Phys. Rev. Letters 6, 231 (1961).

[2]Measurements of proton scattering of high-energy protons from C and d indicate that this "elastic peak" probably arises from single and double quasi-elastic scattering from the nucleons in the Be nuclei. G. Cocconi, A. N. Diddens, E. Lillethun, G. Manning, A. E. Taylor, T. G. Walker, and A. M. Wetherell (to be published).

[3]This was previously called a "quasi-elastic bump" but this nomenclature is now dropped because of confusion with the normal use of quasi-elastic, namely to describe elastic scattering from nucleons in a nucleus.

[4]J. M. Dickson and T. C. Randle, Proc. Phys. Soc. (London) 64, 902 (1951); E. Baker, G. Friedländer, and J. Hudis, Phys. Rev. 112, 1319 (1958); P. A. Penioff, University of California Radiation Laboratory Report UCRL-8780, 1959 (unpublished).

[5]B. Cork, W. A. Wenzel, and C. W. Causey, Phys. Rev. 107, 859 (1957).

[6]G. A. Smith, H. Courant, E. C. Fowler, H. Kraybill, J. Sandweiss, and H. Taft, Phys. Rev. 123, 2160 (1961).

[7]S. A. Azimov, B. P. Bannik, V. G. Grishin, Do In Seb, L. F. Kirillova, P. K. Markov, V. A. Nikitin, L. G. Popova, I. N. Silin, L. V. Silvestrov, E. N. Tsyganov, M. G. Shafranova, B. A. Shahbazyan, A. A. Yuldashev, A. Zlateva, A. Peieva, L. Khristov, and Ch. Chernev, Proceedings of the 1960 Annual International Conference on High-Energy Physics at Rochester (Interscience Publishers, Inc., New York, 1960), p. 91.

[8]B. T. Feld and C. Iso, Nuovo cimento 21, 59 (1961).

[9]Feld has considered isobar excitation by "quasi-elastic diffraction" scattering using a black-sphere optical model. It does not seem useful to compare the present observations with this theory as the momenta and scattering angles were such that the data lie well outside the first minimum of the black-sphere diffraction pattern. B. T. Feld, CERN Internal Reports TH-178, TH-193, 1961 (unpublished).

[10]L. Van Hove has suggested that it may be possible to explain the inelastic bump in terms of diffraction disintegration of the target nucleons (private communication).

[11]D. Amati (private communication).

[12]S. D. Drell and K. Hiida, Phys. Rev. Letters 7, 199 (1961).

[13]In similar experiments performed in the energy region 1-2.7 Gev a peak corresponding to the $(\frac{3}{2},\frac{3}{2})$ resonance has been observed. The results indicate that the

excitation of this state decreases compared to the excitation of the higher "resonances" as the momentum transfer increases. The momentum transfers in these experiments were ~0.1 (Gev/c)^2. G. B. Chadwick, G. B. Collins, P. J. Duke, T. Fujii, N. C. Hien, and F. Turkot, International Conference on Elementary Particles, Aix-en-Provence, 1961 (unpublished). See also G. B. Chadwick, G. B. Collins, S. DeBenedetti, P. J. Duke, N. C. Hien, A. Roberts, and C. E. Swartz, Phys. Rev. Letters 4, 611 (1960).

π-MESON PRODUCTION IN 2.9-Bev p-p COLLISIONS*

A. C. Melissinos, G. G. Fazio, and T. Yamanouchi
Department of Physics and Astronomy, University of Rochester, Rochester, New York
and
S. J. Lindenbaum and L. C. L. Yuan
Brookhaven National Laboratory, Upton, New York
(Received November 29, 1961)

The momentum spectrum of charged π mesons produced in proton-proton collisions at an incident energy of 2.9 Bev has been measured by counter techniques. Related experiments have been recently performed in a 20-in. hydrogen bubble chamber[1,2] and the study of the recoil nucleons has been pursued with counters.[3] The present experiment, however, provides detailed momentum spectra of the π mesons as a function of angle. The shape of the momentum spectra at various angles, especially 0°, provides a crucial test for the most current theories on π production.[4]

The experiment was performed at Brookhaven's Cosmotron using the external proton beam III and a liquid H_2 target. The spectra were measured at 0°, 17°, and 32° in the laboratory and the setup is shown in Fig. 1; the circulating beam intensity ranged from 2×10^{10} to 2×10^{11} protons/pulse with 30% extraction efficiency to the second focus.

As seen in Fig. 1 all secondary beams were provided with focusing quadrupole doublets; however,

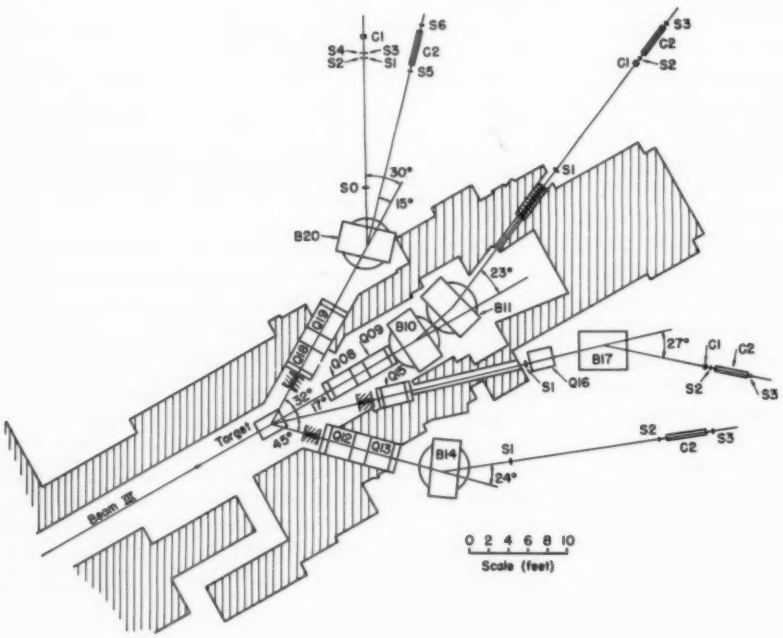

FIG. 1. The experimental setup.

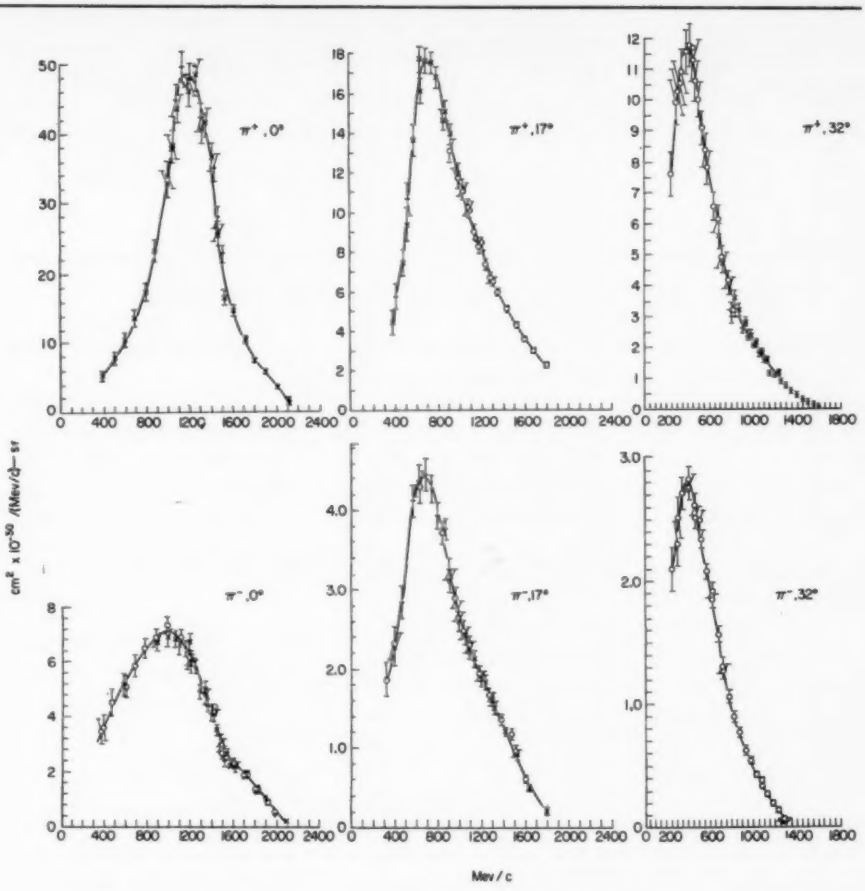

FIG. 2. The solid curves give the laboratory spectra for π^+ and π^- mesons at 0°, 17°, and 32°, after all corrections have been applied.

in the 17° and 32° case collimators were used to reduce the effective source width. With the quadrupoles "tuned" the magnification and momentum width (~2%) remain constant for all momenta. The absolute cross sections were obtained by measuring a few points of the spectrum with the quadrupoles turned off, so as to exclude any errors that may be introduced by the lens magnification or adjustment.

The π mesons were detected by a counter telescope consisting of plastic scintillators and a 4-ft long gas (SF_6) Čerenkov counter; a water Čerenkov counter was also used when required to complement time-of-flight identification in the lower momentum ranges. Corrections were applied to the data for nuclear absorption and multiple scattering in the telescope elements; such corrections were determined both experimentally and by calculation.[5]

The contamination of electrons ($e^{\pm}$) was determined experimentally over the whole spectrum by using the gas counter; the μ-meson contamination was measured at some points of the spectrum and then calculated for the remaining range. Finally the spectra had to be corrected for π-meson decay.

Figure 2 gives the momentum spectra for π^+ and π^- mesons in the laboratory at 0°, 17°, and 32°. The experimental points have been corrected for nuclear absorption, Coulomb scattering, empty target background, $\mu^{\pm}$ and $e^{\pm}$ contamination, and pion decay. The flags on the experimental points represent statistical and other estimated relative errors. The over-all reproducibility can be judged by the scatter of the points; in general the results of two or more completely different runs are shown on the same graph.

The analysis of the spectra has been performed in the c.m. system of the two incoming protons. The transformed c.m. spectra are shown in Figs. 3(a) and 3(b) and do exhibit a striking anisotropy both in shape and in their integrated (over momentum) values. A summary of the integrated cross sections is given in Table I; for comparison the

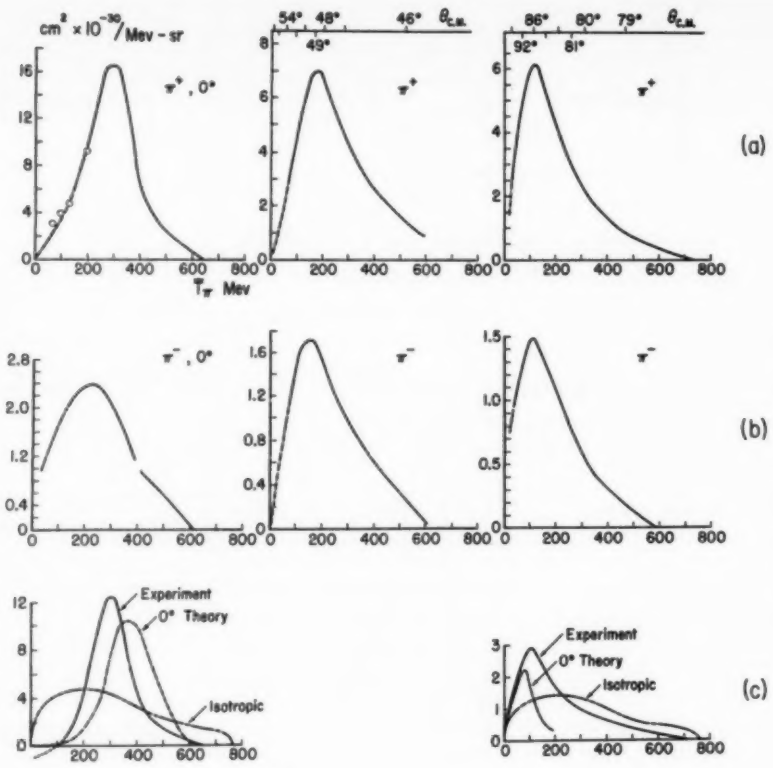

FIG. 3. The c.m. spectra for (a) π^+ mesons, (b) π^- mesons, (c) single production of π^+ mesons. In (c) the experimental spectrum is given by the solid curve and is obtained by subtraction, the dashed curve gives the 0° theory prediction, and the dot-dash curve gives the isotropic theory prediction. The 0° theory predictions have been normalized to fit the area under the experimental spectrum at 0°.

results of the bubble chamber work are also included and are in agreement. The c.m. spectra can now be used for a stringent test of any π-production theory. This is possible because each momentum spectrum is available at an almost fixed production angle and has been accurately determined in detail. In this communication we have tested only the "isobar model"[6] by assuming alternatively two extreme conditions: (a) that the isobars are produced isotropically in the p-p rest frame (isotropic theory); (b) that the isobars are produced in the p-p rest frame only at 0° and 180° (what we call the 0° theory). In both cases the isobars are assumed to decay isotropically in their own rest frame (no polarization). In Table II are compared the positions of the maxima of the experimental spectra, with the positions calculated according to these two extreme hypotheses.

It is evident from Table II that the predictions of the 0° theory are much closer to the experimental results for single pion production, and one may conclude that if the production of single π mesons proceeds through an intermediate isobaric state[1,3,6] then this state is produced (in the p-p rest frame) with an angular distribution ap-

Table I. Summary of integrated cross sections.

	$(d\sigma/d\Omega)_{c.m.}$ (mb/sr)					
	0°	47°	80°	Ang. distr.	σ_t	σ_t(bubble chamber)
π^+	3.92	2.25	1.53	$1+1.5\cos^4\theta$	25.0 ±5.0 mb	24.9 ±1.2 mb[a,b]
π^-	0.81	0.52	0.37	$1+1.2\cos^4\theta$	5.8 ±1.5 mb	4.7 ±0.7 mb[b]

[a] See reference 1.
[b] W. Willis et al. (private communication).

Table II. Position of maxima (in Mev) in pion spectra.

$\theta_{c.m.}$	π^+ singles spectrum Experiment	Isotropic theory	0° theory	π^- spectrum Experiment	Isotropic theory
0°	310	225	370	220	150
47°	200	225	•••	155	150
80°	115	225	80	115	150

proaching a δ function in the forward-backward direction.

For a more detailed and sensitive test of our results with theory we have attempted to isolate the spectra corresponding to different multiplicities. At 2.9-Bev proton energy, the π^+ spectrum contains single, double, and triple production:

$$p+p \rightarrow p+n+\pi^+ \ (pn+),$$

$$p+p \rightarrow (pp+-) \text{ or } (pn+0) \text{ or } (nn++),$$

$$p+p \rightarrow (pp+-0) \text{ or } (pn+00) \text{ or } (nn++0) \text{ or } (pn++-)$$

while the π^- spectrum includes only double and triple production:

$$p+p \rightarrow (pp+-),$$

$$p+p \rightarrow (pp+-0) \text{ or } (pn++-).$$

The branching ratios for the various channels are known[1] or can be calculated using charge independence if one accepts a production mechanism through the $T=\frac{3}{2}$ and $T=\frac{1}{2}$ isobaric states ($p\pi$) of the nucleon.[6] It is then possible to subtract a fraction of the π^- spectrum from the π^+ spectrum and obtain the spectrum for single production at a given angle. These spectra for singles at 0° and 80° are shown in Fig. 3(c); on the same diagrams are given the predictions of the "isobar theory" under the simplified extreme assumptions of 0°-180°, or isotropic production. It is seen that the 0° spectrum is in complete disagreement with the "isotropic theory" and that a strong component of δ-function production is needed; on the contrary the 80° spectrum appears to be a composite of the two theoretical spectra. It is interesting to note that both the 0° and 80° spectra can be explained simultaneously if one assumes for the total cross section an almost equal mixture of isotropic and 0°-180° production.

Finally the contribution of the $T=\frac{1}{2}$ isobar cannot be clearly seen in the single production. The effects due to contributions from this isobar are more pronounced in the 0° spectrum for π^- mesons.

A detailed report of this work including the analysis of the spectra at all angles is being prepared for submittal to The Physical Review.

It is a pleasure to acknowledge the help of Mr. J. S. Weaver in the early stages of this experiment and of Mr. J. Robbins with some calculations. Also we thank the Cosmotron staff, operating crew, and experimental support group as well as the members of the University of Rochester 130-in. Cyclotron Laboratory for their generous cooperation. One of us (ACM) wants to thank R. Sugarman, R. Sternheimer, and G. Collins and his group for many helpful discussions.

*This work was supported by the U. S. Atomic Energy Commission.

[1]G. A. Smith, H. Courant, E. C. Fowler, H. Kraybill, J. Sandweiss, and H. Taft, Phys. Rev. 123, 2160 (1961).

[2]W. Fickinger, E. Pickup, D. Robinson, and E. Salant, Phys. Rev. Letters 7, 196 (1961).

[3]G. Chadwick, G. Collins, C. Schwartz, A. Roberts, S. DeBenedetti, N. Hien, and P. Duke, Phys. Rev. Letters 4, 611 (1960).

[4]F. Selleri, Phys. Rev. Letters 6, 64 (1961); F. Salzman and G. Salzman, Phys. Rev. Letters 5, 377 (1960); S. Drell and K. Hiida, Phys. Rev. Letters 7, 199 (1961).

[5]R. M. Sternheimer, Rev. Sci. Instr. 25, 1070 (1954).

[6]S. J. Lindenbaum and R. M. Sternheimer, Phys. Rev. 105, 1874 (1957); R. M. Sternheimer and S. J. Lindenbaum, Phys. Rev. 123, 333 (1961).

EXPERIMENTAL PROOF OF THE SPIN DEPENDENCE OF THE MUON CAPTURE INTERACTION, AND EVIDENCE FOR ITS (F - GT) CHARACTER*

G. Culligan, J. F. Lathrop,† V. L. Telegdi, and R. Winston
The Enrico Fermi Institute for Nuclear Studies, The University of Chicago, Chicago, Illinois

and

R. A. Lundy
Argonne National Laboratory, Argonne, Illinois
(Received November 21, 1961)

The ground state of a μ-mesonic atom of nuclear spin I consists of a hyperfine doublet, $F_\pm = I \pm \frac{1}{2}$. Spin dependence of the μ-capture interaction means that these two hyperfine states capture at distinct rates, $\Lambda_\pm^{\rm cap}$. These two rates depend more sensitively on $x \equiv C_{\rm GT}/C_{\rm F}$, the ratio of the effective Gamow-Teller and Fermi coupling constants, than the F-averaged capture rate, $\bar{\Lambda}^{\rm cap} \equiv n_+\Lambda_+^{\rm cap} + n_-\Lambda_-^{\rm cap} \equiv (2I+1)^{-1}[(I+1)\Lambda_+^{\rm cap} + I\Lambda_-^{\rm cap}]$. In fact, one has for the basic p-μ atoms $\Lambda_-^{\rm cap}({}_1H^1) \sim (1-3x)^2$, $\Lambda_+^{\rm cap}({}_1H^1) \sim (1+x)^2$, $\bar{\Lambda}^{\rm cap}({}_1H^1) \sim (1+3x^2)$, and with $\Delta\Lambda \equiv \Lambda_-^{\rm cap} - \Lambda_+^{\rm cap}$,

$$\Delta\Lambda({}_1H^1)/\bar{\Lambda}^{\rm cap}({}_1H^1) = 8x(x-1)/(1+3x^2). \qquad (1)$$

Thus, an (F + xGT) type interaction leads with x = -(+)1 to maximal (minimal) spin dependence; the currently favored "universal V-A" interaction, as yet unproved in the case of μ capture, corresponds to $x \simeq -1$. Hence, even a qualitative measurement of (1) should enable one to check whether this favored interaction holds indeed.

A direct experimental study of the fundamental ${}_1H^1$ rates entering (1) meets with many difficulties. Fortunately, as was emphasized by Bernstein, Lee, Yang, and Primakoff,[1,2] experiments with complex nuclei can provide almost equally valuable information. A light nucleus Z with one proton outside a spinless "core" ($I = l \pm \frac{1}{2}$) should yield spin-dependence effects of order $1/Z$; clearly, the lightest nuclide with an odd $s_{1/2}$ proton should approximate ${}_1H^1$ best. For such a nuclide, reference 1 indeed predicts simply

$$\Delta\Lambda(Z)/\bar{\Lambda}^{\rm cap}(Z) = (1/Z\xi)\Delta\Lambda({}_1H^1)/\bar{\Lambda}^{\rm cap}({}_1H^1), \qquad (2)$$

where $\xi(\leq 1)$ is a factor introduced to allow for the possibility that the Pauli principle may have a weaker inhibitory effect on the odd proton.[3]

Guided by these considerations, and following a recent suggestion,[4] we have now measured the time dependence of the rates at which neutral products (neutrons or/and nuclear gamma rays) are emitted in the capture of muons by ${}_9F^{19}$ in order to determine the spin dependence (2). ${}_9F^{19}$ was chosen on two grounds: (a) Its magnetic moment is essentially that of ${}_1H^1$, so that it can justifiably be attributed to an $s_{1/2}$ proton; (b) the conversion rate R, at which $F_+ \to F_-$ transitions take place through atomic processes, has for ${}_9F^{19}$ a predicted[4] magnitude ($\sim 3\times 10^6$ sec^{-1}) that, while being sufficiently large ($\Delta\Lambda/R \ll 1$), leads to observable effects over a time range ($\sim 1/R$) that is both statistically advantageous and electronically convenient.

Let us first predict qualitatively the time dependence $N_n(t)$ of, say, the capture neutron rate. Assume that $\Delta\Lambda/R \ll 1$, and that α_n neutrons are counted per muon capture (from either F_+ or F_-). At times $t > R^{-1}$, practically all neutrons will come from the lower (F_-) state, at a rate $N_n(t) = \alpha_n\Lambda_-^{\rm cap}\exp(-\Lambda_- t)$ (per muon). At $t = 0$ (when the muon reaches its K shell), the rate will be $N_n(0) = \alpha_n\bar{\Lambda}^{\rm cap}$ (and not $\alpha_n\Lambda_-^{\rm cap}$). Hence, to order $\Delta\Lambda/R$, one will observe for all t

$$N_n(t) = \alpha_n\Lambda_-^{\rm cap}(1 - A_n' e^{-Rt})\exp(-\Lambda_- t), \qquad (3)$$

with

$$1 - A_n' = \bar{\Lambda}^{\rm cap}/\Lambda_-^{\rm cap} \qquad (3a)$$

The gamma rate will have (assuming again an equal yield, α_γ, for either F_+ or F_-) a dependence $N_\gamma(t)$ like (3), with $\alpha_\gamma \neq \alpha_n$, but $A_\gamma' = A_n'$. In general, however, the n/γ branching ratios α_n/α_γ may differ for F_+ and F_-, in which case $A_n' \neq A_\gamma'$ and Eq. (3a), yielding the quantities of interest, need not apply. For this reason, one should measure independently both A_n' and A_γ'.

We measured $N_n(t)$ and $N_\gamma(t)$ for ${}_9F^{19}$, using a LiF target T (Li has a negligible capture rate) in the setup schematically indicated in Fig. 1. The neutral capture products were detected with a liquid scintillator 9; a pulse-shape discriminator circuit (p.s.d.) at this counter's output, patterned after the ideas of Brooks and Owen,[5] enabled one to select either γ- or n-induced pulses. The threshold of counter 9 was set at $E_\gamma \simeq 1.7$ Mev.

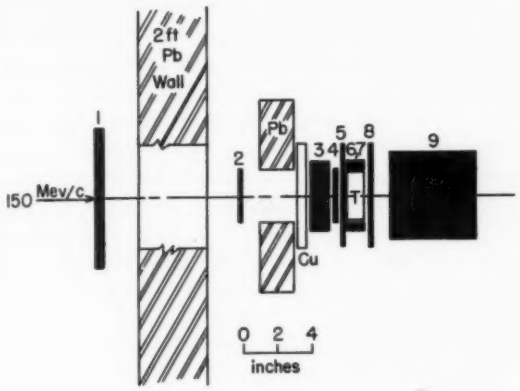

FIG. 1. Experimental setup. 1, 2, 4, 5, and 8, square scintillators; 3, Lucite Čerenkov counter; 6 and 7, yoke-shaped scintillators enclosing a target T from above and below; 9, 5-in. diameter and 5-in. long liquid scintillator counter followed by pulse-shape discriminator (p.s.d.); Cu, 23-g/cm^2 moderator; Pb, collimators; $(2\bar{3}45\bar{6}\bar{7}\bar{8})$ = "muon" signature; $\bar{1}(5\bar{6}\bar{7}\bar{8})9$ +p.s.d. = neutron or gamma signature.

The incident negative "muon" beam consisted of π's, μ's, and e's; π's were suppressed by range (Cu absorber), while e's were rejected with a Čerenkov anticoincidence counter, 3. The target T was enclosed first in a scintillator "house": front and back between counters 5 and 8, and from above and below between two yoke-shaped counters, 6 and 7. This "house" (5678) was put in anticoincidence with 9 and served a double purpose: (a) to reduce accidental background by vetoing decay events; (b) to reduce the chances that bremsstrahlung accompanying such events be counted by 9. A large counter 1, traversed by all beam particles that went through the setup, was further put in anticoincidence with 9 to reduce background. Thus, the signature of a neutral capture product was $(n/\gamma) = \bar{1}(5\bar{6}\bar{7}\bar{8})9$ +p.s.d., while that of a stopped muon was $(\mu) = 2\bar{3}45\bar{6}\bar{7}\bar{8}$. The time intervals between (μ) and (n/γ) pairs were measured with a digitalized instrument ("digitron"[6,7]) that stored their distributions in the memory of a 400-channel analyzer (PHA). Suitable logic, as described in references 6 and 7, was provided in "digitron" to reject multistart and multistop events (to decrease accidentals), as well as to route n- and γ-induced events to distinct 200-channel subsections of the PHA. Thus, $N_n(t)$ and $N_\gamma(t)$ could be recorded simultaneously, each over a time interval of 5 μsec. Under our running conditions (200 μ-stops/sec at a duty factor of 5), background events (accidentals) were ~5% of the real events at $t = 0$.

Figure 2(a) displays in the form $N_{n\gamma}\exp(+\Lambda_- t)$ the sum total of our (background-corrected) neutron and gamma data; $\Lambda_-(_9F^{19}) = (6.9 \pm 0.12) \times 10^5$ sec^{-1} was determined from the late ($t > 0.5$ μsec) parts of these data. This rate agrees well with measurements based on electron rates from KHF_2,[8] PbF_2,[9] and UF_6. If spin-dependence effects were absent, this display should yield a horizontal line; there is, however, a striking dip at early times, and the points are well fitted (dashed line) by an expression like Eq. (3), with $A_{n\gamma}' = 0.31 \pm 0.02$, and $R = (5.8 \pm 0.6) \times 10^6$ sec^{-1}. The separate data for $N_{n/\gamma}$ are quite similar and yield the parameters listed in Table I. $A_\gamma' \neq A_n'$ suggests a small branching ratio effect (see below), while the two values for R agree, as they should.

The anticoincidences in the (μ) and (n/γ) signals reduce the recorded $N_{n/\gamma}(t)$ near $t = 0$. For this

Table I. Comparison of observed parameters with theory.

	Observed from $N_n(t)$	Observed from $N_\gamma(t)$	$\bar{\Lambda}^{cap}, \Lambda_-{}^{cap}$	Predicted for F − GT	Predicted for F + GT
A'	0.36 ±0.04	0.25 ±0.04	0.35 ±0.03[a]	+0.25[b]	+0.04[b]
				+0.37[c]	+0.07[c]
R (10^6 sec^{-1})	6.2 ±1.0	5.8 ±1.4	...	5[d]	

[a] Using $A' = 1 - \bar{\Lambda}^{cap}/\Lambda_-{}^{cap}$; see text.
[b] From Eq. (1) with $x = \pm 1.25$, and Eq. (2) with $\xi = 1$.
[c] Shell-model prediction (reference 3).
[d] Estimate from reference 4, corrected for F^{19} moment contribution.

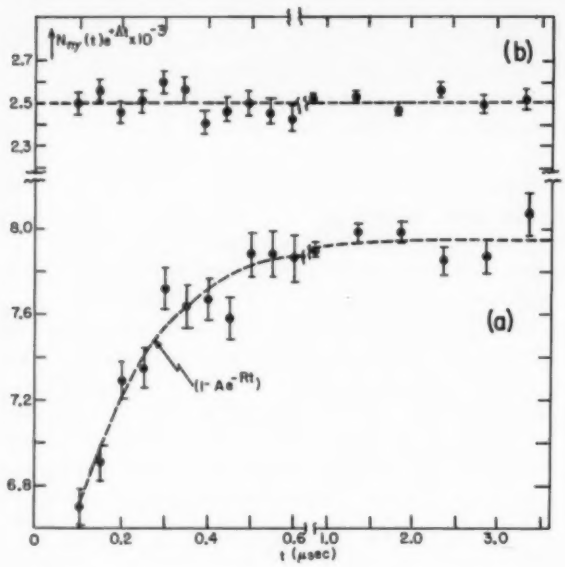

FIG. 2. (a) Time dependence of neutral capture products (neutrons and gammas), $N_{n\gamma}(t)$, from (Li)F, corrected for asymptotic exponential dependence, $\exp(-\Lambda t)=\exp(-\Lambda_- t)$ ($\Lambda_-=6.9\times10^5$ sec^{-1}). Dashed curve corresponds to $A'=0.31\pm0.02$, $R=(5.9\pm0.8)\times10^6$ sec^{-1}. (b) Time dependence of neutral capture products (neutrons and gammas), $N_{n\gamma}(t)$, from (Li)O(H), corrected for asymptotic exponential dependence, $\exp(-\Lambda t)$ ($\Lambda=6.1\times10^5$ sec^{-1}). The dashed horizontal line is the fitted mean. (Note the change in time scale near 0.6 μsec.)

reason, the data for $0<t\leq0.1$ μsec were discarded and are not plotted. To prove, however, that the effects for $t>0.1$ μsec are not instrumental ones, we ran under identical conditions with a LiOH target, in which essentially only $_8O^{16}$ ($I=0$) captures. From these control data as displayed in Fig. 2(b), we conclude that the effect exhibited in Fig. 2(a) is genuine. Further confidence is derived from a comparison of the observed and predicted values of the rate R (see Table I).

As a further check, we compared, using the precession method, the decay asymmetry parameters a of μ^- bound to $_9F^{19}$ (UF_6 target) and to $_6C^{12}$ (graphite). With $R=0$ (and in the absence of spin relaxation effects), one predicts $a(_9F^{19})=\frac{1}{2}a(_6C^{12})$; while with $R\neq0$, one should have $a(_9F^{19})=0$ for $t>R^{-1}$, where only $F_-=0$ systems survive. We find, for $t>0.7$ μsec, $|a(_9F^{19})|<0.003$, and, under identical conditions, $a(_6C^{12})=-(0.027\pm0.002)$.

Table I shows that A_n' and A_γ' closely bracket the values predicted for an F - GT interaction. As branching ratio effects appear to be present ($A_n'\neq A_\gamma'$), it is not obvious which of these two A''s should be compared quantitatively with theory. This difficulty can be circumvented: One can obtain $\bar{\Lambda}^{cap}(_9F^{19})$ by interpolation on the Primakoff plot,[7] and get from it and the observed Λ_-^{cap} a third estimate of A'. This estimate coincides with A_n', i.e., points to a particularly large effect.

We conclude that, in general,

1. μ^- capture is spin dependent ($A'\neq0$);

and, for $_9F^{19}$ in particular,

2. this spin dependence is such that $\Lambda_->\Lambda_+$ ($A'>0$);

3. its magnitude is close to the maximum possible one, i.e., to that predicted for an $(F+xGT)$ interaction with $x\simeq-1$;

4. both the absolute rates and their spin dependence agree with the prediction of a "universal ($V-A$)" interaction, and exclude a ($V+A$) interaction;

5. there is a fast $F_+\rightarrow F_-$ conversion process, of the predicted rate.

Clearly the assignments $F=V$ and $GT=A$ cannot be derived from nonrelativistic experiments, but must be sought elsewhere.

It is a pleasure to acknowledge the assistance of W. A. Cramer in this work.

---

[1]J. Bernstein, T. D. Lee, C. N. Yang, and H. Primakoff, Phys. Rev. 111, 313 (1958).
[2]H. Primakoff, Revs. Modern Phys. 31, 802 (1959).
[3]Shell-model calculations of H. Überall [Phys. Rev. 121, 1219 (1961)] indicate that $\xi=0.57$ for $_9F^{19}$.
[4]R. Winston and V. L. Telegdi, Phys. Rev. Letters 7, 104 (1961).
[5]F. D. Brooks, Nuclear Instr. and Methods 4, 151 (1959); R. B. Owen, IRE Trans. on Nuclear Sci. NS-5, 198 (1958).
[6]R. A. Swanson, Rev. Sci. Instr. 31, 149 (1960).
[7]R. A. Lundy, Phys. Rev. (to be published).
[8]J. C. Sens, Phys. Rev. 113, 679 (1958).
[9]A. Astbury, I. M. Blair, M. Hussain, M. A. R. Kemp, and H. Muirhead (to be published).

SPIN OF Y_1^*†

Robert P. Ely, Sun-Yiu Fung, George Gidal, Yu-Li Pan, Wilson M. Powell, and Howard S. White
Lawrence Radiation Laboratory, University of California, Berkeley, California
(Received November 16, 1961)

The observation of a resonance at 1385 ± 3 Mev in the $\Lambda\pi$ system[1] has renewed interest in the problem of higher symmetries among the strange particles. Global symmetry predicts the existence of hyperonic analogs to the observed pion-nucleon resonances.[2] In particular, a $T=1$ resonance with a mass of 1380 Mev, a half-width $\Gamma/2=23$ Mev, and a total angular momentum $J=3/2$ has been predicted from the measured parameters of the first pion-nucleon resonance.[3,4] This mass and width are in qualitative agreement with the observed Y^* parameters.[5,6] Dalitz has suggested an alternative interpretation which associates the Y^* with a bound S state of the K-nucleon system, requiring the Y^* to have $J=1/2$.[7] In this Letter we present correlations in the production and decay angular distributions of the Y^* that support $J \geq 3/2$.

We have studied the properties of the $T=1$ Y^* produced by the interaction of 1.11 ± 0.03 Bev/c K^- mesons[8] in the 30-inch propane bubble chamber at the Bevatron, via the reaction

$$K^- + p \rightarrow \Lambda + \pi^+ + \pi^-. \qquad (1)$$

The film was scanned for all V^0, π^+, and π^- type events. Eleven hundred such events were found and subjected to both Λ-decay and hydrogen-production constraints via reaction (1), with the FOG, CLOUDY, and FAIR kinematic analysis programs. From a comparison with the events that failed, we can set upper limits of (a) 5% for the fraction of those accepted events that were produced in carbon, and (b) 10% to 15% for those that involve Σ^0 production. The corrections for scanning bias include an escape correction for Λ's that leave the chamber, which varies from 5% to 15% over the momentum range of the Λ, and a 4% correction (15 events) for Λ's below 300 Mev/c, in which the decay proton was too short to be visible. The cross section for reaction (1) is 2.8 ± 0.5 mb, in agreement with the cross section of 3.4 ± 0.5 mb measured by Alston et al.[1]

The pion that resonates with the Λ has been chosen by examination of the invariant mass $M(\Lambda,\pi) = [(E_\Lambda + E_\pi)^2 - (\vec{p}_\Lambda + \vec{p}_\pi)^2]^{1/2}$ of each system. Weighted histograms of $M(\Lambda,\pi^-)$ and $M(\Lambda,\pi^+)$ for all events are shown in Figs. 1(a) and 1(b), respectively. The average error in M is less than, or equal to, the box width over the range of values shown.

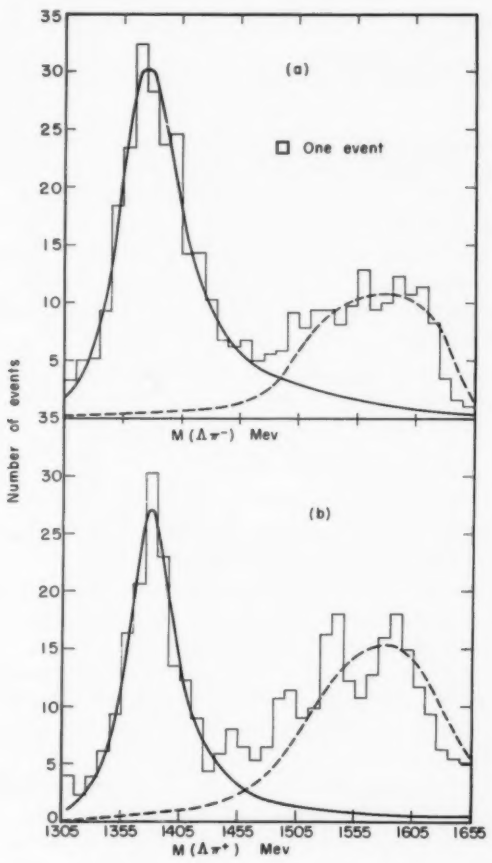

FIG. 1. Weighted histograms of the distribution in invariant mass $M(\Lambda,\pi) = [(E_\Lambda + E_\pi)^2 - (\vec{p}_\Lambda + \vec{p}_\pi)^2]^{1/2}$ for (a) $M(\Lambda,\pi^-)$ and (b) $M(\Lambda,\pi^+)$. The solid lines are the fits to a curve of the form $[(M-M_0)^2 + (\Gamma/2)^2]^{-1}$ of the data near the resonance energy. The corresponding values of M and $\Gamma/2$ are given in Table I. The dashed curves represent the expected values of $M(\Lambda,\pi)$ when the other pion resonates with the Λ.

We have fitted a resonance curve of the form $[(M-M_0)^2 + (\Gamma/2)^2]^{-1}$, modified by the three-body relativistic phase space, to the data near the resonance energy. The solid lines represent the best fits, and the corresponding values of M_0 and $\Gamma/2$ are given in Table I. It should be recognized that the values quoted were derived from a simplified model that omits momentum dependence of the

Table I. Summary of Y^* data.

	Number of events	M_0 (Mev)	$\Gamma/2$ (Mev)	Production angular distributions
Y^{*+}	154	1376 ± 3	24 ± 4	$(7.9 \pm 1.9) - (19.9 \pm 5.7)\cos\theta + (62.1 \pm 16.1)\cos^2\theta + (22.6 \pm 8.9)\cos^3\theta - (63.0 \pm 19.7)\cos^4\theta$
Y^{*-}	224	1376 ± 3	33 ± 5	$(15.5 \pm 2.0) - (0.1 \pm 6.0)\cos\theta + (15.5 \pm 5.1)\cos^2\theta - (21.9 \pm 9.7)\cos^3\theta$

matrix elements[9] and Bose-statistics symmetrization effects.[10] The dashed curves represent the expected values of $M(\Lambda, \pi)$ when the other pion resonates with the Λ.

Although our data allow as much as a 10% nonresonating background, the data are consistent with the assumption that all reactions (1) proceed in two stages:

$$\text{(a) } K^- + p \to Y^{*\pm} + \pi_1^{\mp}$$

and

$$\text{(b) } Y^{*\pm} \to \Lambda + \pi_2^{\pm}.$$

The ratio of $\sigma(K^- + p \to Y^{*-} + \pi^+)/\sigma(K^- + p \to Y^{*+} + \pi^-) = 1.45 \pm 0.15$ indicates that both $T=0$ and $T=1$ production amplitudes are present.

Only those 378 events with 1310 Mev $< M_{\Lambda\pi} <$ 1450 Mev are used in the subsequent analysis. Restricting the range of accepted mass values to $M_0 \pm 30$ Mev does not alter any of our conclusions.

The Y^*-production angular distributions in the K-p center-of-mass system are shown in Fig. 2. The marked difference between the Y^{*+} and Y^{*-} distributions illustrates the interference between the $T=1$ and $T=0$ production amplitudes. The best fits to a power series in $\cos\theta$ are shown as the solid lines, with coefficients as listed in Table I. In each case the addition of higher powers of $\cos\theta$ did not improve the fit, but the $\cos^3\theta$ and $\cos^4\theta$ terms were necessary.

The large negative coefficient of the $\cos^4\theta$ term in the Y^{*+} distribution is characteristic of D-wave production of a $J=3/2$ resonance (the expected distribution for D-wave production of a $J=3/2$ Y^* from a $j=5/2$ initial state is $1+10\cos^2\theta-10\cos^4\theta$.[11] The D-wave production of a Y^* with $J=1/2$ always predicts a positive coefficient for $\cos^4\theta$. However, the negative coefficient depends strongly on the relatively small number of Y^{*+} events produced with $\cos(\vec{Y}^*, \vec{K}) < -0.8$. This region is especially subject to the bias against low-momentum Λ's mentioned above. A correction for this bias does not alter the above conclusions, but reduces their statistical significance.

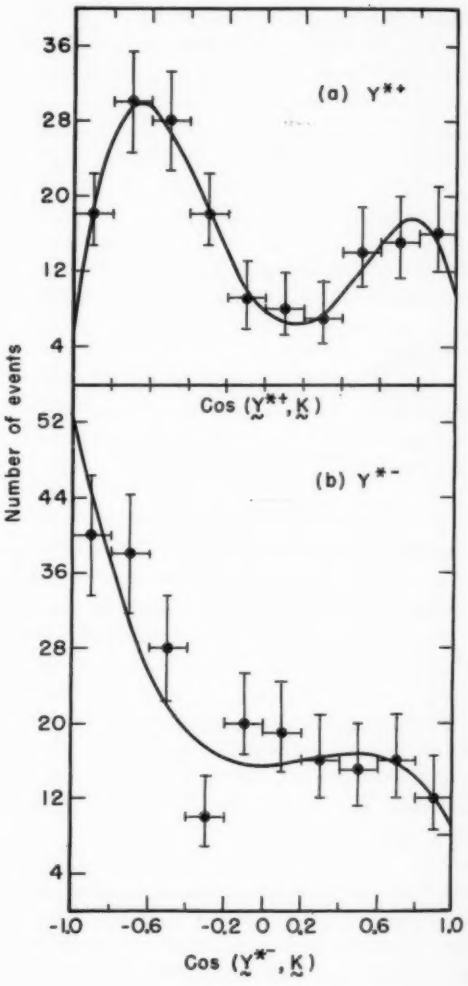

FIG. 2. Production angular distributions of (a) Y^{*+} and (b) Y^{*-} events. The solid curves represent the best fits to a power series in $\cos(\vec{Y}^*, \vec{K})$. The equations for these curves are given in Table I.

Several tests have been suggested that relate the decay angular distributions to the spin state of the Y^*.[12-14] In general, the interpretation of these

tests assumes that there are no interactions between the recoil pion, π_1, and the decay products, Λ and π_2; and that the Y^* is in a state of definite parity. If $J=1/2$, the momentum vector ($\vec{\Lambda}$) of the Λ in the Y^* center of mass must be isotropically distributed. If $J \geq 3/2$, it is possible to achieve an alignment of the Y^* in the production process, which will in turn produce an anisotropy in the distribution of $\vec{\Lambda}$ about the axis of alignment.

Adair[12] has shown that for reaction (a), conservation of the component of angular momentum along the incoming beam direction requires, for $J>1/2$, an alignment for those Y^*'s that are produced along the incident beam direction ($\vec{K}$). Specifically, for $J=3/2$, the Λ distribution must be $1+3\cos^2(\vec{\Lambda},\vec{K})$. The necessity of using nonzero production angles reduces this effect when partial waves with $l>0$ are present in the production process. For D-wave production of a $J=3/2$ Y^*, the process of averaging over a cone of production angles with $|\cos(\vec{Y}^*,\vec{K})| \geq 0.9$ is expected to dilute the distribution to approximately $1+\cos^2(\vec{\Lambda},\vec{K})$. The histogram in $\cos(\vec{\Lambda},\vec{K})$ for those 41 events with $|\cos(\vec{Y}^*,\vec{K})| \geq 0.9$ is shown in Fig. 3(a). The solid curve is a fit to the distribution $1+a\cos^2(\vec{\Lambda},\vec{K})$, with $a=1.0\pm0.8$. Since only 41 events are used, this result cannot distinguish $J=1/2$ from higher spins.

However, Stapp[13] has pointed out that a $J=3/2$ Y^* may preferentially emit Λ's perpendicular to the K axis, either in or perpendicular to the production plane.[15] This preferential emission is expected to be maximal when the Y^* is produced at 90 deg. We find a decided preference for decay perpendicular to the production plane. Figure 3(b) shows the distribution in $\cos(\vec{\Lambda},\vec{K}\times\vec{Y}^*)$ for those 143 events with $|\cos(\vec{Y}^*,\vec{K})|<0.5$. (Note that these events are different from those used in the Adair analysis.) The distribution fits the form $1+a\cos^2(\vec{\Lambda},\vec{K}\times\vec{Y}^*)$ with $a=1.5\pm0.4$. A χ^2 test yields a probability of 10^{-4} that this distribution would arise from an isotropic population. Indications of this effect were found by Alston et al.,[1] and serve to increase the confidence level for anisotropy. This result clearly favors $J \geq 3/2$ for the Y^* system.

As a check on the validity of the isolated Y^* model, we have examined the decay distributions for asymmetries that cannot be present in the decay of an isolated Y^*. In previous experiments at lower K^- momenta, the distributions of $\vec{\Lambda}$ relative to the Y^* direction have shown forward-backward asymmetries. These asymmetries have been attributed to the Bose-statistics symmetrization effects, which are expected to be less important at a K^- momentum of 1.11 Bev/c.[10] A fit of all Y^* events to a $1+a\cos(\vec{\Lambda},\vec{Y}^*)$ distribution gives the values $a_+ = -0.31\pm0.17$ for the Y^{*+}, and $a_- = -0.13 \pm 0.13$ for the Y^{*-}. These coefficients have the same sign as, but are a factor of 3 smaller in magnitude than, those found at a K^- momentum of 800 Mev/c.[16] The distributions in $\cos(\vec{\Lambda},\vec{K})$ and $\cos(\vec{\Lambda},\vec{K}\times\vec{Y}^*)$, for those events used in Fig. 3, show no asymmetry, i.e., the coefficients of $\cos\theta$ are $+0.24\pm0.31$ and $+0.07\pm0.24$, respectively.[17]

If the interference effects are as small as estimated, the observed anisotropy about the production normal implies $J \geq 3/2$. The production angular distribution and the Adair distributions are both consistent with this hypothesis.

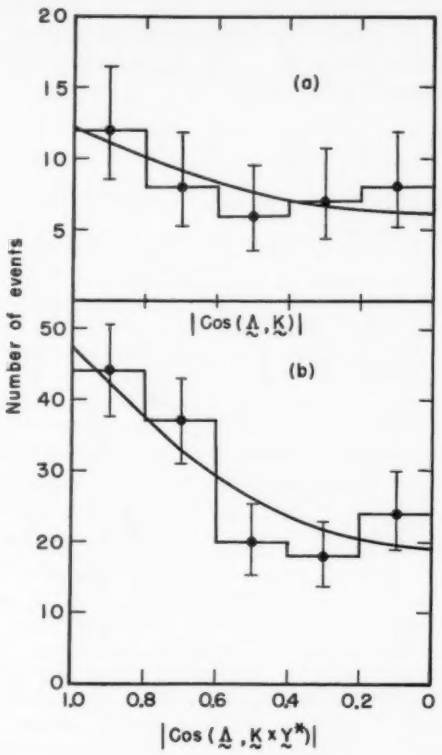

FIG. 3. Two methods used in testing for the spin of the Y^*: (a) The Adair distribution in $\cos(\vec{\Lambda},\vec{K})$ for those 41 events with $|\cos(\vec{Y}^*,\vec{K}| \geq 0.9$. The solid curve is the best fit to $1+a\cos^2(\vec{\Lambda},\vec{K})$ with $a=1.0\pm0.8$. (b) The distribution in $\cos(\vec{\Lambda},\vec{K}\times\vec{Y}^*)$ for those 143 events with $|\cos(\vec{Y}^*,\vec{K})|<0.5$. The solid curve is the best fit to $1+a\cos^2(\vec{\Lambda},\vec{K}\times\vec{Y}^*)$ and yields $a=1.5\pm0.4$.

We are indebted to Dr. A. Pais, Dr. R. H. Dalitz, and Dr. D. Miller for stimulating discussions. It is a pleasure to acknowledge the scanning effort of Mrs. Mattie L. Woodford.

---

†Work done under the auspices of the U. S. Atomic Energy Commission.

[1]M. Alston, L. W. Alvarez, P. Eberhard, M. L. Good, W. Graziano, H. K. Ticho, and S. G. Wojcicki, Phys. Rev. Letters 5, 520 (1960); 7, 472(E) (1961).

[2]M. Gell-Mann, Phys. Rev. 106, 1296 (1957).

[3]D. Amati, B. Vitale, and A. Stanghellini, Phys. Rev. Letters 5, 524 (1960).

[4]L. T. Kerth and A. Pais, Lawrence Radiation Laboratory Report UCRL-9706, 1961 (unpublished).

[5]J. P. Berge, P. Bastien, O. Dahl, M. Ferro-Luzzi, J. Kirz, D. H. Miller, J. J. Murray, A. H. Rosenfeld, R. D. Tripp, and M. B. Watson, Phys. Rev. Letters 6, 557 (1961).

[6]H. J. Martin, L. B. Leipuner, W. Chinowsky, F. T. Shively, and R. K. Adair, Phys. Rev. Letters 6, 283 (1961); R. P. Ely, S. Y. Fung, G. Gidal, Y. L. Pan, W. M. Powell, and H. S. White, Bull. Am. Phys. Soc. 6, 291 (1961); and M. M. Block, E. B. Brucker, R. Gessaroli, T. Kikuchi, A. Kovacs, C. M. Meltzer, R. Kraemer, M. Nussbaum, A. Pevsner, P. Schlein, R. Strand, H. O. Cohn, E. M. Harth, J. Leitner, L. Lendinara, L. Monari, and G. Puppi, Nuovo cimento 20, 724 (1961).

[7]R. H. Dalitz and S. F. Tuan, Phys. Rev. Letters 2, 425 (1959); R. H. Dalitz, Phys. Rev. Letters 6, 239 (1961).

[8]P. Eberhard, M. L. Good, and H. K. Ticho, Rev. Sci. Instr. 31, 1054 (1960).

[9]R. K. Adair, Revs. Modern Phys. 33, 406 (1961).

[10]R. H. Dalitz and D. H. Miller, Phys. Rev. Letters 6, 562 (1961).

[11]We wish to thank Dr. Donald H. Miller for calling this to our attention.

[12]R. K. Adair, Phys. Rev. 100, 1540 (1955).

[13]H. P. Stapp, Lawrence Radiation Laboratory Report UCRL-9526, 1960 (unpublished).

[14]See, for example, R. Gatto and H. P. Stapp, Phys. Rev. 121, 1553 (1961); R. H. Capps, Phys. Rev. 122, 929 (1961); and G. Morpurgo, Nuovo cimento 3, 1069 (1956).

[15]This distribution is kinematically related to Eq. (5) of reference 13. We have performed the suggested weighted average, and find a result 3 standard errors from that which is predicted if $J=1/2$. However, the number of events is insufficient to test the detailed shape of Eq. (5).

[16]J. P. Berge, M. Ferro-Luzzi, and A. H. Rosenfeld, Lawrence Radiation Laboratory, University of California, Berkeley (private communication).

[17]Although we have not estimated the Bose effect in detail, a calculation of the S and P wave production of an $s_{1/2}$ resonance can have a distribution in $\cos(\vec{\Lambda},\vec{K}\times\vec{Y}^*)$ no stronger than $1+0.2\cos^2(\vec{\Lambda},\vec{K}\times\vec{Y}^*)$. The introduction of D waves does not appear to alter these conclusions.

K^* AND $K^+-3\pi$ DECAY

Riazuddin
Physics Department, Panjab University, Lahore, Pakistan

and

Fayyazuddin
Physics Department, Imperial College, London, England

(Received November 3, 1961)

It is well known[1] that the spectrum of the unlike pion in the τ^+-decay mode of K^+ mesons deviates noticeably from the pure statistical distribution. Many people[2] have tried to explain this deviation as due to pion-pion "final state" interaction. On the basis of their analysis of the τ-decay spectrum, these people,[2] however, obtained pion-pion S-wave scattering lengths which do not agree with those obtained[3] on the basis of the crossing relations developed by Chew and Mandelstam.[4] In this note we wish to show that the observed deviation of the spectrum of the unlike pion in τ^+ decay from the statistical distribution can be simply explained if τ^+ decay proceeds via K^* (see Fig. 1) provided that K^* has spin unity, in favor of which there is some slight evidence.[5] On this model the spectrum of the unlike pion in $\tau^{+\prime}$ decay comes out to be the same as given by Weinberg[6] on the basis of $|\Delta\vec{I}|=\frac{1}{2}$ rule and is consistent with experiment.[7] Below we give the details of the calculation.

Denote the 4-momenta of the three emerging pions from K-meson decay by k_1, k_2, and k_3, where k_3 will always refer to the unlike pion in the τ or τ' decay mode. Let K denote the 4-momentum of the K-meson ($K^2=-m_K^2$). We introduce the

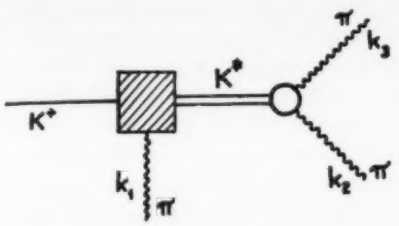

FIG. 1. Feynman diagram for the τ decay mode of the K meson via K^*.

three scalar variables,

$$s_1 = -(K - k_1)^2,$$
$$s_2 = -(K - k_2)^2,$$
$$s_3 = -(K - k_3)^2, \tag{1}$$

where

$$s_1 + s_2 + s_3 = m_K^2 + 3m_\pi^2. \tag{2}$$

Let T_1, T_2, and T_3 denote the kinetic energies of the three pions in the rest system of the K meson. In a nonrelativistic treatment of the decay spectrum, it is convenient to introduce the Dalitz[1] variables

$$x = \sqrt{3}\,(T_1 - T_2)/Q,$$
$$y = (3T_3 - Q)/Q, \tag{3}$$

where $Q = T_1 + T_2 + T_3$. Then, aside from a constant factor, the decay spectrum is given by

$$dw(x, y) = |M|^2 dx dy, \tag{4}$$

where M is the matrix element for $K - 3\pi$ decay and $x^2 + y^2 \leq 1$.

Gell-Mann and Rosenfeld[8] showed that a good empirical fit to the τ^+-decay data, obtained from a plot compiled by Dalitz,[1] is obtained with

$$M_\tau \sim 1 + \tfrac{1}{10} y. \tag{5}$$

We now show that the Feynman diagram shown in Fig. 1 leads to a matrix element of the form (5) for τ^+ decay provided that K^* has spin unity. If K^* has spin unity, Fig. 1 gives, for τ^+ decay, a matrix element of the form

$$g_{K^{0*}} f_{K^{0*}} (s_2 - s_3)/(-s_1 + m_{K^*}^2),$$

where $g_{K^{0*}}$ is the strong coupling constant for the reaction $K^* \to K + \pi$ and $f_{K^{0*}}$ is the weak coupling constant for the decay $K^{0*} \to \pi^+ + \pi^-$. Hence the matrix element for τ^+ decay is given by

$$M_\tau(s_1, s_2, s_3) = \lambda + g_{K^{0*}} f_{K^{0*}} (s_2 - s_3)/(-s_1 + m_{K^*}^2) + \text{same expression with } s_1 \text{ and } s_2 \text{ interchanged}$$

$$= \lambda + g_{K^{0*}} f_{K^{0*}} \left[\frac{s_2 - s_3}{-s_1 + m_{K^*}^2} + \frac{s_1 - s_3}{-s_2 + m_{K^*}^2} \right], \tag{6}$$

where λ is a constant which represents the contribution from intermediate states of higher energy (and corresponds to the subtraction constant in dispersion relations). If we consider the matrix element M_τ at the symmetric point $s_1 = s_2 = s_3 = s_0 = \frac{1}{3} m_K^2 + m_\pi^2$, we find $\lambda = M_\tau(s_0, s_0, s_0)$. Now the maximum value of s_1 or s_2 in τ decay is $(m_K - m_\pi)^2 \approx 6.25\, m_\pi^2$, while $m_{K^*}^2 \approx 40\, m_\pi^2$. Therefore we can neglect s_1 and s_2 as compared with $m_{K^*}^2$ in the denominators of the above expression, so that (6) becomes

$$M_\tau = \lambda + g_{K^{0*}} f_{K^{0*}} (s_1 + s_2 - 2s_3)/m_{K^*}^2,$$

which, on using (2) and (3), becomes

$$M_\tau = \lambda \left[1 + \frac{g_{K^{0*}} f_{K^{0*}}}{\lambda} \left(\frac{2 m_K Q}{m_{K^*}^2} \right) y \right] \tag{7}$$

Now putting in the experimental values of m_K, m_{K^*}, and Q (≈ 75 Mev), we get $2m_K Q/m_{K^*}^2 \approx \frac{1}{10}$. Hence if we take $\lambda \approx g_{K^{0*}} f_{K^{0*}}$ (or, what is the same thing, $\lambda \approx f_{K^{0*}}$ since $g_{K^{0*}}$ has been shown to be of the order of unity by Chan[5]), Eq. (7) reduces to (5) which has been shown to fit the τ^+-decay data by Gell-Mann and Rosenfeld[8] and Weinberg.[6]

Note that if K^* has spin zero, then in Eq. (6), $(s_2 - s_3)$ and $(s_1 - s_3)$ do not appear and if we neglect s_1 and s_2 as compared with $m_{K^*}^2$, the matrix element is constant and the spectrum will not deviate from the statistical distribution.

For $\tau^{+\prime}$ decay, we get the matrix element (corresponding to the diagram in Fig. 1)

$$M_{\tau'} = \lambda' + g_{K^{+*}} f_{K^{+*}} (2m_K Q/m_{K^*}^2) y,$$

where $\lambda' = M_{\tau'}(s_0, s_0, s_0)$. It is well known that the $|\Delta\vec{I}| \leq \frac{3}{2}$ rule[2,6,8] gives $\lambda' = \lambda/2$. It can be shown that

$$g_{K^{+*}} = -g_{K^{0*}}/\sqrt{2},$$

and, if we assume the $|\Delta\vec{I}| = \frac{1}{2}$ rule,

$$f_{K^{+*}} = \sqrt{2} f_{K^{0*}},$$

so that

$$M_{\tau'} = \tfrac{1}{2}\lambda\left[1 - 2\frac{g_{K^{0*}} f_{K^{0*}}}{\lambda}\left(\frac{2m_K Q}{m_{K^*}{}^2}\right)y\right]. \qquad (8)$$

Note that the factors multiplying y in Eqs. (7) and (8) are in the ratio 1:-2 which is the same result as obtained by Weinberg[6] on the basis of the $|\Delta\vec{I}| = \frac{1}{2}$ rule. Now taking as before $g_{K^{0*}} f_{K^{0*}} \approx \lambda$, Eq. (8) becomes

$$M_{\tau'} = \tfrac{1}{2}\lambda[1 - 2\tfrac{1}{10}y], \qquad (9)$$

which is consistent with the experiment.[6,7]

Note that for $\tau^{+\prime}$ decay another diagram, which is obtained from Fig. 1 by replacing $k_1(\pi^0)$ with $k_3(\pi^+)$, is also possible. But it is easy to see that on symmetrization between k_1 and k_2 this gives zero.

We are indebted to Dr. P. T. Matthews and Professor A. Salam for encouragement and advice. We gratefully acknowledge the financial help given by the Pakistan Atomic Energy Commission. One of us (R) would like to thank CERN and the Physics Department, Imperial College, London, where this work was done, for hospitality. The other (F) is grateful to the British Department of Technical Cooperation for the award of a Fellowship under the Colombo Plan.

[1]S. McKenna et al., Nuovo cimento 10, 763 (1958); R. H. Dalitz, Reports on Progress in Physics (The Physical Society, London, 1957), Vol. 20, p. 163; and Phys. Rev. 94, 1046 (1954). See also E. Fabri, Nuovo cimento 11, 479 (1954).

[2]B. S. Thomas and W. G. Holladay, Phys. Rev. 115, 1329 (1959); N. N. Khuri and S. B. Treiman, Phys. Rev. 119, 1115 (1960); R. F. Sawyer and K. C. Wali, Phys. Rev. 119, 1929 (1960). See also A. N. Mitra and E. Lomon, Proceedings of the 1960 Annual International Conference on High-Energy Physics at Rochester (Interscience Publishers, New York, 1960). See also T. N. Truong, Phys. Rev. Letters 6, 308 (1961).

[3]B. R. Desai, Phys. Rev. Letters 6, 497 (1961); B. H. Bransden and J. W. Moffat, Phys. Rev. Letters 6, 708 (1961).

[4]G. F. Chew and S. Mandelstam, Phys. Rev. 119, 467 (1960); G. F. Chew and S. Mandelstam, Lawrence Radiation Laboratory Report UCRL-9126, 1960 [Nuovo cimento (to be published)].

[5]M. A. B. Bég and P. C. DeCelles, Phys. Rev. Letters 6, 145, 428(E) (1961); C. H. Chan, Phys. Rev. Letters 6, 383 (1961).

[6]S. Weinberg, Phys. Rev. Letters 4, 87 and 585(E) (1960).

[7]S. Bjorklund, E. L. Koller, and S. Taylor, Phys. Rev. Letters 4, 424, 475(E) (1960).

[8]M. Gell-Mann and A. H. Rosenfeld, Ann. Rev. Nuclear Sci. 7, 407 (1957).

VECTOR MESONS AND POSSIBLE VIOLATIONS OF CHARGE SYMMETRY IN STRONG INTERACTIONS

Sergio Fubini
Istituto di Fisica dell'Università, Torino, Italy and CERN, Geneva, Switzerland
(Received November 22, 1961)

The two vector bosons, $\rho \to 2\pi$ [1] and $\omega \to 3\pi$,[2] needed to understand the main features of the electromagnetic form factors of the nucleon, have been recently observed in several experiments, the masses of the ρ and ω being very close but the observed width of the ρ being much larger than that of ω.

A very important result has recently been obtained by the Berkeley group[3] which found that the wide ρ^0 resonance is split into two levels $\rho_1{}^0$, $\rho_2{}^0$ whose experimental widths are of the same order of magnitude as that of ω^0. The first tentative attribution of quantum numbers identifies the vector boson with the higher level $\rho_2{}^0$.

So the present very preliminary values of the masses of ρ^0 and ω^0 are the following:

$$m_{\omega^0} = 787 \pm 10 \text{ Mev}, \quad m_{\rho^0} = 775 \pm 10 \text{ Mev}.$$

The observed widths, ~10 Mev, coincide with the experimental resolution.

The equality, within experimental errors, of m_{ρ^0} and m_{ω^0} is quite intriguing since both particles have the same quantum numbers except

isospin (the 2π decay mode requires $T=1$ and the 3π, $T=0$), and both widths are smaller than 10 Mev and might well turn out to coincide.

Another important regularity appears if one considers the role of ρ^0 and ω^0 in the explanation of the main features of the electromagnetic form factors of the nucleon.[4] The equality of the masses together with the observed vanishing charge radius of the neutron imply that the residues of the ρ^0 and ω^0 poles in the charge form factors are nearly equal.

It seems unlikely that, if confirmed by future experiments, these amazing coincidences should be due to pure chance.

A first way of dealing with this situation is to assume the existence of some new kind of symmetry law, which must be satisfied very accurately by strong interactions leading to the near equality of the masses in the supermultiplet $\rho\,\omega^0$. This interpretation is somewhat artificial since we do not have in elementary particle physics other supermultiplets with such a small mass difference. For the supermultiplet $\Lambda\Sigma$, for example, the mass difference is about 70 Mev.

Another possibility is that ω^0 and ρ^0 are two decay modes of the same particle (which we shall denote by Γ), which, like the photon, does not have a well-defined isotopic spin.

In this Letter we wish to discuss the theoretical implications and experimental consequences of the existence of a neutral vector meson of mass of 780 Mev which can decay both into two pions and three pions.[5]

First of all, we have to consider whether the violation of charge symmetry (C.S.) in strong interactions, caused by the existence of the Γ meson, is in contradiction with the present experimental evidence for C.S. At first sight one would say that, since the width of Γ is certainly less than 10 Mev and probably even smaller, the coupling of Γ to the other strongly interacting particles is of the order of magnitude of the electromagnetic coupling and so the C.S. violation due to the presence of Γ will be rather small and compatible with experiment. This interpretation is, however, incorrect since we know that Γ's are produced in about 50% of the $p\bar{p}$ annihilation events.

So the question of the size of the C.S. violation induced by the Γ depends in our theory upon the role played by Γ in the different reactions and in particular on the manner in which its long lifetime can be reconciled with the large production rate.

A simple physical model is the following. The Γ is strongly coupled to nucleons but, due to its large mass, its density will be large only in the inner part $[\sim 1/(5.6\,m_\pi)]$ of the nucleon cloud. So the probability of producing a Γ will be quite large in those phenomena, like $p\bar{p}$ annihilation, in which the nucleon cores are essentially involved.

On the other hand, the 2π and 3π decay processes have to pass through a nucleon-antinucleon virtual state. This means that the interaction region has a very small radius $\sim 1/2M$. The small decay rates of the Γ might be therefore due to the strong effect of the centrifugal barrier since the pions are produced in p waves.[6]

Coming back to the question of charge symmetry, we observe that the only existing experimental tests of C.S. come from nuclear physics and low-energy pion physics at energies in which no real Γ can be produced so that the C.S. violation will only come from exchange of virtual Γ's. This effect can enter in two different manners: first in renormalizing the fundamental pion-nucleon vertex, secondly in the direct Γ exchange, for example, in nuclear forces.

Now the first effect is small due to the weak effective coupling $(\Gamma\pi)$; the second is unimportant at low energy, because of the short range of the contribution of nuclear forces from Γ exchange (1.5 times shorter than the range of the repulsive core). We think therefore that the large Γ mass together with its weak coupling to pions will probably make the C.S. violations small enough not to contradict the existing experiments.

We now come to the question of possible experimental checks of the validity of the proposed scheme. The most direct test has been suggested to me by J. Prentki. In the hypothesis of the unique Γ particle the ratio of the number of ρ^0 to that of ω^0 produced in any reaction will not depend on the kind of reaction, but only on the branching ratio $(\Gamma \to 2\pi)/(\Gamma \to 3\pi)$. For example, one can verify that the ratio of ρ^0 to ω^0 produced in $p\bar{p}$ annihilation is then the same as the ratio in pion-nucleon collisions.[7]

The violations of C.S. due to the existence of the Γ meson will occur mostly in those reactions in which the important effects come from the inner part of the nucleon cloud. So one expects important deviations from C.S. in nucleon-antinucleon annihilation and in pion-nucleon and nucleon-nucleon elastic scattering at large energy (~Bev) and large angles. A possible experiment is to

verify deviations of the branching ratio,

$$p+p \begin{cases} \nearrow \mathrm{He}^3+\pi^0 \\ \searrow \mathrm{H}^3+\pi^+, \end{cases}$$

from the value $\frac{1}{2}$ predicted by charge independence.

The existence of the Γ meson leads to an explanation of the main features of the nucleon form factors by means of a unique particle. The absence of any charge structure of the neutron at small momentum transfers can be now interpreted by saying that the coupling of the Γ to the nucleon is of the form $(1+\tau_3)/2$. The similarity of the Γ to the photon is now very striking: Both particles have the same quantum number and violate charge symmetry in the same manner.

It is amusing to note the analogy existing between our problem and the θ-τ puzzle. In the latter case one had two particles with equal masses and lifetimes having all the same quantum numbers except parity, the first decaying into two pions, the second into three. Also in that case two explanations were proposed: (1) a new kind of symmetry between couples of particles of opposite parity; the so-called "parity doublets." (2) θ and τ are two decay modes of the same particle which decays violating the conservation of parity. Nature has chosen the second possibility. One can also note the interesting analogy between the $(1+\gamma_5)$ appearing in parity-nonconserving interactions and the $(1+\tau_3)$ appearing in the interactions violating charge symmetry: In both cases there is maximum violation of the symmetry law.

When the first results on nucleon structure were showing a large charge structure for the proton and none for the neutron, the first reaction of many physicists was to consider these experiments as an indication for a violation of charge symmetry. Maybe this naive point of view will finally turn out to be the correct one.

The author has benefited by very useful criticism from many people in the CERN Theoretical Division. He wants to offer his special thanks to Professor D. Amati, Professor J. Prentki, Professor L. Van Hove, and Professor V. F. Weisskopf for their illuminating discussions.

---

[1]A. R. Erwin, R. March, W. D. Walker, and E. West, Phys. Rev. Letters 6, 628 (1961); D. Stonehill, C. Baltay, H. Courant, W. Fickinger, E. C. Fowler, H. Kraybill, J. Sandweiss, J. Sanford, and H. Taft, Phys. Rev. Letters 6, 624 (1961); E. Pickup, D. K. Robinson, and E. O. Salant, Phys. Rev. Letters 7, 192 (1961). Bologna, Orsay, and Saclay groups, presented by G. Puppi, Report at the International Conference on Elementary Particles, Aix-en-Provence, 1961 (unpublished).

[2]B. C. Maglić, L. W. Alvarez, A. H. Rosenfeld, and M. L. Stevenson, Phys. Rev. Letters 7, 178 (1961); A. Pevsner, Report at the International Conference on Elementary Particles, Aix-en-Provence, 1961 (unpublished).

[3]B. C. Maglić (private communication); J. Button, G. R. Kalbfleisch, G. Lynch, B. Maglić, A. H. Rosenfeld, and M. L. Stevenson, University of California Radiation Laboratory Report UCRL-9814 (to be published).

[4]S. Bergia, A. Stanghellini, S. Fubini, and C. Villi, Phys. Rev. Letters 6, 367 (1961).

[5]The matrix element for Γ decaying into three pions is of the form

$$\sum_{\alpha\beta\gamma} \epsilon_{\mu\alpha\beta\gamma} k_\alpha^{(1)} k_\beta^{(2)} k_\gamma^{(3)} F(k^{(1)}k^{(2)}, k^{(1)}k^{(3)}).$$

So the three final pions must be either in a p or in a higher l state. In the first case the final-state wave function is antisymmetric in the exchange of any pair of pions, which (because of Bose statistics) must all have different charge. From this we can see that the charged partner of Γ (which must go into either $\pi^+\pi^+\pi^-$ or $\pi^+\pi^0\pi^0$) can only decay into three pions in d wave and so the centrifugal barrier will make this decay rate very small.

[6]See matrix element in reference 5.

[7]In the case of $N\bar{N}$ annihilation, one has to measure the ratio of the number of ρ^0 produced in $N+\bar{N} \to (n+2)$ pions to the number of ω^0 produced in $N+\bar{N} \to (n+3)$ pions since they both correspond to the process $N+\bar{N} \to \Gamma+n$ pions.

IS ISOTOPIC SPIN A GOOD QUANTUM NUMBER FOR THE NEW ISOBARS?

Sheldon L. Glashow*

Institute of Theoretical Physics, Department of Physics, Stanford University, Stanford, California

(Received November 27, 1961)

Recent numbers of this Journal report discoveries of several relatively long-lived meson and hyperon isobars. Some of these display remarkable regularities in mass beyond what may be anticipated from known symmetry principles—the three members of the ($T=1$, $J=1$) 750-Mev two-pion resonance[1] (ρ) differ in mass from the ($T=0$, $J=1$) 785-Mev three-pion resonance[2] (ω) by only 4%; stranger yet, the masses of $Y_{(1)}$ (the $T=1$ hyperon isobar at 1385 Mev)[3] and $Y_{(0)}$ (the $T=0$ hyperon at 1400 Mev)[4] differ by about 1%. In both cases there is a near degeneracy in mass between an isotopic singlet and triplet.

Among particles of better pedigree, Σ and Λ hyperons also show this quadruplet structure, with a Σ,Λ mass splitting of 7%. This suggests the speculation[5] that the symmetry group of the strongest interactions is greater than the isotopic rotation group, and is such that these interactions leave degenerate Σ and Λ hyperons. The even more marked quadruplet structure of both vector bosons and hyperon isobars offers additional support to this view.

Whether nearly degenerate quadruplets are portents of symmetries to come, or whether they are mere acts of chance is not for now to say. In either case, the existence of two particles, identical in essential (i.e., rigorously conserved) quantum numbers and with neighboring masses, can cause a novel enhancement of virtual electromagnetic effects.

Suppose that ω and ρ_0 differ by no quantum number respected by electromagnetism. What linear combinations of these fields propagate with definite mass and definite lifetime? They are ω and ρ_0 themselves, so long as electromagnetism is ignored, for the strong interactions—we presume—conserve isotopic spin. But electromagnetism fails to conserve isotopic spin: The electric current includes both an isoscalar and isovector part. Thus electromagnetism may induce nonradiative transitions between ω and ρ_0.[6] Said another way, the mass (and lifetime) eigenstates, when electromagnetism operates, are no longer simply ρ_0 and ω but become superpositions of the two fields. The amount of admixing does not directly depend upon the relative strength of electromagnetic and strong couplings, but rather, upon the relative size of the transition matrix element between ρ_0 and ω and their mass difference. Thus the closeness of the two vector mesons' masses may greatly enhance the extent that their decays violate isotopic invariance.

In order to identify the "particles," we must diagonalize a two-by-two effective mass matrix describing the ρ_0,ω system: $M=M_0+M_1$. The complex diagonal matrix M_0 assigns to ρ_0 and ω their masses and lifetimes without radiative correction. The matrix M_1, in general complex and symmetric, describes the electromagnetic effects—its matrix elements are of order 1/137 those of M_0. The off-diagonal matrix element of M_1, which we call η, is just half the transition matrix element connecting ρ_0 and ω.

In any higher symmetry scheme, M_0 describes the ρ_0,ω mass splitting caused by the intermediate strength symmetry-breaking interactions (Issbi) as well as their mean mass determined by the symmetric strong interactions. As an approximation, Issbi may be neglected in the evaluation of M_1. Then, the "electromagnetic eigenstates," or eigenvectors of M_1, depend only on the structure of the higher symmetry group (they would be the "particles" were Issbi absent). In global symmetry,[5] they are $(1/\sqrt{2})(\rho_0\pm\omega)$. In the eightfold way[7] they are $\frac{1}{2}\rho_0\pm\frac{1}{2}\sqrt{3}\,\omega$ and $\frac{1}{2}\omega-\frac{1}{2}\sqrt{3}\,\rho_0$. The determination of the electromagnetic mass splitting between these states (and thereby, of η) is a dynamical problem far beyond the scope of this note.

For the ρ_0,ω system, we may expect that the electromagnetic matrix elements are small compared to the mass difference due to strong interactions. [Electromagnetic effects are typically several Mev, whereas the masses of the two vector particles differ by $\mathrm{Re}(\delta m)\sim 35$ Mev. Actually, we must also take into account their difference in lifetime, so that $|\delta m|\sim 50$ Mev.] Thus, one of the two eigenstates is dominantly ρ_0, the other dominantly ω. Dropping terms of order $\eta^2(\delta m)^{-2}$, we find for these eigenstates:

$$\tilde{\rho}_0=\rho_0+\eta(\delta m)^{-1}\omega,$$

$$\tilde{\omega}=\omega-\eta(\delta m)^{-1}\rho_0.$$

Because δm is relatively small, the amount of admixing is not at all negligible. When the isotopic spin conserving interactions of ρ_0 and ω are expressed in terms of the "particles" $\tilde{\rho}_0$ and $\tilde{\omega}$, a

significant probability is revealed for the $\tilde{\rho}_0$ to decay into the three-pion channel and for $\tilde{\omega}$ to decay into the two-pion channel. The narrower experimental width of the three-pion channel means that the second effect is far the more important of the two. With $\eta \sim 5$ Mev as a pure guess, about 5% of all $\tilde{\omega}$ should decay into two pions. Experimentally, this effect might be misinterpreted as evidence for a second ρ_0 at 790 Mev, except that it is absent for the charged partners of ρ_0.[8]

The case for $Y_{(1)}^0$ and $Y_{(0)}$ is similar. The mass difference is smaller, $|\delta m| \sim 20$ Mev, so that the departures from charge independence could be more pronounced. With $\eta \sim 5$ Mev, the eigenstates,

$$\tilde{Y}_{(1)}^0 = Y_{(1)}^0 + \eta(\delta m)^{-1} Y_{(0)},$$

and

$$\tilde{Y}_{(0)} = Y_{(0)} - \eta(\delta m)^{-1} Y_{(1)}^0,$$

involve admixtures of 25% in amplitude. The principal decay mode of $\tilde{Y}_{(0)}$ is $\tilde{Y}_{(0)} \to (\Sigma + \pi)_{T=0}$ and that of $\tilde{Y}_{(1)}^0$ is $\tilde{Y}_{(1)}^0 \to \Lambda + \pi^0$.[9] Radiative corrections allow the isospin-violating modes $\tilde{Y}_{(0)} \to \Lambda + \pi^0$ and $\tilde{Y}_{(1)}^0 \to (\Sigma + \pi)_{T=0}$. With the $(\Sigma + \pi)_{T=0}$ channel assumed three times narrower than the $\Lambda + \pi$ channel (in accordance with phase space—for experimentally there are as yet only upper bounds for the widths), we find for the branching ratios of the anomalous modes: 2% for $\tilde{Y}_{(1)}^0$ and 20% for $\tilde{Y}_{(0)}$. Since we have guessed both η and the relative widths of the two states, this result could be very much in error. However, the existence of such an effect as we discuss depends critically on the assumption that $Y_{(0)}$ and $Y_{(1)}$ share the same values of spin and parity. The observation of a significant branching ratio for $\tilde{Y}_{(0)} \to \Lambda + \pi^0$ would be very convincing evidence for this assertion.

I wish to thank Professor M. Baker, Professor J. Dreitlein, Professor D. Walecka, and Mr. K. Nordtvedt for their helpful comments.

*Work supported in part by the U. S. Air Force through the Air Force Office of Scientific Research.

[1]J. Anderson, V. Bang, P. Burke, D. Carmony, and N. Schmitz, Phys. Rev. Letters 6, 365 (1961); A. Erwin, R. March, W. Walker, and E. West, Phys. Rev. Letters 6, 628 (1961).

[2]B. Maglić, L. Alvarez, A. Rosenfeld, and M. Stevenson, Phys. Rev. Letters 7, 178 (1961); N. Xuong and G. Lynch, Phys. Rev. Letters 7, 327 (1961).

[3]M. Alston, L. Alvarez, P. Eberhard, M. Good, W. Graziano, H. Ticho, and S. Wojcicki, Phys. Rev. Letters 5, 520 (1960); later references may be found in our reference 4.

[4]M. Alston, L. Alvarez, P. Eberhard, M. Good, W. Graziano, H. Ticho, and S. Wojcicki, Phys. Rev. Letters 6, 698 (1961); P. Bastien, M. Ferro-Luzzi, and A. Rosenfeld, Phys. Rev. Letters 6, 702 (1961).

[5]There have been many such ideas, starting perhaps with the contributions of M. Gell-Mann, J. Schwinger, and J. Tiomno, in the Proceedings of the 1957 International Conference on High-Energy Physics at Rochester (Interscience Publishers, Inc., New York, 1957), Vol. IX, pp. 6-29.

[6]Should both ρ_0 and ω contribute to electromagnetic form factors, the virtual sequence $\rho_0 \leftrightarrow \gamma \leftrightarrow \omega$ is allowed and generates a nonvanishing matrix element connecting ω and ρ_0. An estimate of the transition rate between ω and ρ_0 due to this diagram may be made if their contributions to the nucleon form factors, their coupling constants to nucleons, and their widths are known. Our guess, $\eta \sim 5$ Mev, is consistent with such an estimate, with current experimental data, the value $(g^2/4\chi)_{\rho\bar{N}N} \sim 0.3$ [W. K. R. Watson (private communication)], and a similar value for the strength of the ω-nucleon coupling. However, this estimate is not reliable. It requires knowledge of form factors and coupling constants near the ω or ρ_0 mass shells, not at low momentum transfer; furthermore, diagrams with other intermediate states like $\rho_0 \leftrightarrow \gamma + \pi^0 \leftrightarrow \omega$, cannot be neglected.

[7]M. Gell-Mann, Phys. Rev. (to be published); Y. Ne'eman, Nuclear Phys. 26, 222 (1961).

[8]The relative size of the two-pion peaks due to $\tilde{\rho}_0$ and $\tilde{\omega}$ depends upon the experiment considered—the anomalous peak would be more striking if more $\tilde{\omega}$ were produced than $\tilde{\rho}_0$.

[9]The decay mode $Y_{(1)}^0 \to (\Sigma + \pi)_{T=1}$ conserves isotopic spin, but mysteriously seems to be absent. It could be forbidden by assuming R invariance. See J. J. Sakurai, Phys. Rev. Letters 7, 426 (1961).

SCALAR NUCLEON FORM FACTOR $F_1^n + F_1^p$ *

Norman K. Glendenning and Gustav Kramer†
Lawrence Radiation Laboratory, University of California, Berkeley, California
(Received October 23, 1961)

All meson-theoretic derivations of nucleon-nucleon potentials agree that the outer region should behave like the one-pion exchange potential (OPEP). The inner region cannot be calculated unambiguously, however, and is therefore usually treated phenomenologically.

The modification of the inner region in such a way as to fit the low-energy n-p data is the subject of a forthcoming work.[1] There we discovered that the integrals that enter the deuteron electromagnetic form factor G^2 are very insensitive to the inner region of the potential for $q \lesssim 3$ f^{-1}, and are therefore determined by the well-established OPEP tail. This fact can be used to extract the sum of the neutron and proton charge form factors $F_1^p + F_1^n$ with practically no uncertainty arising from our imperfect knowledge of the n-p force. The sum $F_1^p + F_1^n$ is obtained from the expression[2]

$$G_{\text{exp}}^2 = (F_1^p + F_1^n)^2 (G_0^2 + G_2^2) + [2\tan^2(\theta/2) + 1] G_{\text{mag}}^2, \quad (1)$$

where G_0, G_2, G_{mag} are, respectively, the contributions from the spherical and quadrupole charge distributions and the magnetic moment.[3] In addition to F_1^p and F_1^n, G_{mag} contains also the magnetic parts of the nucleon form factors F_2^p and F_2^n. Since G_{mag} is almost everywhere at least two orders of magnitude less than $G_0^2 + G_2^2$, its value will effect at most the third figure of $F_1^p + F_1^n$ (except at large angles, which we avoid). Since the already published neutron form factors of Hofstadter et al.[4] should allow us to compute G_{mag} to at least one significant figure, we shall use the published values of the nucleon form factors in G_{mag}.

We have used the experimental cross section for elastic electron-deuteron scattering of Friedman, Kendall, and Gram[5] to find $G_{\text{exp}}^2 = (d\sigma/d\Omega)_{\text{exp}}/(d\sigma/d\Omega)_0$, where $(d\sigma/d\Omega)_0$ is the cross section for electron scattering from a spinless point charge.

Drawing a smooth curve through a recent experimental measurement[6] of the proton charge form factor F_1^p, we obtained values for this quantity which we subtracted from our value of $F_1^p + F_1^n$ to get the neutron charge form factor. Our results are tabulated in Table I. The upper and lower limit on $F_1^n + F_1^p$ come both from the experimental uncertainty in G_{exp}^2 and the slight uncertainty in the integrals appearing on the right side of Eq. (1) arising from our imperfect knowledge of the nucleon force at small distances.

As can be seen from the table, it is consistent with the existent data to say that the neutron charge form factor F_1^n is zero, at least up to a momentum transfer $q = 3$ f^{-1}. However, most of the data suggest a very small negative value of the form factor.

Our results do not agree with those of the Stan-

Table I. Upper and lower limits on the scalar nucleon form factor $F_1^n + F_1^p$ and the neutron form factor F_1^n deduced from the experimental proton and deuteron form factors F_1^p and G are shown. We obtain F_1^p by drawing a smooth curve through the experimental points of reference 6.

q (f^{-1})	θ (deg)	G^2 exp	$F_1^n + F_1^p$ Lower	$F_1^n + F_1^p$ Upper	F_1^p exp	F_1^n Lower	F_1^n Upper
0.99	60.0	0.266 ±0.025	0.781	0.877	0.901	-0.120	-0.024
1.07	70.0	0.241 ±0.023	0.789	0.890	0.889	-0.100	0.001
1.36	90.0	0.151 ±0.015	0.779	0.897	0.839	-0.060	0.058
1.51	105.0	0.101 ±0.009	0.716	0.824	0.809	-0.093	0.015
1.79	43.0	0.0496 ±0.0048	0.638	0.751	0.748	-0.110	0.003
1.99	48.5	0.0290 ±0.0027	0.574	0.685	0.706	-0.132	-0.021
2.22	55.0	0.0225 ±0.0022	0.610	0.744	0.658	-0.048	0.086
2.41	61.0	0.0107 ±0.0009	0.489	0.600	0.619	-0.130	-0.019
2.61	67.5	0.00733 ±0.00077	0.467	0.598	0.578	-0.111	0.020
2.82	75.0	0.00422 ±0.00042	0.413	0.537	0.538	-0.125	-0.001

ford[4] and Cornell[7] groups who analyzed the inelastic (deuteron breakup) process. However, no analysis of the inelastic process to date has accounted for the presence of the D state in the deuteron, nor all of the final-state interactions, except in a rough manner.[2,8]

There is some uncertainty introduced into our results by unknown relativistic and meson-current effects. Nevertheless we feel that these effects will be small in the region of low momentum transfer considered here.[9]

---

*Work supported by the U. S. Atomic Energy Commission.

†On leave from the University of Heidelberg, Heidelberg, Germany.

[1]N. K. Glendenning and G. Kramer, Lawrence Radiation Laboratory Report UCRL-9904 (to be published). The potentials were required to yield the deuteron binding energy and quadrupole moment and give a scattering phase shift at zero energy consistent with the known scattering length. In addition, the phase shifts at higher energies were calculated and they agree roughly with the analysis of the experimental data at 95 Mev by M. H. MacGregor, Phys. Rev. 123, 2154 (1961), and with two of the solutions in the energy range up to 300 Mev of M. H. Hull, K. E. Lassila, H. M. Ruppel, F. A. McDonald, and G. Breit, Phys. Rev. 122, 1606 (1961).

[2]V. Z. Jankus, Phys. Rev. 102, 1586 (1956).

[3]R. Hofstadter, Ann. Rev. Nuclear Sci. 7, 231 (1957).

[4]R. Hofstadter, C. de Vries, and R. Herman, Phys. Rev. Letters 6, 290 (1961); R. Hofstadter and R. Herman, Phys. Rev. Letters 6, 293 (1961). We used Eqs. (9) through (12) in the second of these references.

[5]J. I. Friedman, H. W. Kendall, and P. A. M. Gram, Phys. Rev. 120, 992 (1960).

[6]F. Bumiller, H. Croissiaux, E. Dally, and R. Hofstadter, Phys. Rev. 124, 1623 (1961).

[7]D. N. Olson, H. F. Schopper, and R. R. Wilson, Phys. Rev. Letters 6, 286 (1961). R. M. Littauer, H. F. Schopper, and R. R. Wilson, Phys. Rev. Letters 6, 141 (1961); 6, 144 (1961).

[8]L. Durand, III, Phys. Rev. Letters 6, 631 (1961); Phys. Rev. 123, 1393 (1961).

[9]R. Blankenbecler, thesis, Stanford University, 1958 (unpublished), has studied relativistic corrections, using a simplified model of the deuteron (two bosons, one of which is charged, bound by a separable potential). In this model the corrections can give rise to a 25 to 30% reduction in the cross section at $q = 3$ f^{-1} which would mean that the scalar charge form factor would be larger by as much as 15%. Whether the corrections would be as large in a realistic model is not clear. However, suppose that this is the correction that obtains at $q = 3$ f^{-1}. Then if we applied a correction that is 15% at $q = 3$ f^{-1} and goes linearly to zero as $q \to 0$, the limits we place on F_1^n would lie one above and one below the zero value for all values of q listed in our table except at $q = 2.2$ f^{-1}, where both limits are positive.

ERRATA

RESONANCE IN THE $\Lambda\pi$ SYSTEM. Margaret Alston, Luis W. Alvarez, Philippe Eberhard, Myron L. Good, William Graziano, Harold K. Ticho, and Stanley G. Wojcicki [Phys. Rev. Letters 5, 520 (1960)].

Due to a typographical error, a sentence in the second paragraph on page 523, line 26, is incorrect and should read: "We find the ratio of events with $|\xi| < 0.5$ to all events is 0.355." The conclusions of the paragraph remain unchanged.

π-π RESONANCE IN π^--p INTERACTIONS AT 1.25 Bev. E. Pickup, D. K. Robinson, and E. O. Salant [Phys. Rev. Letters 7, 192 (1961)].

Due to a computational error, the mean value of the $\pi^-\pi^0$ and $\pi^-\pi^+$ cross sections at the maximum of the resonance was incorrectly stated as $\sigma_{\pi-\pi} = 95$ mb. The correct value is 65.0 ± 7.5 mb. The values of the ordinate in Fig. 3 should be multiplied by 0.68.

LIFETIME EFFECTS IN CONDENSED FERMION SYSTEMS. A. Bardasis and J. R. Schrieffer [Phys. Rev. Letters 7, 79 (1961)].

It has been pointed out by P. Nozières that a more accurate estimate of the damping coefficient α for He^3 can be made with the aid of the theoretical expression for the thermal conductivity given by Abrikosov and Khalatnikov.[1] Our original assumption that the thermal conductivity relaxation time is given by

$$\tau = \hbar/2\alpha(kT)^2,$$

leads to $\alpha = 9.1 \times 10^{16}$ erg$^{-1} \simeq 37.6/E_F$. The more refined estimate using $m^* = 2.82\ m$ gives $\alpha = 4.27 \times 10^{15}$ erg$^{-1} \simeq 1.77/E_F$. With this value one finds that damping effects reduce the transition temperature T_c^0, predicted in the absence of damping, to

$$T_c \simeq 0.32\ T_c^0.$$

[1]A. A. Abrikosov and I. M. Khalatnikov, Reports on Progress in Physics (The Physical Society, London, 1959), Vol. 22, p. 329.

AUTHOR INDEX TO VOLUME 7

References with (E) are to Errata

ABASHIAN, ALEXANDER (see Booth, Norman E.) 35

ABEL, W. R., A. C. ANDERSON, and J. C. WHEATLEY. Propagation of sound in He^3 299

ALDER, B. J. and R. H. CHRISTIAN. Behavior of strongly shocked carbon 367

ALEXANDER, GIDEON, JARED A. ANDERSON, FRANK S. CRAWFORD, JR., WILLIAM LASKAR, and LESTER J. LLOYD. Interactions of lambdas with protons 348

ALEXEFF, I. and R. V. NEIDIGH. Observations of ionic sound waves in plasmas 223

ALMQVIST, E. (see Litherland, A. E.) 98

ALSTON, MARGARET, LUIS W. ALVAREZ, PHILIPPE EBERHARD, MYRON L. GOOD, WILLIAM GRAZIANO, HAROLD K. TICHO, and STANLEY G. WOJCICKI. Resonance in the $\Lambda\pi$ system 472(E)

ALVAREZ, LUIS W. (see Alston, Margaret) 472(E)

—— (see Maglić, B. C.) 178

ANDERSON, A. C., W. REESE, R. J. SARWINSKI, and J. C. WHEATLEY. Self-diffusion coefficient and nuclear susceptibility of liquid helium-three 220

——, W. REESE, and J. C. WHEATLEY. Magnetic properties of He^3 at pressures near the minimum in the melting curve 366

——, G. L. SALINGER, W. A. STEYERT, and J. C. WHEATLEY. Specific heat of He^3 under pressure 295

—— (see Abel, W. R.) 299

ANDERSON, J. D. and C. WONG. Evidence for charge independence in medium weight nuclei 250

ANDERSON, JARED A. (see Alexander, Gideon) 348

ANDREWS, D. J. (see Zickendraht, W.) 252

ARMBRUSTER, R. (see Gorodetzky, S.) 170

ARMSTRONG, J., N. BLOEMBERGEN, and D. GILL. Linear effect of applied electric field on nuclear quadrupole resonance 11

BAKER, W. F., R. L. COOL, E. W. JENKINS, T. F. KYCIA, S. J. LINDENBAUM, W. A. LOVE, D. LÜERS, J. A. NIEDERER, S. OZAKI, A. L. READ, J. J. RUSSELL, and L. C. L. YUAN. Particle production by 10-30 Bev protons incident on Al and Be 101

BALL, JAMES S. and WILLIAM R. FRAZER. Possible explanation of the higher pion-nucleon and K^--p resonances in terms of inelastic thresholds 204

—— and DAVID Y. WONG. Solutions of the pion-pion partial wave dispersion relations 390

BARDASIS, A. and J. R. SCHRIEFFER. Lifetime effects in condensed fermion systems 79, 472(E)

BARDEEN, JOHN. Quantization of flux in a superconducting cylinder 162

BARDON, MARCEL, PAOLO FRANZINI, and JULIET LEE. Helicity of μ^- mesons; Mott scattering of polarized muons 23

BARNES, V. E., D. V. BUGG, W. P. DODD, J. B. KINSON, and L. RIDDIFORD. Peripheral collisions and the $(\frac{3}{2},\frac{3}{2})$ resonance in the reaction $p+p \rightarrow n+p+\pi^+$ at 970 Mev 288

BARTELINK, D. J. (see Moll, J. L.) 87

BEALL, E. F., BRUCE CORK, D. KEEFE, P. G. MURPHY, and W. A. WENZEL. Asymmetry parameters in the decays $\Sigma^+ \rightarrow p+\pi^0$ and $\Lambda \rightarrow p+\pi^-$ 285

BENEDEK, G. B. (see Pound, R. V.) 405

BERLINCOURT, T. G. (see Thorsen, A. C.) 244

BERNSTEIN, A. M. (see Posner, M.) 173

BIONDI, M. A. (see Kasner, W. H.) 321

BLAIR, J. and A. C. SMITH. Phase transition in mercury telluride 124

BLAMONT, J. E. and F. RODDIER. Precise observation of the profile of the Fraunhofer strontium resonance line. Evidence for the gravitational red shift on the sun 437

BLATT, J. M. Persistent ring currents in an ideal Bose gas 82

BLAUGHER, R. D. (see Hulm, J. K.) 302

BLOCK, M. (see Leitner, J.) 264

—— (see Pevsner, A.) 421

BLOEMBERGEN, N. Linear effect of

applied electric field on magnetic hyperfine interaction 90
——— (see Armstrong, J.) 11
——— (see Pershan, P. S.) 165
BOERSCH, H., C. RADELOFF, and G. SAUERBREY. Experimental detection of transition radiation 52
BOLSTERLI, M. and D. A. GEFFEN. K_{e3} decay as a test of universal V-A lepton coupling 203
BOOTH, NORMAN E., ALEXANDER ABASHIAN, and KENNETH M. CROWE. Anomaly in meson production in $p+d$ collisions 35
BORST, L. B., S. L. BORST, L. KOYSOOKO, H. PATEL, and E. STUSNICK. Nuclear spin states in molecular crystals 343
BORST, S. L. (see Borst, L. B.) 343
BOWEN, P. H., G. C. COX, G. B. HUXTABLE, A. LANGSFORD, J. P. SCANLON, and J. J. THRESHER. Polarization in neutron-proton scattering below 100 Mev 248
BOWERS, R., C. LEGENDY, and F. ROSE. Oscillatory galvanomagnetic effect in metallic sodium 339
BOZORTH, R. M. (see Matthias, B. T.) 160
BRADNER, HUGH (see Stubbs, Theodore F.) 188
BRENIG, W. Remark concerning quantized magnetic flux in superconductors 337
BREWER, H. R., D. S. HARMER, and D. H. HAY. M-shell, relativistic electron wave functions 319
BROCKHOUSE, B. N., K. R. RAO, and A. D. B. WOODS. Image of the Fermi surface in the lattice vibrations of lead 93
BROWN, JOHN L., JOHN A. KADYK, GEORGE H. TRILLING, REMY T. VAN de WALLE, BRYON P. ROE, and DANIEL SINCLAIR. Experimental study of the $K_{e3}{}^{+}$ decay interaction 423
——— (see Roe, Byron P.) 346
BROWN, M. A. C. S. and E. G. S. PAIGE. Electric-field-induced modulation of the absorption due to interband transitions of free holes in germanium 84
BROWN, M. R., B. A. COLES, J. OWEN, and R. W. H. STEVENSON. Ferromagnetic exchange interaction between Mn^{2+} ions in Mn, ZnF_2 246
BRUCKER, B. (see Leitner, J.) 264
BRUGGER, K. and W. P. MASON. Relation between thermal conductivity defect in sodium chloride and acoustic relaxation effects at low temperatures 270
BRUNER, L. J. and ROBERT W. KEYES. Electronic effect in the elastic constants of germanium 55
BUEHLER, E. (see Kunzler, J. E.) 215(E)
BUGG, D. V. (see Barnes, V. E.) 288
BUGG, W. (see Leitner, J.) 264
BURDICK, GLENN A. Topology of the Fermi surface of copper 156
BUTLER, S. T. and C. A. PEARSON. Deuterons from high-energy proton bombardment of matter 69
BYERS, N. and C. N. YANG. Theoretical considerations concerning quantized magnetic flux in superconducting cylinders 46

CABIBBO, NICOLA. Measurement of the linear polarization of γ rays by the elastic photoproduction of π^0 on He^4 386
CALDWELL, DAVID O. Method for determining the spin of the K-π resonance 259
CARERI, G., S. CUNSOLO, and P. MAZZOLDI. Critical drift velocity of ions in liquid helium 151
CAVERZASIO, C. (see Garron, J. P.) 261
CHANDA, RICHARD N. (see Sheline, Raymond K.) 446
CHASMAN, RICHARD R. New approximation for pairing forces in nuclei 418
CHEVALLIER, P. (see Gorodetzky, S.) 170
CHEW, GEOFFREY F. and S. C. FRAUTSCHI. Principle of equivalence for all strongly interacting particles within the S-matrix framework 394
CHILTON, FRANK. Nuclear de-excitation following muon capture and the bound muon decay anomaly 31
CHINOWSKY, WILLIAM (see Slater, William) 378
——— (see Stubbs, Theodore F.) 188
CHRISTIAN, R. H. (see Alder, B. J.) 367
CLARK, M. A. (see Litherland, A. E.) 98
CLINE, THOMAS L. Search for high-energy cosmic gamma rays 109
CLOGSTON, A. M. (see Matthias, B. T.) 7
COCCONI, G., A. N. DIDDENS, E. LILLETHUN, G. MANNING, A. E. TAYLOR, T. G. WALKER, and A. M. WETHERELL. Elastic and inelastic scattering of high-

energy protons from hydrogen 450
COHEN, MORREL H. and L. M. FALICOV. Magnetic breakdown in crystals 231
COHN, H. O. (see Leitner, J.) 264
COLES, B. A. (see Brown, M. R.) 246
COLLINS, HARRY D. (see Putnam, Lawrence H.) 77
COMPTON, W. DALE (see Faraday, Bruce J.) 57; 433(E)
COOK, V., D. KEEFE, L. T. KERTH, P. G. MURPHY, W. A. WENZEL, and T. F. ZIPF. Total cross-section measurements of K^+-p and K^+-n interactions in the momentum region 0.77 to 2.83 Bev/c 182
COOL, R. L. (see Baker, W. F.) 101
CORBETT, J. W. and G. D. WATKINS. Silicon divacancy and its direct production by electron irradiation 314
CORENZWIT, E. (see Matthias, B. T.) 7
CORK, BRUCE (see Beall, E. F.) 285
CORNWELL, J. F. (see Wohlfarth, E. P.) 342
COSTELLO, D. G. (see Walters, W. L.) 284
COX, G. C. (see Bowen, P. H.) 248
CRAIG, PAUL P. Drag forces in rotating He II 331
CRAWFORD, FRANK S., JR. (see Alexander, Gideon) 348
CROWE, KENNETH M. (see Booth, Norman E.) 35
CULLIGAN, G., J. F. LATHROP, V. L. TELEGDI, R. WINSTON, and R. A. LUNDY. Experimental proof of the spin dependence of the muon capture interaction, and evidence for its (F-GT) character 458
CUNSOLO, S. (see Careri, G.) 151

De ALFARO, V. and B. VITALE. Possibility of a 4-pion structure in the $T=J=1$ pion-pion scattering amplitude 72
DEAVER, BASCOM S., JR., and WILLIAM M. FAIRBANK. Experimental evidence for quantized flux in superconducting cylinders 43
DICKE, R. H. Experimental tests of Mach's principle 359
DICKEY, D. H. (see Harman, T. C.) 403
DIDDENS, A. N. (see Cocconi, G.) 450
DIEBOLD, R., R. GOMEZ, R. TALMAN, and R. L. WALKER. Photoproduction of single neutral pions from hydrogen at 60° in the 600-1100 Mev region 323
DIEKE, G. H. (see Varsanyi, F.) 442
DODD, W. P. (see Barnes, V. E.) 288
DOLL, R. and M. NÄBAUER. Experimental proof of magnetic flux quantization in a superconducting ring 51
DOUGLASS, D. H., JR. Direct experimental measurement of the magnetic field dependence of the superconducting energy gap of aluminum 14
DRELL, S. D. and K. HIIDA. Quasi-elastic peak in high-energy nucleon-nucleon scattering 199
DRESSELHAUS, M. S. (see Harman, T. C.) 403
DREVER, R. (see Pound, R. V.) 405

EBERHARD, PHILIPPE (see Alston, Margaret) 472(E)
ECK, T. G. (see Joseph, A. S.) 334
EISLER, F., J. M. GAILLARD, J. KEREN, M. SCHWARTZ, and S. WOLF. Example of the decay $\Lambda^0 \to p + \mu^- + \bar{\nu}$ 136
ELY, ROBERT P., SUN-YIU FUNG, GEORGE GIDAL, YU-LI PAN, WILSON M. POWELL, and HOWARD S. WHITE. Spin of Y_1^* 461
ENGELER, W., H. LEVINSTEIN, and C. STANNARD, JR. Oscillatory photoconductivity in InSb 62
ENGLER, A. (see Leitner, J.) 264
——— (see Pevsner, A.) 421
ERWIN, A. R., R. MARCH, W. D. WALKER, and E. WEST. Evidence for a π-π resonance in the $I=1$, $J=1$ state 39(E)

FAIRBANK, WILLIAM M. (see Deaver, Bascom S., Jr.) 43
FALICOV, L. M. (see Cohen, Morrel H.) 231
FARADAY, BRUCE J., HERBERT RABIN, and W. DALE COMPTON. Evidence for the double F model of the M center 57; 433(E)
FAWCETT, E. Magnetoresistance of transition metals in the high-field limit 370
FAYYAZUDDIN (see Riazuddin) 464
FAZIO, G. G. (see Melissinos, A. C.) 454
FEINBERG, G., F. GÜRSEY, and A. PAIS. Lepton pairings in the two-neutrino theory 208

FERRARI, E. and F. SELLERI. Pionic form factor effects in peripheral nucleon-nucleon collisions 387
FESHBACH, H., E. LOMON, and A. TUBIS. Proton-proton interaction 39(E)
FETISOV, E. P. (see Silin, V. P.) 374
FICKINGER, W. J., E. PICKUP, D. K. ROBINSON, and E. O. SALANT. One-pion exchange in p-p collisions at 2 Bev 196
FOLEN, V. J. (see Rado, G. T.) 310
FORD, KENNETH W., VERNON W. HUGHES, and JOHN G. WILLS. Theoretical values for magnetic moments of μ-mesonic atoms 134
FRANCK, J. P. Beta-gamma phase transformation in solid He^3 435
FRANKEN, P. A., A. E. HILL, C. W. PETERS, and G. WEINREICH. Generation of optical harmonics 118
FRANZINI, PAOLO (see Bardon, Marcel) 23
FRASER, J. S. (see Milton, J. C. D.) 67
FRAUTSCHI, S. C. (see Chew, Geoffrey F.) 394
FRAZER, WILLIAM R. (see Ball, James S.) 204
FRIEDLÄNDER, E. M., M. MARCU, and M. SPÎRCHEZ. Relative inelasticity and anisotropy of proton interactions at 9 and 23.5 Gev 25
FUBINI, SERGIO. Vector mesons and possible violations of charge symmetry in strong interactions 466
FUNG, SUN-YIU (see Ely, Robert P.) 461

GAILLARD, J. M. (see Eisler, F.) 136
GARRETT, C. G. B. (see Kaiser, W.) 229
GARRON, J. P., J. C. JACMART, M. RIOU, C. RUHLA, J. TEILLAC, C. CAVERZASIO, and K. STRAUCH. Quasi-elastic interaction of 155-Mev protons with protons in Li^6 and Li^7 261
GEBALLE, T. H. (see Hulm, J. K.) 302
GEFFEN, D. A. (see Bolsterli, M.) 203
GESSAROLI, R. (see Leitner, J.) 264
——— (see Pevsner, A.) 421
GIBSON, W. M., T. D. THOMAS, and G. L. MILLER. Structure in the kinetic energy spectrum of fragments from thermal-neutron-induced fission of U^{235} 65
GIDAL, GEORGE (see Ely, Robert P.) 461
GILL, D. (see Armstrong, J.) 11
GINTSBURG, M. A. Electromagnetic radiation from solar corpuscular streams 399
GLASER, DONALD A. (see Roe, Byron P.) 346
GLASHOW, SHELDON L. Is isotopic spin a good quantum number for the new isobars? 469
GLENDENNING, NORMAN K. and GUSTAV KRAMER. Scalar nucleon form factor $F_1^n + F_1^p$ 471
GOLDHABER, GERSON (see Slater, William) 378
——— (see Stubbs, Theodore F.) 188
GOLDHABER, SULAMITH (see Slater, William) 378
——— (see Stubbs, Theodore F.) 188
GOMEZ, R. (see Diebold, R.) 323
GOOD, MYRON L. (see Alston, Margaret) 472(E)
GOODING, TERENCE J. and GEORGE IGO. Scattering of 915-Mev α particles from carbon and helium: direct evidence for α-particle clustering in nuclei 28
GORDON, G. (see Jacobs, S.) 415
GORDON, W. L. (see Joseph, A. S.) 334
GORODETZKY, S., G. SUTTER, R. ARMBRUSTER, P. CHEVALLIER, P. MENNRATH, F. SCHEIBLING, and J. YOCCOZ. Double gamma emission in the 6.06-Mev monopole transition of O^{16} 170
GOSSARD, A. C., V. JACCARINO, and J. P. REMEIKA. Experimental test of the spin-wave theory of a ferromagnet 122
GOVE, H. E. (see Litherland, A. E.) 98
GRAY, L. (see Leitner, J.) 264
GRAZIANO, WILLIAM (see Alston, Margaret) 472(E)
GREEN, JOHN M. and JOHN L. JOHNSON. Stability criterion for arbitrary hydromagnetic equilibria 401
GRINELLINI, N. T. (see Leitner, J.) 264
GÜRSEY, F. (see Feinberg, G.) 208

HAM, FRANK S. Linear effect of applied electric field in electron spin resonance 242
HAMILTON, D. R. (see Posner, M.) 173
HARMAN, T. C., A. J. STRAUSS, D. H. DICKEY, M. S. DRESSELHAUS, G. B. WRIGHT, and J. G. MAVROIDES. Low electron effective masses and energy gap in $Cd_xHg_{1-x}Te$ 403

HARMER, D. S. (see Brewer, H. R.) 319
HART, M. and A. R. LANG. Direct determination of x-ray reflection phase relationships through simultaneous reflection 120
HARTH, E. (see Leitner, J.) 264
HAY, D. H. (see Brewer, H. R.) 319
HEEGER, A. J., A. M. PORTIS, DALE T. TEANEY, and GERALD WITT. Double resonance and nuclear cooling in an antiferromagnet 307
HELTEMES, E. C. and C. A. SWENSON. Specific heat of solid He^3 363
HERB, R. G. (see Walters, W. L.) 284
HIIDA, K. (see Drell, S. D.) 199
HILL, A. E. (see Franken, P. A.) 118
HOH, F. C. and B. LEHNERT. Screw instability of a plasma column 75
HOPFIELD, J. J. (see Thomas, D. G.) 316
HSU, F. S. L. (see Kunzler, J. E.) 215(E)
HUGHES, VERNON W. (see Ford, Kenneth W.) 134
HULM, J. K., R. D. BLAUGHER, T. H. GEBALLE, and B. T. MATTHIAS. Superconductivity of niobium-molybdenum alloys below 1°K 302
HUTCHINSON, D. P., J. MENES, G. SHAPIRO, A. M. PATLACH, and S. PENMAN. Magnetic moment of positive and negative muons 129
HUTSON, A. R., J. H. McFEE, and D. L. WHITE. Ultrasonic amplification in CdS 237
HUXTABLE, G. B. (see Bowen, P. H.) 248

IGO, GEORGE (see Gooding, Terence J.) 28

JACCARINO, V. (see Gossard, A. C.) 122
JACMART, J. C. (see Garron, J. P.) 261
JACOBS, S., G. GORDON, and P. RABINOWITZ. Coherent light amplification in optically pumped Cs vapor 415
JENKINS, E. W. (see Baker, W. F.) 101
JOHNSON, JOHN L. (see Greene, John M.) 401
JONES, LAWRENCE W. (see Lai, Kwan W.) 125
JOSEPH, A. S., W. L. GORDON, J. R. REITZ, and T. G. ECK. Evidence for spin-orbit splitting in the band structure of zinc and cadmium 334

KADYK, JOHN A. (see Brown, John L.) 423
——— (see Roe, Byron P.) 346
KAISER, W. and C. G. B. GARRETT. Two-photon excitation in $CaF_2:Eu^{2+}$ 229
KALBFLEISCH, G. R. (see Maglić, B. C.) 137
KANE, W. E. (see Walters, W. L.) 284
KÄNZIG, W. Paraelasticity, a mechanical analog of paramagnetism 304
KAPLAN, SELIG, GEORGE A. PAULIKAS, and ROBERT V. PYLE. Dissociation of H_2^+ ions by a magnetic field 96
KASAI, PAUL H. and YOSHIRO OTOMO. Paramagnetic resonance detection of luminescent centers and traps 17
KASNER, W. H., W. A. ROGERS, and M. A. BIONDI. Electron-ion recombination coefficients in nitrogen and in oxygen 321
KEEFE, D. (see Beall, E. F.) 285
——— (see Cook, V.) 182
KELLER, J. B. and B. ZUMINO. Quantization of the fluxoid in superconductivity 164
KEMP, JAMES C. Field-swept maser oscillation 21
KEREN, J. (see Eisler, F.) 136
KERN, C. WILLIAM and WILLIAM N. LIPSCOMB. Magnetic shielding constants in heteropolar diatomic molecules 19
KERST, D. W. (see Ohkawa, T.) 41
KERTH, L. T. (see Cook, V.) 182
KEYES, ROBERT W. (see Bruner, L. J.) 55
KIKUCHI, T. (see Leitner, J.) 264
KINSON, J. B. (see Barnes, V. E.) 288
KNIFFEN, D. A. (see Naugle, J. E.) 3
KOVACS, A. (see Leitner, J.) 264
KOYSOOKO, L. (see Borst, L. B.) 343
KRAEMER, R. (see Pevsner, A.) 421
KRAMER, GUSTAV (see Glendenning, Norman K.) 471
KUEHNER, J. A. (see Litherland, A. E.) 98
KUNZLER, J. E., E. BUEHLER, F. S. L. HSU, and J. H. WERNICK. Superconductivity in Nb_3Sn at high current density in a magnetic field 215(E)
KUSHIDA, TOSHIMOTO and KUNIOMI SAIKI. Shift of nuclear quadrupole resonance frequency by electric field 9
KYCIA, T. F. (see Baker, W. F.) 101

LAI, KWAN W., LAWRENCE W. JONES, and MARTIN L. PERL. Negative pion-proton elastic scattering at 1.51, 2.01, and 2.53 Bev/*c* outside the diffraction peak 125

LANE, A. M. and J. M. SOPER. Persistence of isobaric correspondence between nuclear states in mass regions where isotopic spin is not a good quantum number 420
LANG, A. R. (see Hart, M.) 120
LANGSFORD, A. (see Bowen, P. H.) 248
LASKAR, WILLIAM (see Alexander, Gideon) 348
LATHROP, J. F., R. A. LUNDY, V. L. TELEGDI, and R. WINSTON. X-ray yields in the K and L series of μ-mesonic atoms 147
———, R. A. LUNDY, V. L. TELEGDI, R. WINSTON, and D. D. YOVANOVITCH. Measurements of muon disappearance rates vs time in C, Mg, Al, Si, and P 107
——— (see Culligan, G.) 458
LEE, JULIET (see Bardon, Marcel) 23
LEE, T. D., PETER MARKSTEIN, and C. N. YANG. Production cross section of intermediate bosons by neutrinos in the Coulomb field of protons and iron 429
LEE, WONYONG (see Slater, William) 378
LEGENDY, C. (see Bowers, R.) 339
LEHNERT, B. Gravitational instability of a magnetized plasma 440
——— (see Hoh, F. C.) 75
LEITNER, J., L. GRAY, E. HARTH, S. LICHTMAN, J. WESTGARD, M. BLOCK, B. BRUCKER, A. ENGLER, R. GESSAROLI, A. KOVACS, T. KIKUCHI, C. MELTZER, H. O. COHN, W. BUGG, A. PEVSNER, P. SCHLEIN, M. MEER, N. T. GRINELLINI, L. LENDINARA, L. MONARI, and G. PUPPI. Helicity of the proton from Λ decay 264
LENDINARA, L. (see Leitner, J.) 264
LEVINSTEIN, H. (see Engeler, W.) 62
LICHTMAN, S. (see Leitner, J.) 264
LILLETHUN, G. (see Cocconi, G.) 450
LINDENBAUM, S. J., W. A. LOVE, J. A. NIEDERER, S. OZAKI, J. J. RUSSELL, and L. C. L. YUAN. Antiproton-proton and proton-proton total cross section from 4 to 20 Bev/c 185
———, W. A. LOVE, J. A. NIEDERER, S. OZAKI, J. J. RUSSELL, and L. C. L. YUAN. $\pi^+ + p$ and $\pi^- + p$ total cross sections from 8 to 20 Bev/c 352
——— (see Baker, W. F.) 101
——— (see Melissinos, A. C.) 454
LINLOR, WILLIAM I. Plasma production by traveling resonant perturbations 115
LIPSCOMB, WILLIAM N. (see Kern, C. William) 19
LITHERLAND, A. E., J. A. KUEHNER, H. E. GOVE, M. A. CLARK, and E. ALMQVIST. Rotational bands in Ne^{20} 98
LITTAUER, R. M., H. F. SCHOPPER, and R. R. WILSON. Scattering of Bev electrons by hydrogen and deuterium 141
———, H. F. SCHOPPER, and R. R. WILSON. Structure of the proton and neutron 144
LLOYD, LESTER J. (see Alexander, Gideon) 348
LOMON, E. (see Feshbach, H.) 39(E)
LOVE, W. A. (see Baker, W. F.) 101
——— (see Lindenbaum, S. J.) 185; 352
LUDWIG, G. W. and H. H. WOODBURY. Splitting of electron spin resonance lines by an applied electric field 240
LÜERS, D., I. S. MITTRA, W. J. WILLIS, and S. S. YAMAMOTO. K_2^0 decays and interactions 255; 361(E)
——— (see Baker, W. F.) 101
LUNDY, R. A. (see Culligan, G.) 458
——— (see Lathrop, J. F.) 107; 147
LYNCH, GERALD R. (see Xuong, Nguyen Huu) 327

MAGLIĆ, B. C., L. W. ALVAREZ, A. H. ROSENFELD, and M. L. STEVENSON. Evidence for a $T=0$ three-pion resonance 178
———, G. R. KALBFLEISCH, and M. L. STEVENSON. Charge asymmetries in the angular distribution of π and K mesons from antiproton annihilations in flight 137
MAHLMAN, G. W. Observation of solid-state photoemission from tin into germanium 408
MANNING, G. (see Cocconi, G.) 450
MARCH, R. (see Erwin, A. R.) 39(E)
MARCU, M. (see Friedländer, E. M.) 25
MARKSTEIN, PETER (see Lee, T. D.) 429
MASON, W. P. (see Brugger, K.) 270
MATTHIAS, B. T., R. M. BOZORTH, and J. H. VAN VLECK. Ferromagnetic interaction in EuO 160
———, A. M. CLOGSTON, H. J. WILLIAMS, E. CORENZWIT, and R. C. SHERWOOD. Ferromagnetism in solid solutions of scandium and indium 7
——— (see Hulm, J. K.) 302
MAVROIDES, J. G. (see Harman, T. C.) 403

MAYER-KUCKUK, T. and F. C. MICHEL. Comparison of the beta spectra of B^{12} and N^{12} 167
MAZZOLDI, P. (see Careri, G.) 151
McFEE, J. H. (see Hutson, A. R.) 237
McLEOD, D., S. RICHERT, and A. SILVERMAN. Evidence for a pion-pion resonance from photoproduction of pion pairs 383
MEER, M. (see Leitner, J.) 264
MELISSINOS, A. C., G. G. FAZIO, T. YAMANOUCHI, S. J. LINDENBAUM, and L. C. L. YUAN. π-meson production in 2.9-Bev p-p collisions 454
MELTZER, C. (see Leitner, J.) 264
—— (see Pevsner, A.) 421
MENES, J. (see Hutchinson, D. P.) 129
MENNRATH, P. (see Gorodetzky, S.) 170
MERMOD, R. (see von Dardel, G.) 127
MEYER, HORST (see Rives, John E.) 217
MEYER, N. I. (see Moll, J. L.) 87
MICHEL, F. C. (see Mayer-Kuckuk, T.) 167
MICHEL, R. E. and B. ROSENBLUM. Multicomponent magnetoplasma resonance in p-type germanium 234
MILLER, G. L. (see Gibson, W. M.) 65
MILTON, J. C. D. and J. S. FRASER. Prompt fission yields and total kinetic energy behavior from time-of-flight measurements 67
MITTRA, I. S. (see Luers, D.) 255; 361(E)
MOLL, J. L., N. I. Meyer, and D. J. BARTELINK. Hot electron emission from silicon pn junctions parallel to the surface 87
MONARI, L. (see Leitner, J.) 264
MURPHY, P. G. (see Beall, E. F.) 285
—— (see Cook, V.) 182

NÄBAUER, M. (see Doll, R.) 51
NARATH, A. Nuclear magnetic resonance of Cr^{53} in antiferromagnetic $CrCl_3$ 410
NASH, F. R. Size-dependent relaxation times at liquid helium temperatures 59
NAUGLE, J. E. and D. A. KNIFFEN. Flux and energy spectra of the protons in the inner Van Allen belt 3
NEIDIGH, R. V. (see Alexeff, I.) 223
NETHERCOT, A. H., JR. Superconducting-normal transition time 226
NIEDERER, J. A. (see Baker, W. F.) 101
—— (see Lindenbaum, S. J.) 185; 352
NUSSBAUM, M. (see Pevsner, A.) 421

O'HALLORAN, THOMAS (see Slater, William) 378
OHKAWA, T. and D. W. KERST. Stable plasma confinement by multipole fields 41
OLESON, NORMAN L. (see Putnam, Lawrence H.) 77
OLNESS, J. W. (see Sprenkel, E. L.) 174
ONSAGER, LARS. Magnetic flux through a superconducting ring 50
OTOMO, YOSHIRO (see Kasai, Paul H.) 17
OWEN, J. (see Brown, M. R.) 246
OZAKI, S. (see Baker, W. F.) 101
—— (see Lindenbaum, S. J.) 185; 352

PAIGE, E. G. S. (see Brown, M. A. C. S.) 84
PAIS, A. Remark on the algebra of interactions 291
—— (see Feinberg, G.) 208
PALMER, D. W. (see Walters, W. L.) 284
PAN, YU-LI (see Ely, Robert P.) 461
PARMENTER, R. H. Enhancement of superconductivity by extraction of normal carriers 274
PATEL, H. (see Borst, L. B.) 343
PATLACH, A. M. (see Hutchinson, D. P.) 129
PAULIKAS, GEORGE A. (see Kaplan, Selig) 96
PEARSON, C. A. (see Butler, S. T.) 69
PENMAN, S. (see Hutchinson, D. P.) 129
PERL, MARTIN L. (see Lai, Kwan W.) 125
PERSHAN, P. S. Absence of antiferromagnetic domain walls in MnF_2 280
—— and N. Bloembergen. Electrically induced shift of the F^{19} resonance frequency in MnF_2 165
PETERS, C. W. (see Franken, P. A.) 118
PEVSNER, A., R. KRAEMER, M. NUSSBAUM, C. RICHARDSON, P. SCHLEIN, R. STRAND, T. TOOHIG, M. BLOCK, A. ENGLER, R. GESSAROLI, and C. MELTZER. Evidence for a three-pion resonance near 550 Mev 421
—— (see Leitner, J.) 264
PICKUP, E., D. K. ROBINSON, and E. O. SALANT. π-π resonance in π^--p interactions at 1.25 Bev 192, 472(E)
—— (see Fickinger, W. J.) 196

PIETENPOL, JERRY L. Auto-ionization of the $(1s2s2p)\ ^4P_{5/2}$ level in Li and He^- 64
PINCUS, P. and J. WINTER. Influence of magnon-phonon coupling on the low-temperature magnetic properties of an antiferromagnet 269
PIROUÉ, P. A. (see von Dardel, G.) 127
POMERANTZ, M. Excitation of spin-wave resonance by microwave phonons 312
PORTER, JOHN F., JR. Fluorescence excitation by the absorption of two consecutive photons 414
PORTIS, A. M. (see Heeger, A. J.) 307
POSNER, M., J. L. SNIDER, A. M. BERNSTEIN, and D. R. HAMILTON. Magnetic moment of N^{13} 173
POUND, R. V., G. B. BENEDEK, and R. DREVER. Effect of hydrostatic compression on the energy of the 14.4-kev gamma ray from Fe^{57} in iron 405
POWELL, WILSON M. (see Ely, Robert P.) 461
PUPPI, G. (see Leitner, J.) 264
PUTNAM, LAWRENCE H., HARRY D. COLLINS, and NORMAN L. OLESON. Experimental evidence for beam-plasma interaction in a low-pressure argon discharge 77
PYLE, ROBERT V. (see Kaplan, Selig) 96

RABIN, HERBERT (see Faraday, Bruce J.) 57; 433(E)
RABINOWITZ, P. (see Jacobs, S.) 415
RADELOFF, C. (see Boersch, H.) 52
RADO, G. T. and V. J. FOLEN. Observation of the magnetically induced magnetoelectric effect and evidence for antiferromagnetic domains 310
RAO, K. R. (see Brockhouse, B. N.) 93
RAUCH, CONRAD J. Millimeter cyclotron resonance experiments in diamond 83
READ, A. L. (see Baker, W. F.) 101
REESE, W. (see Anderson, A. C.) 220; 366
REITZ, J. R. (see Joseph, A. S.) 334
REMEIKA, J. P. (see Gossard, A. C.) 122
RIAZUDDIN and FAYYAZUDDIN. K^* and $K^+-3\pi$ decay 464
RICHARDS, P. L. Anisotropy of the superconducting energy gap in pure and impure tin 412
RICHARDSON, C. (see Pevsner, A.) 421
RICHERT, S. (see McLeod, D.) 383
RIDDIFORD, L. (see Barnes, V. E.) 288
RIOU, M. (see Garron, J. P.) 261
RIVES, JOHN E. and HORST MEYER. Density of liquid helium-3 between 0.045 and 1.3°K 217
ROBINSON, D. K. (see Fickinger, W. J.) 196
——— (see Pickup, E.) 192, 472(E)
RODBELL, D. S. Possibility of exchange magnetostriction yielding negative thermal expansion in solid He^3 1
RODDIER, F. (see Blamont, J. E.) 437
ROE, BYRON P., DANIEL SINCLAIR, JOHN L. BROWN, DONALD A. GLASER, JOHN A. KADYK, and GEORGE H. TRILLING. New determination of the K^+-decay branching ratios 346
——— (see Brown, John L.) 423
ROGERS, W. A. (see Kasner, W. H.) 321
ROSE, F. (see Bowers, R.) 339
ROSE-INNES, A. C. and B. SERIN. Superconductivity of superimposed metals 278
ROSENBLUM, B. (see Michel, R. E.) 234
ROSENFELD, A. H. (see Maglić, B. C.) 178
ROSS, MARC H. (see Shaw, Gordon L.) 210
RUDERFER, MARTIN. First-order terrestrial ether drift experiment using the Mössbauer radiation 361(E)
RUHLA, C. (see Garron, J. P.) 261
RUSSELL, J. J. (see Baker, W. F.) 101
——— (see Lindenbaum, S. J.) 185; 352
RUSTGI, M. L. (see Zickendraht, W.) 252

SAIKI, KUNIOMI (see Kushida, Toshimoto) 9
SAKURAI, J. J. Existence of two $T=0$ vector mesons 355
——— New resonances and strong interaction symmetry 426
SALANT, E. O. (see Fickinger, W. J.) 196
——— (see Pickup, E.) 192, 472(E)
SALINGER, G. L. (see Anderson, A. C.) 295
SARWINSKI, R. J. (see Anderson, A. C.) 220
SAUERBREY, G. (see Boersch, H.) 52
SAWYER, R. F. Anomalous thresholds and final-state interactions in production processes 213
SCANLON, J. P. (see Bowen, P. H.) 248
SCHEIBLING, F. (see Gorodetzky, S.) 170
SCHLEIN, P. (see Leitner, J.) 264
——— (see Pevsner, A.) 421
SCHMIDT-TIEDEMANN, K. J. Experimental evidence of birefringence by free carriers in semiconductors 372

SCHOPPER, H. F. (see Littauer, R. M.) 141; 144
SCHRIEFFER, J. R. (see Bardasis, A.) 79, 472(E)
SCHWARTZ, M. (see Eisler, F.) 136
SEGALL, B. Calculated shape of the Fermi surface of copper 154
SEGEL, R. E. (see Sprenkel, E. L.) 174
SEITZ, FREDERICK. Nature of the V_1 center 282
SELLERI, F. (see Ferrari, E.) 387
SERIN, B. (see Rose-Innes, A. C.) 278
SHAPIRO, G. (see Hutchinson, D. P.) 129
SHAW, GORDON L. and MARC H. ROSS. $\Lambda\pi$ resonance and s-wave K^--p reactions 210
SHELINE, RAYMOND K., TORBJØRN SIKKELAND, and RICHARD N. CHANDA. Experimental observation of a new region of nuclear deformation 446
SHERWOOD, R. C. (see Matthias, B. T.) 7
SHULMAN, R. G. and S. SUGANO. Calculation of the crystal field splitting 157
SIKKELAND, TORBJØRN (see Sheline, Raymond K.) 446
SILIN, V. P. and E. P. FETISOV. Interpretation of the electromagnetic radiation from electron passage through metal films 374
SILVERMAN, A. (see McLeod, D.) 383
SINCLAIR, DANIEL (see Brown, John L.) 423
—— (see Roe, Byron P.) 346
SKOFRONICK, J. G. (see Walters, W. L.) 284
SLATER, WILLIAM, DONALD H. STORK, HAROLD K. TICHO, WONYONG LEE, WILLIAM CHINOWSKY, GERSON GOLDHABER, SULAMITH GOLDHABER, and THOMAS O'HALLORAN. K^++d charge-exchange reaction from 52 to 456 Mev 378
—— (see Stubbs, Theodore F.) 188
SMITH, A. C. (see Blair, J.) 124
SNIDER, J. L. (see Posner, M.) 173
SNITZER, E. Optical maser action of Nd^{+3} in a barium crown glass 444
SOPER, J. M. (see Lane, A. M.) 420
SPÎRCHEZ, M. (see Friedländer, E. M.) 25
SPRENKEL, E. L., J. W. OLNESS, and R. E. SEGEL. Identification of doublet states at 5.16 Mev in B^{10} 174
STANNARD, C., JR. (see Engeler, W.) 62
STEVENSON, M. L. (see Maglić, B. C.) 137; 178
STEVENSON, R. W. H. (see Brown, M. R.) 246
STEYERT, W. A. (see Anderson, A. C.) 295
STORK, DONALD H. (see Slater, William) 378
—— (see Stubbs, Theodore F.) 188
STRAND, R. (see Pevsner, A.) 421
STRAUCH, K. (see Garron, J. P.) 261
STRAUSS, A. J. (see Harman, T. C.) 403
STUBBS, THEODORE F., HUGH BRADNER, WILLIAM CHINOWSKY, GERSON GOLDHABER, SULAMITH GOLDHABER, WILLIAM SLATER, DONALD H. STORK, and HAROLD K. TICHO. K^+-p interaction at 455 Mev 188
STUSNICK, E. (see Borst, L. B.) 343
SUGANO, S. (see Shulman, R. G.) 157
SUTTER, G. (see Gorodetzky, S.) 170
SWENSON, C. A. (see Heltemes, E. C.) 363

TALMAN, R. (see Diebold, R.) 323
TAYLOR, A. E. (see Cocconi, G.) 450
TEANEY, DALE T. (see Heeger, A. J.) 307
TEILLAC, J. (see Garron, J. P.) 261
TELEGDI, V. L. (see Culligan, G.) 458
—— (see Lathrop, J. F.) 107; 147
—— (see Winston, R.) 104
THOMAS, D. G. and J. J. HOPFIELD. Bound exciton complexes 316
THOMAS, T. D. (see Gibson, W. M.) 65
THORSEN, A. C. and T. G. BERLINCOURT. de Haas–van Alphen effect in rhenium, niobium, and tantalum 244
THRESHER, J. J. (see Bowen, P. H.) 248
TICHO, HAROLD K. (see Alston, Margaret) 472(E)
—— (see Slater, William) 378
—— (see Stubbs, Theodore F.) 188
TOOHIG, T. (see Pevsner, A.) 421
TRILLING, GEORGE H. (see Brown, John L.) 423
—— (see Roe, Byron P.) 346
TUBIS, A. (see Feshbach, H.) 39(E)

VAN de WALLE, REMY T. (see Brown, John L.) 423
VAN VLECK, J. H. (see Matthias, B. T.) 160
VARSANYI, F. and G. H. DIEKE. Ion-

pair resonance mechanism of energy transfer in rare earth crystal fluorescence 442
VITALE, B. (see De Alfaro, V.) 72
VIVARGENT, M. (see von Dardel, G.) 127
von DARDEL, G., R. MERMOD, P. A. PIROUÉ, M. VIVARGENT, G. WEBER, and K. WINTER. Total cross sections for pions on protons in the momentum range 4.5 to 10 Gev/c 127

WALKER, R. L. (see Diebold, R.) 323
WALKER, T. G. (see Cocconi, G.) 450
WALKER, W. D. (see Erwin, A. R.) 39(E)
WALTERS, W. L., D. G. COSTELLO, J. G. SKOFRONICK, D. W. PALMER, W. E. KANE, and R. G. HERB. Lewis effect in resonance yield curves 284
WATKINS, G. D. (see Corbett, J. W.) 314
WEBER, G. (see von Dardel, G.) 127
WEINREICH, G. (see Franken, P. A.) 118
WENZEL, W. A. (see Beall, E. F.) 285
——— (see Cook, V.) 182
WERNICK, J. H. (see Kunzler, J. E.) 215(E)
WEST, E. (see Erwin, A. R.) 39(E)
WESTGARD, J. (see Leitner, J.) 264
WETHERELL, A. M. (see Cocconi, G.) 450
WHEATLEY, J. C. (see Abel, W. R.) 299
——— (see Anderson, A. C.) 220; 295; 366
WHITE, D. L. (see Hutson, A. R.) 237
WHITE, HOWARD S. (see Ely, Robert P.) 461
WILLIAMS, H. J. (see Matthias, B. T.) 7
WILLIS, W. J. (see Luers, D.) 255; 361(E)
WILLS, JOHN G. (see Ford, Kenneth W.) 134
WILSON, R. R. (see Littauer, R. M.) 141; 144
WINSTON, R. and V. L. TELEGDI. Fast atomic transitions within μ-mesonic hyperfine doublets, and observable effects of the spin dependence of muon absorption 104
——— (see Culligan, G.) 458
——— (see Lathrop, J. F.) 107; 147
WINTER, J. (see Pincus, P.) 269
WINTER, K. (see von Dardel, G.) 127
WITT, GERALD (see Heeger, A. J.) 307
WOHLFARTH, E. P. and J. F. CORNWELL. Critical points and ferromagnetism 342
WOJCICKI, STANLEY G. (see Alston, Margaret) 472(E)
WOLF, S. (see Eisler, F.) 136
WONG, C. (see Anderson, J. D.) 250
WONG, DAVID Y. (see Ball, James S.) 390
WOODBURY, H. H. (see Ludwig, G. W.) 240
WOODS, A. D. B. (see Brockhouse, B. N.) 93
WRIGHT, G. B. (see Harman, T. C.) 403

XUONG, NGUYEN HUU and GERALD R. LYNCH. Evidence confirming the $T=0$ three-pion resonance 327

YAMAMOTO, S. S. (see Luers, D.) 255; 361(E)
YAMANOUCHI, T. (see Melissinos, A. C.) 454
YANG, C. N. (see Byers, N.) 46
——— (see Lee, T. D.) 429
YOCCOZ, J. (see Gorodetzky, S.) 170
YOVANOVITCH, D. D. (see Lathrop, J. F.) 107
YUAN, L. C. L. (see Baker, W. F.) 101
——— (see Lindenbaum, S. J.) 185; 352
——— (see Melissinos, A. C.) 454

ZACHARIASEN, FREDRIK. Self-consistent calculation of the mass and width of the $J=1$, $T=1$, $\pi\pi$ resonance 112; 268(E)
ZICKENDRAHT, W., D. J. ANDREWS, and M. L. RUSTGI. Photodisintegration of polarized and aligned deuterons 252
ZIPF, T. F. (see Cook, V.) 182
ZUMINO, B. (see Keller, J. B.) 164

104
458
7; 147
269
127
307

342

472(E)
136
250
390
240
93
403

327

361(E)
454
46
429
170
) 107
101
5; 352
454

268(E)

252
182
164